Syracuse University
SURFACE at Syracuse University

Dissertations - ALL | SURFACE at Syracuse University

Summer 7-16-2021

Effects of Acid Deposition and Changing Climate on the Hydrochemistry and Critical Loads of Watersheds in the Adirondack Region of New York

Shuai Shao
Syracuse University

Follow this and additional works at: https://surface.syr.edu/etd

 Part of the Biogeochemistry Commons, and the Civil and Environmental Engineering Commons

Recommended Citation

Shao, Shuai, "Effects of Acid Deposition and Changing Climate on the Hydrochemistry and Critical Loads of Watersheds in the Adirondack Region of New York" (2021). *Dissertations - ALL*. 1532.
https://surface.syr.edu/etd/1532

This Dissertation is brought to you for free and open access by the SURFACE at Syracuse University at SURFACE at Syracuse University. It has been accepted for inclusion in Dissertations - ALL by an authorized administrator of SURFACE at Syracuse University. For more information, please contact surface@syr.edu.

Abstract

Despite decreases in acidic deposition since the 1970s, the recovery of surface waters from acidification has been limited primarily due to the depletion of exchangeable base cations, net mineralization of organic sulfur and nitrogen and release of previously retained SO_4^{2-} and NO_3^-, and increases in concentrations of naturally occurring organic acids from soil. The future recovery of stream chemistry from acidic deposition may be altered by projected increases in temperature and precipitation associated with a changing climate. The goals of this study were to conduct a modeling analysis of the response of soils and streams in the Adirondack Park, New York, USA to future changes in acidic deposition and climate.

I conducted the research for this dissertation in three phases. In phase one, the integrated biogeochemical model PnET-BGC was applied to 25 forested watersheds that represent a range of acid sensitivity in the Adirondack region to simulate the response of streams to past and future changes in atmospheric S and N deposition, and to calculate the target loads of acidity for protecting and restoring stream water quality and ecosystem health. Using measured data, the model was calibrated and applied to simulate soil and stream chemistry at all study sites. Model hindcasts indicate that historically, stream water chemistry in the Adirondacks was variable, but inherently sensitive to acid deposition. Model projections suggest that simultaneous decreases in sulfate, nitrate and ammonium deposition are more effective in restoring stream ANC than individual decreases in sulfur or nitrogen species in deposition. However, the increases in stream ANC per unit equivalent decrease in S deposition is greater than for equivalent decreases in N deposition. Using empirical algorithms, fish community density and biomass are projected to increase under several deposition-control scenarios that coincide with increases in stream ANC.

However, model projections suggest that even under the most aggressive deposition-reduction scenarios, stream chemistry and fisheries will not fully recover to pre-industrial values by 2200 due to legacy effects of historical acidification.

In phase two, the PnET-BGC model was applied to two montane forested watersheds in the Adirondack region to evaluate the effects of future climate change on the recovery of surface waters from historical acidification in response to future changes in atmospheric sulfur and nitrogen deposition. Statistically downscaled climate scenarios, on average, projected warmer temperatures and greater precipitation for the Adirondacks by the end of the century. Model simulations suggest under constant climate, acid-sensitive Buck Creek would gain more acid neutralizing capacity (ANC) than acid insensitive Archer Creek by 2100 from large reductions in acidic deposition. However, climate change could limit those improvements in stream acid-base status. Under climate change, acid-insensitive Archer Creek is projected to experience less of an ANC increase than Buck Creek by 2100. Calculated target loads for 2150 for both sites decreased when future climate change was considered in model simulations, which suggests further reductions in acid deposition may be necessary to restore ecosystem structure and function under a changing climate.

In phase three, the "One-at-A-Time (OAT) first-order sensitivity index method and Monte Carlo method were used to analyze the uncertainty in modeling Adirondack stream ANC. The results of first-order sensitivity analysis indicated that in general the model simulations of stream ANC are most sensitive to variation in precipitation quantity, Ca^{2+} and Na^{+} weathering rates, maximum monthly air temperature, SO_4^{2-} wet deposition, and DOC site density (the moles of organic anions per moles of organic carbon). The results of the first-order sensitivity analysis showed that even if the order of the most sensitive parameters between different research sites

were consistent, there were differences in projected uncertainty of stream ANC among sites. Monte Carlo analysis was conducted under the assumption of a 30% interval uncertainty (± 15%) in 16 input factors for 500 simulations that were normally distributed around the original simulated stream ANC for year 2050. The Monte Carlo analysis indicated that the model simulation of ANC is most sensitive to precipitation quantity, Ca^{2+} weathering rate, Na^{+} weathering rate, SO_4^{2-} wet deposition, and maximum monthly air temperature. Future simulations could be improved with further research to improve characterization of these inputs.

Effects of Acid Deposition and Changing Climate on the Hydrochemistry and Critical Loads of Watersheds in the Adirondack Region of New York

by

Shuai Shao

B.S., Beijing Jiaotong University, 2011
M.S., Syracuse University, 2014

Dissertation

Submitted in partial fulfillment of the requirements for the degree of

Doctor of Philosophy in Civil Engineering.

Syracuse University

July 2021

Copyright © Shuai Shao 2021

All Rights Reserved

Acknowledgement

I would like to thank my advisor Dr. Charles Driscoll for his support and guidance. Words are powerless to express my gratitude to Charley for his encouragements and the intelligence he shared. His dedication helped enormously on my study at Syracuse University and this dissertation. I thank Maureen Hale and Heather Flaherty for their patience and acknowledge financial supports from U.S. Environmental Protection Agency through the STAR program, the New York State Energy Research and Development Authority, and Department of Civil and Environmental Engineering at Syracuse University.

I sincerely appreciate committee members of my dissertation, Drs. Andria Staniec, Christa Kelleher, Svetoslava Todorova, Douglas Burns, and Peng Gao for their flexibility and suggestions on this dissertation.

I thank Professors David Chandler, Cliff Davidson, Chris Johnson, Svetoslava Todorova, Christa Kelleher, Peng Gao, Peter Plumley, Ruth Yanai with whom I had classes and worked as a teaching assistant at Syracuse University. I thank coauthors of my papers Dr. Timothy Sullivan Gregory Lawrence, Douglas Burns, Todd McDonnell, Barry Baldigo, Huizhong Shen, Yilin Chen, Armistead Russell, Chris Johnson, Timothy Fahey, John Battles, Joel Blum for their comments and suggestions. I would like to thank our department and college staff for their help at various times with my studies at Syracuse University: Heather Flaherty, Nick Clarke, Elizabeth Buchanan, Maureen Hale, Michael Rice, Morgan Narkiewicz and Mario Montesdeoca.

I would like to thank my wife Jiao (Alyssa) Sui, my daughters Kate and Lena and my parents. They made sacrifice for me and supported me doing whatever I want. I am sure I was not able to finish my Ph.D. without their love. I would like to dedicate this dissertation to them.

Table of Contents

List of Tables

Table A-10. Predicted fish biomass (g/0.1 ha) for the 25 model sites under preindustrial (1850), ambient (2015), and future (2150) scenario summer baseflow ANC Q_{27} conditions.

List of Figures

among 17 models and the gray area represents the 95% confidence interval. The Mann-Kendall Trend test was applied to each climate variable to assess significant trend direction.

Figure 4-4. Comparisons of measured (red circle) and model simulated (black lines) annual values of SO_4^{2-}, NO_3^-, ANC, DOC and stream flow over the period 1999–2013 at Archer Creek (a) and Buck Creek (b).

Figure 4-5. Projected annual volume-weighted average of SO_4^{2-}, NO_3^-, ANC, DOC in streamwater and soil BS% at Archer Creek over the period 2000–2100 for scenarios of pre-industrial (a) and 20% increase (b) deposition (red lines) which consider variation of simulations of 17 atmosphere-ocean general circulation models and two RCPs. The gray shaded area represents the 95% confidence interval of this variation. The blue circles represent the measured annual average value. The black line represents the projection for stationary meteorological conditions and business as usual deposition scenario (reference scenario).

Figure 4-6. Projected annual volume-weighted average of SO_4^{2-}, NO_3^-, ANC, DOC in streamwater and soil BS% at Buck Creek over the period 2000–2100 for scenarios of pre-industrial (a) and 20% increase (b) deposition (red lines) which consider variation of simulations of 17 atmosphere-ocean general circulation models and two RCPs. The gray shaded area represents the 95% confidence interval of this variation. The blue circles represent the measured annual average value. The black line represents the projection for stationary meteorological conditions and business as usual deposition scenario (reference scenario).

Figure 4-7. Time series of model simulations of ANC for Archer Creek (a) and Buck Creek (b), comparing deposition only scenarios with combined climate and deposition scenarios. The solid lines represent the scenarios in which climate remains at current conditions with deposition

Chapter 1. Introduction

1.1 General introduction

Atmospheric deposition of sulfur (S) and nitrogen (N) increased substantially in the eastern United States through most of the 20th century due to increases in human-caused emissions (Galloway & Cowling, 2002; Husar et al., 1991). For more than a century, air pollution has affected sensitive terrestrial and aquatic ecosystems largely in forested mountain landscapes, causing substantial damage at some locations, including the southwestern Adirondack Mountain region in New York State (Greaver et al., 2012). Federal and state legislation and rules and changes in energy generation have facilitated reductions in S and N emissions and atmospheric deposition prior to and since the turn of the 21st century. As a result, some ecosystem recovery (both chemical and biological change) has been documented for watersheds in the Adirondacks (Driscoll et al., 2016, 2007; Sullivan, 2017; Sutherland et al., 2015). However, decreases in acidic deposition have not resulted in complete recovery of soil and surface waters to estimated preindustrial conditions (Fakhraei et al., 2014; Gregory B. Lawrence et al., 2012; Shao et al., 2020). Moreover, changing climate may affect the recovery of forest ecosystems from historical acidification (Robison & Scanlon, 2018).

Past and recent climatic observations suggest an intensification of extreme temperature and precipitation events in the United States, as abnormally wet or dry conditions occur simultaneously with anomalously high temperatures (Karl et al., 2012; U.S. Global Change Research Program, 2018). Statistical and dynamical downscaling of coarse-scale climate model forecasts indicate that larger increases in temperature will occur at high latitude, inland regions

in the Northeast US (Hayhoe et al., 2008). Predicting the interaction of climate change and acidification on ecosystems is difficult because of their complex long-term, spatially variable effects on hydrologic and biogeochemical processes and the high uncertainty of future emissions of CO_2, SO_x, and NO_x (Campbell et al., 2009). Many variables affected by climate change may either exacerbate or mitigate the rate and degree of chemical and biological response to acidification and recovery. A better understanding of the biogeochemical interactions between the effects of climate and acid deposition will help improve projections of the response of watersheds impaired by elevated acidic deposition to future emission control programs.

Biogeochemical models have been used to investigate how future changes in climate are likely to interact with other drivers such as atmospheric deposition and land disturbance in forest watersheds over broad regions (Aber et al., 1997; Campbell et al., 2009; Ollinger et al., 1993; Robison & Scanlon, 2018; Valipour et al., 2018). Compared with other biogeochemical models that have been used to evaluate acidification of soil and surface water, PnET-BGC has some advantages including the depiction of major abiotic and biotic processes (Gbondo-Tugbawa et al., 2001). Models that only focus on abiotic processes may be inadequate to investigate the long-term effects of climate change, as resulting changes in living biomass and detrital organic matter affect hydrology and major element cycles (Cosby et al., 1985). PnET-BGC has proven to be an effective tool to assess the interactive effects of climate change and other disturbances, such as atmospheric deposition and land disturbance on the hydrology and pools and fluxes of elements at diverse watersheds sites (Dong et al., 2019a; Dong et al., 2019b; Pourmokhtarian et al., 2012, 2017).

Target loads (TLs) represent the level of atmospheric deposition that allows for specified levels of protection for an ecosystem that can be achieved within a given time frame. The TL concept and its calculation can account for spatial variation and temporal elements of the response of ecosystems to changes in atmospheric deposition and recovery (Burns, 2015). The development of TLs helps inform resource managers understand deposition effects thresholds; determine whether air quality conditions will meet or exceed thresholds for ecosystem damage; quantify protection afforded by various levels of emissions controls; and facilitate a science-based dialog between stakeholders and managers. Generally, TLs are calculated for a specific time frame by which the specified level of protection will be attained.

Acid deposition to sensitive landscapes can affect fish and other biotic communities in freshwater ecosystems (Lovett et al., 2009). Surface water acidification is characterized by elevated concentrations of strong acid anions (sulfate (SO_4^{2-}), nitrate (NO_3^-)), low pH and acid neutralizing capacity (ANC), and mobilization of calcium (Ca^{2+}) and inorganic monomeric aluminum (Al_i), which can impair the health of resident fish populations and their communities (Baldigo et al., 2019a, 2007). Developing TLs for N and S deposition using ANC as the chemical indicator can help quantify the protection of surface water afforded by various levels of emissions controls, and predict the corresponding response of fish communities in acid sensitive regions (U.S. Environmental Protection Agency, 2010). Moreover, empirical relations between chemical indicators of acidification stress, such as ANC, and fish-health metrics can help inform management decisions regarding the recovery of fish assemblages to potential future changes in acid deposition.

1.2 Objectives of this study

The primary objective of the first phase was to develop past, present (ambient), and future projections of effects of changing S and N deposition on the acid-base status of stream ecosystems in the Adirondack region of New York. I applied the dynamic biogeochemical model PnET-BGC to quantify historical acidification and projected the future chemical response of 25 stream watersheds in the Adirondacks to changes in S and N (both oxidized and reduced N) deposition. The specific goals of this study are to 1) assess the past, ambient, and future acidification of streams in the Adirondack Park, as affected by acidic deposition; 2) develop TLs of acidity for two endpoints, a fixed and site-specific endpoint, that could be used to project the future spatial extent and rates of stream water recovery; and 3) assess historical effects of acidification and potential future recovery of fish assemblages using the contemporary relations between fish metrics and water chemistry from Baldigo et al., (2019b).

The primary objective of second phase was to improve the understanding of the biogeochemical interactions between the effects of climate change and acidic deposition by investigating how changes in climatic conditions (e.g., temperature, precipitation) will affect watershed response to recovery from acidic deposition and to identify the processes through which this interaction will be manifested. In this study, the integrated biogeochemical model PnET-BGC was applied to explore the biogeochemical interactions at the watershed level of possible future acidic deposition scenarios with statistically downscaled climate projections over the next century in the Adirondack region of New York.

The primary objective of third phase was to improve understanding of the uncertainty in modeling of stream acidity using PnET-BGC. For this phase I used two methods to perform the

sensitivity and uncertainty analysis to quantify parameter uncertainty in PnET-BGC modeling work. First, I applied the “One-at-A-Time” (OAT) first-order sensitivity analysis to screen the input factors that have the greatest influence on model output. Next, a Monte Carlo uncertainty analysis using a Latin Hypercube Sample scheme (LHS) was employed to describe the uncertainty in model simulated stream ANC.

Chapter 2. Literature review

2.1 Acidic deposition

Acidic deposition includes many forms of sulfur (S) and nitrogen (N) that are released to the atmosphere from combustion of fossil fuels. Acidic deposition causes a range of effects across the largely montane forested landscape, including acidification of soil and drainage water; toxicity to fish and other aquatic biota; depletion of available soil nutrient base cations, such as Ca and magnesium (Mg^{2+}); reduced growth and regeneration of various plant species; increased susceptibility of foliage to winter injury; and changes in species composition and biodiversity. Such effects have been thoroughly studied in the Adirondack Mountain region of New York State (Driscoll et al., 2001; Fakhraei et al., 2014; Lawrence et al., 2008; Sutherland et al., 2015). Investigations have included long-term monitoring, process studies, and mathematical modeling of ecosystem responses and determining target loads (TLs) of acidity, focused largely on lakes and soils.

Acidification of soil and drainage water caused by atmospheric deposition of S and N has had environmental and economic consequences (Beier et al., 2017). Both S and N acidify base-poor soils and reduce nutrient cation availability. Increased N supply can increase primary production, alter species composition, and affect biodiversity (Bobbink et al., 2010). Ecosystem effects of increasing N supply include changes in N and carbon (C) cycling and ecological responses (Gilliam et al., 2019; Neff et al., 2002). Acidic deposition not only acidifies sensitive soils, resulting in depletion of base cations, but also mobilizes aluminum (Al) from soil to soil-solution and subsequently to drainage water in chemical forms that are toxic to aquatic life and

plant roots. Some plant species are highly susceptible to stress from soil and soil solution acidification (U.S. Environmental Protection Agency, 2008), most notably sugar maple (*Acer saccharum*; Sullivan et al., 2013) and red spruce (*Picea rubens*; Schaberg et al., 2000).

The mobility of atmospherically deposited strong acid anions such as SO_4^{2-} and NO_3^- in the soil and in water is dependent on soil characteristics, hydrologic flow paths and other watershed characteristics. Neutralization of acid inputs largely occur by the release of base cations to drainage water through the processes of weathering and ion exchange (van Breemen et al., 1983). Sulfate and NO_3^- leach to surface waters and their charge is largely balanced by base cations (Ca^{2+}, Mg^{2+}, K^+, and Na^+) and acidic cations, including hydrogen ion (H^+) and Al_i. Base cation loss from the soil caused by acidic deposition occurs in combination with cation loss caused by the natural leaching associated with organic and carbonic acids. Thus, acidic deposition enhances natural base cation loss from the soil rooting zone (Cronan et al., 1978), promotes transport of Al_i to surface waters, and affects the health of a variety of plant and animal species, especially those that require substantial supplies of Ca^{2+} and/or Mg^{2+} or prefer higher pH values. Thus, acidic deposition can contribute to changes in species distributions and abundance in both the terrestrial and aquatic communities (Sullivan, 2015).

Atmospheric deposition of S and N increased substantially in the eastern United States throughout the 20th century due to human emission sources (Galloway & Cowling, 2002). For more than a century, air pollution has affected sensitive aquatic and terrestrial resources and caused substantial damage in the Adirondack Mountain region in New York State (Sullivan, 2015). Acidification of soil and drainage water in the Adirondack Park has been caused primarily by atmospheric deposition of acid derived from sulfur dioxide emissions. Nitrogen oxides (NO_x)

also contribute to the process of acidification but to a lesser extent (Fakhraei et al., 2014). However, N deposition is becoming proportionally more important to overall acidic deposition with large recent reductions in S emissions and deposition (Fakhraei et al., 2014; Sullivan, 2015). Emissions of S and N into the atmosphere at locations upwind from the Adirondack Park increased several-fold during the late 19th and the 20th centuries to levels high enough to impair sensitive terrestrial and aquatic ecosystems (Fakhraei et al., 2014; Shao et al., 2020). Reductions in atmospheric sulfur dioxide (SO_2) and NO_x emissions have occurred across the eastern United States since the 1970s in response to the Clean Air Act (CAA), with especially sharp decreases in emissions since the 1990s in accordance with Title IV of the 1990 CAA Amendments and associated rules. These reductions have led to large decreases in atmospheric deposition of S and N (Driscoll et al., 2001, 2016). Decreases in acidic deposition have coincided with marked decreases in SO_4^{2-} and NO_3^- concentrations, increases in pH and acid neutralizing capacity (ANC), and decreases in concentrations of Al_i in acid-impacted surface waters, such as the Adirondack region of New York State (Driscoll et al., 2016; Lawrence et al., 2011; Sullivan et al., 2018). Despite these improvements, the recovery of surface water chemistry has been limited primarily due to three factors. First, long-term depletion of soil exchangeable base cations due to decades of acidic deposition has limited the ability of the soil to offset declines in S and N deposition (Johnson et al., 2008a). Second, declines in S and N deposition are increasingly buffered by internal soil sources of SO_4^{2-} and NO_3^- that have accumulated largely from legacy deposition to surface waters (Mitchell et al., 2011). Third, increases in dissolved organic carbon (DOC) concentrations in many Adirondack surface waters have been noted during this recovery period, and the strong acid fraction of the DOC has likely slowed the rate of recovery in pH and ANC (Driscoll et al., 2016; Fakhraei & Driscoll, 2015; Lawrence et al., 2011).

2.2 Climate change

The greenhouse gases (GHG) emissions have significant increased after the Industrial Revolution and affecting climate and ecosystems. These anthropogenic emissions and production of heat-trapping gases (CO_2, CH_4, N_2O and O_3) are the main cause for most of the averaged global warming since 1950 (IPCC, 2014). Over the past century, climate warming has increased the mean annual air temperatures of the Earth by 0.74°C and temperatures are predicted to rise by as much as 5°C by 2100 (IPCC, 2014). Some studies have shown that mountainous areas may be more sensitive to global climate change and are experiencing a higher rate of warming than the global average (Beniston et al., 1997; Rangwala & Miller, 2012). Statistical and dynamical downscaling of coarse-scale climate model forecasts indicate that larger increases in temperature will occur at high latitude, inland regions in the Northeast US (Hayhoe et al., 2008). Since 1970, the Northeast US region has been heating up at a rate of nearly 0.27°C per decade (NECIA, 2006). Winter temperature shows a higher rate of increase, from 1970 to 2000 0.72°C per decade (NECIA, 2006). The total precipitation increased by 100 mm, which is characterized by increased temporal variability (Hayhoe et al., 2007). The climate predictions coupled with atmosphere-ocean general circulation models (AOGCMs) indicate that in the 21st century, the annual average temperature and precipitation in the northeastern United States will continue to increase.

Future climate predictions include global temperature rise, changes in precipitation patterns (including increased severity and duration of precipitation events), frequent occurrences of extreme weather events, geophysical changes (changes in albedo), and sea level rise (IPCC,

2014). In the northeastern US, climate models predict an increase in temperature of 2-10°C by 2050 under continued high greenhouse gas emissions scenarios and about 2-6°C under low emission conditions (NOAA, 2013). The length of the growing season is also projected to increase concurrent with spring temperatures from approximately 141 days (1970-1999) to over 180 days by the end of the 21st century (Guilbert et al., 2014). In addition, many climate models also indicate larger inter-annual variation in both temperature and precipitation and higher variability in resulting erratic weather patterns (Hayhoe et al., 2007). According to the Intergovernmental Governmental Panel on Climate Change (IPCC) (2014) report, global warming exceeds the pre-industrial baseline by about 2°C, which is likely to cause more frequent high temperatures and extreme precipitation in most parts of North America, although most precipitation will fall in rainfall rather than snow. In the Northeast, due to the increase in runoff caused by the increase in temperature and rainfall, the time of spring snowmelt is advanced, and it may be accompanied by an increase in evapotranspiration and a joint increase in temperature, which may increase the frequency of summer droughts (Frumhoff et al., 2007). As a result of higher temperatures and higher evaporation, soil moisture will decrease in late summer and early autumn. It is expected that the increase in precipitation will not make up for this decrease, resulting in increases in the occurrence of short-term drought (Campbell et al., 2009). Compared with low-emission scenarios, these effects are more pronounced under high-emission scenarios, which highlights the impact of temperature on the hydrological cycle in the Northeast (NECIA, 2006).

Predicting the interaction of climate change and acidification on ecosystems is difficult because of their complex long-term, spatially variable effects on hydrologic and biogeochemical processes and the high uncertainty of future emissions of CO_2, S, and N (Campbell et al., 2009).

Many variables affected by climate change may either exacerbate or mitigate the rate and degree of chemical and biological response to acidification and recovery. A better understanding of the biogeochemical interactions between the effects of climate and acid deposition will help improve projections of the response of watersheds impaired by elevated acidic deposition to future emission control programs.

2.3 Biogeochemical models

PnET-BGC, an integrated forest vegetation-soil-water biogeochemical model that has been widely used to assess the effects of air pollution, climate change and land disturbance on forest and aquatic ecosystems (Gbondo-Tugbawa et al., 2001; Pourmokhtarian et al., 2017; Valipour et al., 2018). This model was formulated by linking two sub-models: PnET- CN (John D. Aber et al., 1997) and BGC (Gbondo-Tugbawa et al., 2001). The biogeochemical processes depicted in the model include tree photosynthesis, growth and productivity, litter production and decay, mineralization of soil organic matter and associated elements, immobilization of N, nitrification, interactions of major elements with vegetation and organic matter, abiotic soil processes, solution speciation, and surface water processes (Gbondo-Tugbawa et al., 2001). The model nominally operates on a monthly time step and is generally applied at the small watershed scale. The Gaines–Thomas formulation is applied to describe cation exchange reactions within the soil. The exchangeable cations considered in the model include Ca^{2+}, Mg^{2+}, Na^{+}, H^{+}, Al^{3+}, K^{+} and NH_4^{+}. pH-dependent isotherms are used to describe SO_4^{2-} and dissolved organic matter (DOM) (organic acids) adsorption processes. Speciation of monomeric Al (Al_m) is calculated in the model, including both organic and inorganic forms. Organic acids are described using a

triprotic analog (Driscoll et al., 1994) and the total amount of organic acid is estimated as a fraction (using the site density) of DOC concentration (Fakhraei & Driscoll, 2015). PnET-BGC simulates ANC as an analog to measured ANC by Gran plot analysis (Grove-Rasmussen, 1961) by considering the contributions of dissolved inorganic carbon (DIC), organic anions, and Al complexes (Driscoll et al., 1994; Fakhraei & Driscoll, 2015). PnET-BGC includes a CO_2 uptake algorithm that considers the effects of increases in atmospheric CO_2 concentration on forest ecosystem processes (Pourmokhtarian et al., 2012). The hydrologic algorithms used in PnET-BGC were summarized by Aber and Federer (1992) and Chen and Driscoll, (2005). More detailed descriptions of the model, including the results of an uncertainty analysis of parameter values, are available in Gbondo-Tugbawa et al. (2001), Pourmokhtarian et al. (2017), Valipour et al. (2018) and Fakhraei et al. (2016). Other biogeochemical models, such as MAGIC (Model Acidification of Groundwater in Catchments) have been used to evaluate chemical impacts of acidic deposition (Helliwell et al., 2014; McDonnell et al., 2013), but do not consider variation in meteorological and hydrological conditions that is critical to the analysis conducted in this work.

PnET-BGC has previously been tested with vegetation, soil and water biogeochemistry data from the Hubbard Brook Experimental Forest (HBEF) in New Hampshire (Gbondo-Tugbawa et al., 2001; Valipour et al. 2018) and then extended successfully to the Adirondack (Fakhraei et al., 2014; Zhai et al., 2008) and Catskill regions (Chen & Driscoll, 2004) of New York, northern New England (Chen & Driscoll, 2005a), and the southern Appalachian Mountain region (Fakhraei et al., 2016). The model has been used to project the response of acid-sensitive forest ecosystems to future controls on atmospheric S and N emissions at the HBEF, the Adirondacks, northern New England and the Great Smoky Mountains (Chen & Driscoll, 2005b;

Driscoll et al., 2016; Fakhraei et al., 2014; Gbondo-Tugbawa & Driscoll, 2003; Wu & Driscoll, 2009; Zhou et al., 2015).

Biogeochemical models have also been used to provide comprehensive approaches to investigate how future changes in climate are likely to interact with other drivers such as atmospheric deposition, increasing atmospheric CO_2 concentrations, and land disturbance in forest watersheds over broad regions. Modeling efforts have been applied to the forest ecosystem to assess impacts of climate change and other drivers (Ollinger et al., 1993; Campbell et al., 2009; Pourmokhtarian et al., 2012, 2017; Robison & Scanlon, 2018; Dong, et al., 2019a; Dong, et al., 2019b) . PnET-BGC has proven to be an effective tool to assess the effects of climate change on hydrology and the cycles and fluxes of elements across multiple watershed sites. The model has been used to evaluate the dynamics of water, carbon, and nitrogen under future climate change at the H. J. Andrews Experimental Forest in the Pacific Northwest, and Niwot Ridge and Loch Vale Watershed in the southern Rocky Mountains (Dong et al., 2019a; Dong et al., 2019b). Pourmokhtarian et al. (2012, 2017) used PnET-BGC to simulate ecohydrological responses to climate change for the forest watersheds in the northeastern United States. The biogeochemical interaction between the effects of climate and acidic deposition for forest watershed in Shenandoah National Park, Virginia was investigated using PnET-BGC model (Robison & Scanlon, 2018).

2.4 Sensitivity and uncertainty

Models are the primary tool scientists and engineers use to estimate the interactive effects of multiple disturbances on ecosystems and project past and future response to environmental change. In ecological studies, models provide representations of complex systems through

mathematical expressions of important processes. Model outputs are based on model structure, meteorological, hydrological, other time-series inputs and the time step used in the model, and a host of parameters that describe the system being simulated. Even if these assumptions and input data are representative of conditions believed to be correct, they will be inaccurate. Models are always simplifications of the real systems. Furthermore, the future cannot be forecasted with precision, so the model outputs of future conditions are at best uncertain. In short, uncertainty in model simulation is inevitable. Uncertainty can be introduced via insufficient and/or inaccurate model inputs and limitations in the underlying assumptions, formulation, and structure of the model (Morris, 1991). Both single-parameter (local) analysis and multi-dimensional parameter (global) techniques can help to identify sensitivity and uncertainty in models.

Local sensitivity analysis methods are usually focused on determining the behavior of the model around some local points (Saltelli et al., 2009). Local sensitivity analysis methods work well for models that are linear but fail to detect any discontinuities or non-linear relationships between model parameters and are usually also computationally costly. The most commonly used local sensitivity methods are screening design or “One-at-A-Time” (OAT) techniques and differential analysis (DA) techniques (Saltelli et al., 2009). OAT is performed by varying one factor at a time while all the other factors are held constant at their nominal values. OAT produces some benefits but is limited to models which are inexpensive computationally and have a small number of variables. Moreover, this method is only helpful in determining first-order effects (Iman et al., 1981; Lilburne et al., 2006). DA involves calculating the derivative of a function about some chosen point of interest which is then used as a measure of the sensitivity.

Global sensitivity analysis methods are used in many applications in engineering and biological sciences and are becoming increasingly popular. Global sensitivity analysis methods

explore the entire parameter space of each variable and all the parameters are varied simultaneously (Saltelli et al., 2009). The basic approach behind Global sensitivity analysis is to vary all variables simultaneously and compute the variance of the output. The relative sensitivity of an input variable is determined by fixing a particular variable and determining the decrease in the output variance. Usually, the larger the decrease in output, the more sensitive the output is to the input variable. The Sobol's method and Fourier Amplitude Sensitivity Test (FAST) method are two variance based global sensitivity analysis methods that have been widely applied (Schwieger, 2004). Sobol's method is used to calculate global sensitivity indices of the input parameters for nonlinear models that are defined either by analytical methods or by a simulation model (Sobol, 2001). The basis of Sobol's method is the decomposition of variance of the model output function into a sum of variances in combinations of input parameters in increasing dimensionality (Zhang & Rundell, 2006). The basic feature of FAST is that the multidimensional space of the input factors is explored by a suitably defined search curve (Saltelli et al., 1999). FAST sensitivity analysis proceeds by relating the probability distribution of each parameter to a frequency (Cukier et al., 1978).

Uncertainty analysis is also classified as local or global. Local uncertainty of a multi-variable function which is either analytic or experimental is determined by first calculating the partial derivatives of the function and using these partial derivatives as magnification factors with the uncertainty in the input parameter to determine the uncertainty of the output (Saltelli et al., 2009). The global uncertainty analysis gives an overall perspective of output uncertainty by determining the key indicators of uncertainty: the output distribution function, including expected values and variance.

The Monte Carlo analyses selects a random set of input data values drawn from their individual probability distributions. These values are then used in the model to obtain values of model output variables. This process is repeated many times (usually more than 100 times). The result is a probability distribution of model output variables and system performance indices that results from variations and possible values of all the input values. One major limitation of applying Monte Carlo methods to estimate the uncertainty for model output variables is the computing power required. Therefore, a sampling method is applied to the Monte Carlo method to reduce the time needed to perform sensitivity analyses. The most widely used sampling scheme is Latin Hypercube Sampling (LHS) (McKay et al., 1979). LHS typically requires less samples and converges faster than Simple Random Sampling (SRS) methods when used in uncertainty analysis. By representing each variable as its Cumulative Distribution Function (CDF) (prior distribution) and partitioning the CDF into n regions and taking a single sample from each region, this approach increases the likelihood that the full range of the posterior distribution is sampled.

Chapter 3. The response of stream ecosystems in the Adirondack region of New York to historical and future changes in atmospheric deposition of sulfur and nitrogen

3.1 Methods

3.1.1 Study sites

The Adirondack region is a 2.4 million ha forested area with about 2800 lakes (>2000 m^2 surface area) and a dense network of streams (Driscoll et al., 1991). The region has historically received high rates of acid deposition, with a spatial pattern of decreasing deposition from the southwest to northeast (Ito et al., 2002) (Figure 3-1). Bedrock geology is composed primarily of gneisses and metasedimentary rocks. Soils are largely Spodosols derived from glacial till. There are pockets of carbonate minerals and calcium rich feldspars in the central and eastern Adirondacks (Driscoll et al. 1991). The climate is characterized by cool summers and cold winters, with mean temperature of 18 ^{o}C in July and -10 ^{o}C in January. The annual mean precipitation is 110 cm for the period from 1980 to 2016 (range 76 to 154 cm) (http://nadp.slh.wisc.edu/; accessed January 15, 2016). The growing season extends from late May to early September. Maximal seasonal snow depths typically range from 0.5 to 1.5 m. Snowmelt typically occurs in late March or early April, resulting in elevated stream flow (Lawrence et al., 2004). Dominant vegetation is northern hardwood forest, consisting largely of yellow birch (*Betula alleghaniensis* Britton), American beech (*Fagus grandifolia* Ehrh.) and sugar maple (*Acer saccharum* Marsh). The region also has about 10% cover by coniferous trees, including red spruce (*Picea rubens*), balsam fir (*Abies balsamea* L. Mill.) and eastern hemlock

(*Tsuga canadensis*). Many forests in the region have undergone historical cutting, and/or experienced blow-down, fire, and various pests (Driscoll et al., 1991).

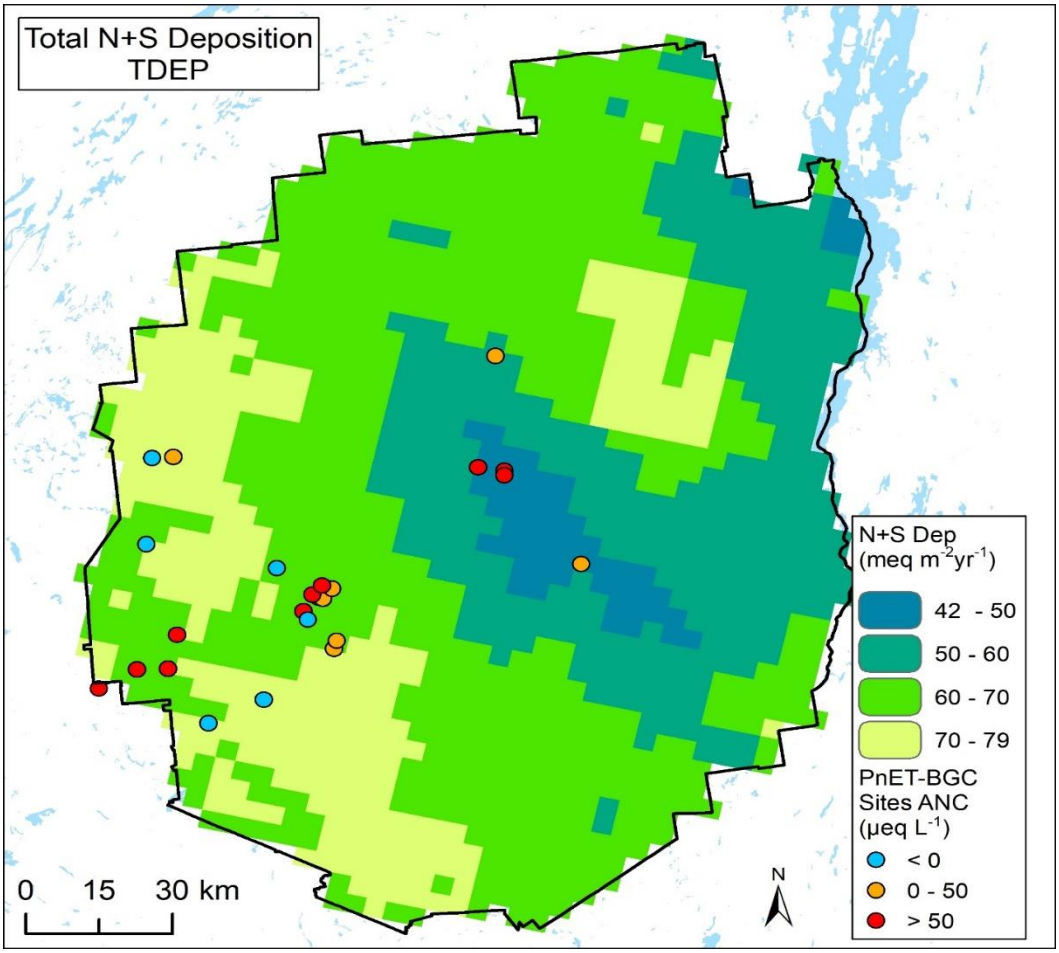

Figure 3-1. Estimated total S+N deposition for 2015 and location of the 25 Adirondack streams to which PnET-BGC was applied in this study. The deposition data were developed from TDep Version 2016.01. Values are an average of years 2014 and 2015. (http://nadp.slh.wisc.edu/committees/tdep/tdepmaps/. Accessed May 11, 2017)

3.1.2 Stream and soil data

Within this landscape, a suite of small watersheds containing first or second order streams, mostly in the western portion of the Adirondack region, were selected for site-specific biogeochemical modeling from among those that had suitable data for required model inputs

(Table A-1). The streams draining the 25 watersheds encompass a wide range of pH, ANC, and concentrations of Al_i. Monthly, or more frequent stream water chemistry data were available for Archer Creek from 1996-2015, Buck Creek from 2001-2015 (ANC and pH records extended from 1991-2015), tributaries of Buck Creek from 1998 to 2015, and watershed T24 at Honnedaga Lake from 2011 to 2015 (U.S. Geological Survey, 2019). For the remainder of the stream sites, water chemistry data were available from the Western Adirondack Stream Survey (WASS) (collected 2004-05) or the Adirondack Sugar Maple Project (ASMP) (collected in 2009-2011) (Lawrence et al., 2018; U.S. Geological Survey, 2019). Among the 25 streams studied, seven had ANC values less than 0 µeq L^{-1}, eight had ANC values between 0 and 50 µeq L^{-1}, and 10 had ANC greater than 50 µeq L^{-1} based on sampling during the high flow spring period (Figure 3-1). Soil chemical data were collected in each of the watersheds through multiple sampling programs. Sampling designs, field and laboratory methods, horizon descriptions and chemical measurements can be accessed in Lawrence et al. (2017) at https:// doi.org/10.5066/F78050TR except for soil chemistry data from T24. Soil chemical parameters used in modeling at T24 were: exchangeable Ca^{2+} = 0.23 $cmol_c$ kg^{-1}, exchangeable Mg^{2+} = 0.06 $cmol_c$ kg^{-1}, exchangeable Na^+ = 0.02 $cmol_c$ kg^{-1}, exchangeable K^+ = 0.06 $cmol_c$ kg^{-1}, exchangeable Al^{3+} = 5.01 $cmol_c$ kg^{-1}, exchangeable H^+ = 1.06 $cmol_c$ kg^{-1}, and pH = 4.19.

3.1.3 Atmospheric deposition and meteorology

The Huntington Forest (HF) in the central Adirondacks (43º 58’ N, 74º 13’ W) was used as a benchmark to estimate wet deposition to the watersheds of the study streams. Wet deposition of the major solutes (Na^+, Mg^{2+}, K^+, Ca^{2+}, Cl^-, NO_3^-, SO_4^{2-}, and NH_4^+) to the HF over the period 1978–2015 were obtained from the National Atmospheric Deposition Program (NADP;

http://nadp.slh.wisc.edu/data/sites/siteDetails.aspx? net=NTN&id=NY20, accessed March 10, 2016). Estimates of wet deposition for the simulation period for which measurements of wet deposition were not available (1900-1978) were developed from linear regression of measured concentrations of wet deposition at HF (NADP: NY20) with national emissions (https://www.epa.gov/air-emissions-inventories/air-pollutant-emissions-trends-data, accessed January 15, 2016) using observations for the years 1979-2015 (Table A-2). To extrapolate wet deposition data at the HF to other Adirondack stream sites modeled in this study, I assumed that the time series of wet deposition for the regional sites was proportional to values observed and recreated for HF. The spatial models developed by Fakhraei et al. (2014), based on wet deposition data from NADP (http://nadp.sws.uiuc.edu/, accessed January 13, 2016) and national emissions data (Nizich et al., 2000) were used to extrapolate the historical wet deposition time series to all other modeled stream sites. Estimates of pre-industrial (~1850) deposition were estimated from measurements obtained from remote sites (SO_4^{2-} : 6.2 µeq L^{-1}, NO_3^- : 2.3 µeq L^{-1}) (Galloway et al., 1984).

Dry deposition inputs of S and oxidized N for PnET-BGC were based on estimates of dry to wet deposition ratios, taken from the regional regression model developed by Ollinger et al. (1993) and modified by Chen and Driscoll (2004) to incorporate effects of forest composition. The forest composition for each study watershed was determined through a GIS data layer obtained from the National Land Cover Database (http://www.mrlc.gov/nlcd06_data.Php, accessed March 10, 2016). The dry to wet deposition ratios for base cations (Ca^{2+}, Mg^{2+}, Na^+, K^+), ammonium (NH_4^+) and chloride (Cl^-) were derived from throughfall measurements at the HF (Shepard et al. 1989). Since temporal and spatial patterns were not observed in dry to wet ratios of base cations, NH_4^+, and Cl^- among CASTNET (U.S. EPA Clean Air Status and Trends

Network) and nearby NADP deposition monitoring sites in the northeastern US, dry-to-wet deposition ratios for these analytes were assumed to be constant at each site throughout the simulation period.

Air temperature, precipitation, and photosynthetically active radiation (PAR) were derived from measurements taken at the HF from 1940 to 2015 (State University of New York, College of Environmental Science and Forestry; http://www.esf.edu/hss/em/huntington/ackerman.html, accessed January 13, 2016). For the years between 1895 and 1939, monthly data from the PRISM model (http://www.prism.oregonstate.edu/, accessed January 13, 2016) were used to reconstruct historical estimates of maximum and minimum temperature and precipitation. Average values for the period 1895-1939 were used to represent historical meteorological data for the HF.

To extrapolate meteorological data from the HF to other sites, I applied the spatial models developed by Fakhraei et al. (2014) using data from the National Climatic Data Center (NCDC; https://www.ncdc.noaa.gov/cdo-web/, accessed January 13, 2016). Solar radiation at other stream sites was scaled from the HF, using the ratios derived from the regression models developed by Aber and Freuder (2000)

3.1.4 Model applications

3.1.4.1 PnET-BGC model formulation

Watershed response to changing levels of acid deposition and TLs were simulated using PnET-BGC, an integrated forest vegetation-soil-water biogeochemical model that has been widely used to assess the effects of air pollution, climate change and land disturbance on forest

and aquatic ecosystems (Gbondo-Tugbawa et al. 2001, Pourmokhtarian et al. 2017, Valipour et al. 2018). This model was formulated by linking two sub-models: PnET- CN (Aber et al., 1997) and BGC (Gbondo-Tugbawa et al. 2001). The biogeochemical processes in the model include tree photosynthesis, growth and productivity, litter production and decay, mineralization of soil organic matter and associated elements, immobilization of N, nitrification, interactions of major elements with vegetation and organic matter, abiotic soil processes, solution speciation, and surface water processes (Gbondo-Tugbawa et al. 2001). The model nominally operates on a monthly time step and is generally applied at the small watershed scale. The Gaines–Thomas formulation is applied to describe cation exchange reactions within the soil. The exchangeable cations considered in the model include Ca^{2+}, Mg^{2+}, Na^{+}, H^{+}, Al^{3+}, K^{+} and NH_4^{+}. pH-dependent isotherms are used to describe SO_4^{2-} and dissolved organic matter (organic acids) adsorption. Organic acids are described using a triprotic analogue (Org^{3-}; Driscoll et al. 1994) and the total amount of organic acid is estimated as a fraction of DOC concentration (Fakhraei and Driscoll 2015). PnET-BGC simulates ANC as an analog to measured ANC by Gran plot analysis (Gran, 1952) by considering the contributions of dissolved inorganic carbon (DIC), organic anions, and Al complexes (Driscoll et al. 1994, Fakhraei and Driscoll 2015). PnET-BGC includes a CO_2 uptake algorithm that considers the effects of increases in atmospheric CO_2 concentration on forest ecosystem processes (Pourmokhtarian et al. 2012). The hydrologic algorithms used in PnET-BGC were summarized by Aber and Federer (1992) and Chen and Driscoll (2005b). More detailed descriptions of the model, including the results of an uncertainty analysis of parameter values, are available in Gbondo-Tugbawa et al. (2001), Pourmokhtarian et al. (2017), and Fakhraei et al. (2016).

PnET-BGC has been tested with vegetation, soil and water biogeochemistry data from the Hubbard Brook Experimental Forest (HBEF) in New Hampshire (Gbondo-Tugbawa et al. 2001) and then extended successfully to watersheds in the Adirondack (Fakhraei et al. 2014, Zhai et al. 2008) and Catskill regions (Chen and Driscoll 2004) of New York, northern New England (Chen and Driscoll 2005a), and the southern Appalachian Mountain region (Fakhraei et al. 2016). The model has been used to project the response of acid-sensitive forest ecosystems to future controls on atmospheric S and N emissions at the HBEF, the Adirondacks, northern New England and the Great Smoky Mountains (Chen and Driscoll 2005a, Fakhraei et al. 2014, Fakhraei et al. 2016, Gbondo-Tugbawa and Driscoll 2003, Wu and Driscoll 2009, Zhou et al. 2015).

3.1.4.2 Model scenarios

Monthly values of atmospheric deposition of all major elements and meteorological data (precipitation, minimum and maximum temperature, solar radiation) were input over the entire simulation period. Forest vegetation type, and soil physical and chemical characteristics were assumed to be constant over time. Known major land disturbance events, including forest cutting and climatic events, were considered in the year they occurred in model simulations (McMartin, 1994). Soil and stream chemistry and stream flow data were used for chemical and hydrological calibration of the model. Weathering rates for major base cations and other soil parameters (e.g., soil SO_4^{2-} and DOC adsorption capacity) in this study were obtained through model calibration by adjusting input parameters until predicted surface water chemistry outputs matched observed values (Table A-3).

Simulations were initiated in the year 1000 under constant pre-industrial meteorology and deposition and no land disturbance, allowing for a spin-up period to achieve steady state (e.g.,

net ecosystem production [NEP] of the simulated forested watershed remains close to zero; Fakhraei et al. 2014) before anthropogenic deposition and land disturbances were applied in the model after 1850. The model was run from 1850 to 2015 based on reconstructed and measured deposition and meteorology data discussed above and information on site forest disturbance, using the vegetation, soil and hydrologic parameters to assess impacts on soil and stream chemistry caused by past and ambient acid deposition. The model simulations of stream chemistry and soil exchangeable cation concentrations were compared with measured values over the recent period to evaluate model performance. Model simulations continued with an implementation year starting in 2015, with a two-step change in deposition. The first step involved ramping deposition changes to target values by 2020. In the second step, deposition from the carbon dioxide management scenario was ramped down incrementally to 2030 over a range of percent reductions with the lowest scenario being estimated pre-industrial deposition. Simulations were continued through the year 2200, considering several future deposition control scenarios (for SO_4^{2-}, NO_3^- and NH_4^+ individually and in combination) (Figure 3-2) (Table 3-1). These included: a "business-as-usual" scenario that held ambient deposition constant until the end of the simulation period; a "possible future" scenario that linearly ramped deposition from ambient values down to levels projected under a proposed carbon dioxide control program (Keyes et al., 2019) and then held values constant; and a suite of "additional reduction" scenarios that linearly decreased deposition from the "possible future"(2020) level to the pre-industrial deposition level (1850) at intervals of 25% decreases; and an "increasing deposition" scenario in which deposition increased 15% from ambient levels to 2020 and then was held constant.

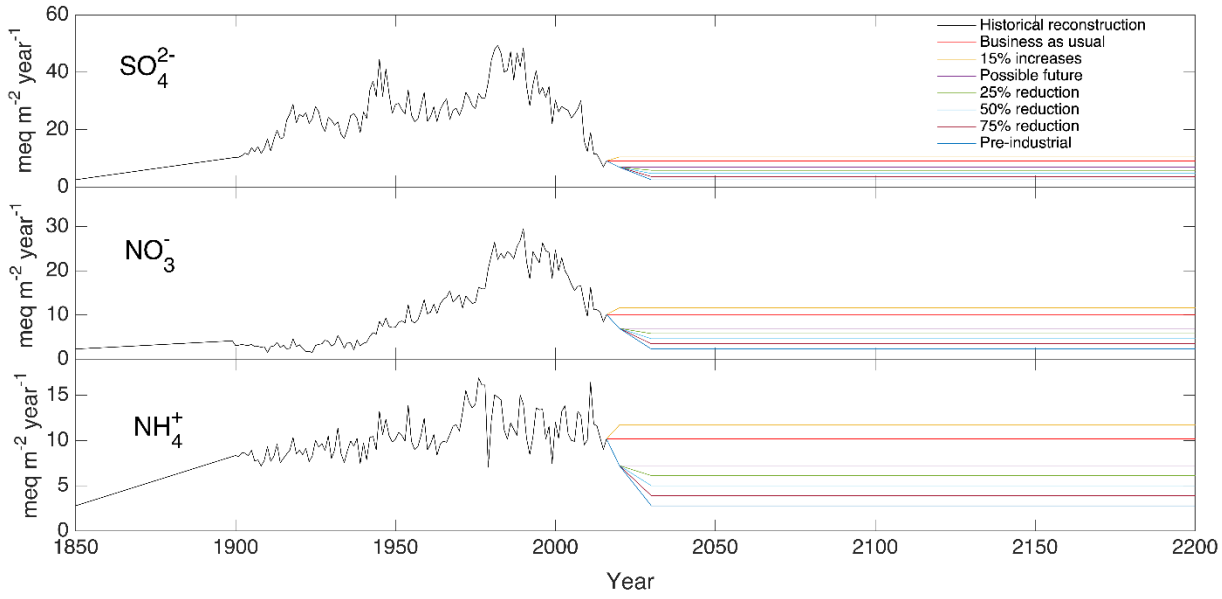

Figure 3-2. Reconstructions of wet atmospheric deposition of SO_4^{2-}, NO_3^- and NH_4^+ at Huntington Forest in the Adirondacks for the period 1850-2200. [Future projections (present-2200) are shown under the "business as usual" scenario, the "possible future" scenario, a 15% increase scenario, and four reductions applied to the "possible future" scenario, including a 100% reduction in anthropogenic emissions (return to preindustrial levels).]

To determine and evaluate the most effective approach to achieve further recovery of Adirondack stream ANC, the scenarios were applied to the model projections of ambient stream ANC as 1) decreases in atmospheric deposition of SO_4^{2-} alone; 2) equal decreases in SO_4^{2-} and NO_3^- deposition; and 3) equal percentage decreases in deposition of SO_4^{2-}, NO_3^-, and NH_4^+ simultaneously. ANC response curves were developed for the two specified endpoint years (2050 and 2150) for use in the TL analyses. These ANC response curves were obtained using the model simulated stream ANC under the different future deposition scenarios (Table 3-1).

Table 3-1. Model scenarios for changing SO_4^{2-}, NO_3^-, and NH_4^+ deposition in the future.

Scenario Number	Description
1	Business as usual (average of 2013-2015)
2	Possible deposition future (associated with carbon dioxide emission control policy for electric utilities)
3	Additional deposition reduction 25%
4	Additional deposition reduction 50%
5	Additional deposition reduction 75%
6	Additional deposition reduction 100%
7	Increased deposition 15%

I used two types of ANC criteria as goals for recovery in the TLs analysis: a fixed ANC criterion and a second based on the model-simulated site-specific ANC at each modeled site (Table 3-2). A fixed value of 20 µeq L^{-1} ANC was selected to represent likely protection of brook trout health against elevated concentrations of Al_i (U.S.EPA, 2009, Baldigo et al. 2007, 2019a). However, note simulations suggest that Adirondack streams had pre-industrial ANC values as low as 10 µeq L^{-1} (see Results). Some of these streams may have had pre-industrial ANC above 20 µeq L^{-1}, yet from model simulations are unable to recover to this level even if acid deposition from anthropogenic emissions is eliminated in the future, suggesting that some of the impact may be irreversible. Thus, benchmarks based on model-simulated pre-industrial ANCs as criteria for recovery may be more appropriate than a fixed ANC benchmark as a basis for establishing recovery goals. However, in our forecast simulations, 20 of 25 sites did not achieve their pre-industrial ANC by 2150 even under the most aggressive emissions reduction scenarios (100% reduction in SO_4^{2-}, NO_3^-, and NH_4^+ deposition). Because of this limitation in the maximum achievable chemical recovery, I used an ANC value that was 20 µeq L^{-1} less than the

simulated pre-industrial ANC as the site-specific target in TL analyses. This reflects recovery to within 20 µeq L^{-1} of the pre-industrial value at a given site.

Table 3-2. Target loads of SO_4^{2-} + NO_3^- + NH_4^+ deposition to reach ANC targets by 2050 and 2150 based upon PnET-BGC model simulations for each of the 25 Adirondack study streams.

Sites	*Preindustrial ANC (µeq L^{-1})*	*Measured ANC (µeq L^{-1})*	*Ambient Deposition (2015) (meq m^{-2} yr^{-1})*	*TL to Reach ANC Criterion of 20 µeq L^{-1} (meq m^{-2} yr^{-1})*		*TL to Reach Site Specific ANC Criterion (meq m^{-2} yr^{-1})*	
				2050	2150	2050	2150
North Buck	22.8	-38.3	39.9	NA[a]	NA	NA	NA
35014	10.1	-35.2	47.3	NA	NA	NA	NA
27026	25.5	-27.1	41.4	NA	NA	NA	NA
T24	28.7	-25.3	40.3	NA	NA	NA	NA
22019	23.4	-16.2	47.7	NA	NA	NA	18.1
12003	28.2	-6.4	46.1	NA	8.8	22.6	34.6
WF	25.9	-3.7	41.4	NA	NA	21.1	36.5
South Buck	53.2	3.6	41.1	13.5	33.7	NA	NA
13008	38.4	3.8	44.2	12.4	19.4	19.0	29.2
24002	37.3	4.2	41.1	4.5	21.8	10.3	28.7
28011	52.6	8.2	42.2	31.2	45.6	NA	32.1
28014	51.8	11.8	39.9	28.6	34.7	15.2	27.1
NW	56.5	12.4	39.9	45.1	53.0	14.4	31.1
Buck Creek	56.3	14.7	42.6	45.6	55.4	NA	33.2
AMP	93.1	42.1	37.5	49.2	62.3	NA	33.4
27019	160.6	95.7	41.8	WB[b]	WB	NA	NA
Archer	148.8	113.0	39.1	WB	WB	29.3	35.2
30009	155.8	116.5	48.1	WB	WB	33.7	42.5
26008	163.2	119.3	42.6	WB	WB	17.5	29.8
30019	163.8	119.8	50.0	WB	WB	31.1	42.2
29012	218.3	164.1	52.8	WB	WB	WB	WB
28030	271.6	219.3	42.6	WB	WB	WB	34.8
N1	285.1	238.0	37.5	WB	WB	39.8	45.2
24001	336.8	262.2	42.6	WB	WB	8.8	46.9
S14	894.1	619.4	36.4	WB	WB	WB	WB

[a] N/A indicates that there is no applicable TL because past base cation depletion is not sufficiently reversible in the model to achieve recovery to preindustrial conditions.

[b] WB indicates that the TL is not a useful statistic because the site is so well buffered.

3.1.5 Estimating Discharge and Adjusting ANC Values

Discharge measurements were not available for most sites to accompany stream chemistry samples and fish collections described in this chapter. Therefore, discharge was estimated for each stream sample and each fish collection by relating the discharge to one of six nearby gauges maintained by the U.S. Geological Survey (USGS) in the region (Table A-1). Flow percentiles were calculated at each gauge based on daily mean discharge values for water years 2003 through 2015, representing the full range of time that included all field data analyzed in this investigation. The gauge closest to each stream site was selected to represent the flow percentile at the ungauged stream location, which in most instances was within 35 km of a sampled stream site. At stream sites represented by Buck Creek (04253296), the flow percentile for the date of collection was assigned to each sample. Because the other five stream gauges used in this analysis have watersheds with drainage areas that ranged from two to three orders of magnitude larger than Buck Creek and the sampled streams, the flow percentile on the day following collection was assigned to each of these samples. This estimate of a 1-day lag at the larger streams was tested and confirmed by exploring correlations between daily mean discharge at Buck Creek with those of each of the five gauges at lags of 0, 1, 2, 3, and 4 days. The one-day lag consistently yielded correlation coefficients that were an average of 0.07 greater than those without a lag.

Prior to performing analyses of the relation between ANC and discharge among samples collected at a given stream, data from some of the sites and samples collected were excluded for the following reasons. First, any stream site which had an ANC greater than 400 μeq L^{-1} for any sample collected was not included because such streams are considered insensitive to both

chronic and episodic acidification and are highly likely to maintain an ANC of greater than 100 μeq L^{-1}, even during the highest flow conditions. Second, any sample at a given stream for which the discharge difference (ΔQ) among any two samples was less than 10% were eliminated based on the assumption that differences of less than this amount could not be reliably estimated at an ungauged site. Finally, stream sites where ANC at low flow (ANC_{max}) was based on a discharge percentile ($Q_{percent}$) value greater than 50% were not considered because these data were not consistent with the goal of representing low-flow ANC values for the stream.

The extent of episodic acidification was defined as the magnitude of the decrease in ANC as a function of the increase in stream discharge relative to the sample with the lowest discharge at each site:

$$\Delta ANC/\Delta Q = (ANC_i - ANC_{max})/(Q_i - Q_{min}) \quad (3\text{-}3)$$

where ANC_i is the value for a given sample, ANC_{max} is the value at the lowest discharge among the samples collected at a given site, Q_i is the discharge for each sample, and Q_{min} is the discharge for the sample represents ANC_{max} at each site.

A $Q_{percent}$ value was assigned to each of the stream samples and fish collections that were used to calculate representative ANC values that were then applied in PnET-BGC model simulations at each of the 25 stream sites. The $Q_{percent}$ values were averaged among the samples and fish collections used to calculate each representative ANC calibration value. The mean $Q_{percent}$ among the dates of fish collections was 27%, the value applied using equation (3-3) to adjust ANC values to simulate fish community responses to future deposition scenarios.

3.1.6 ANC and fish metrics

The chemical indicator ANC was used to illustrate how acidification currently affects local fish assemblages; predict how historical deposition loads of S and N (and acidification) likely affected fish assemblages in ~1850; and how different TLs will likely affect these assemblages (biological recovery) in the future. Nonlinear empirical relationships between fish metrics and ANC were developed by Baldigo et al. (2019b) using fish-community surveys conducted in 47 streams in the western Adirondack region under summer base flow conditions during 2014, 2015, and 2016:

$$\text{Fish density} = -0.0033ANC^2 + 2.75ANC + 113.5 \quad (3\text{-}1)$$

$$\text{Fish biomass} = 9 \times 10^{-10}ANC^5 - 10^{-6}ANC^4 + 0.0006ANC^3 - 0.15ANC^2 - 0.0033ANC^2 + 20.9ANC + 616 \quad (3\text{-}2)$$

The units for ANC are µeq L^{-1}, fish density are number of fish per 0.1 ha and the units for fish biomass are grams per 0.1 ha. Observations for these relationships were obtained during summer flow condition; however, the modeled simulated stream chemistry is a volume-weighted annual average. Therefore, I applied an approach in which an empirically-calculated flow percentile based on the period Oct. 2001 to Sept. 2015 from a nearby stream gauge was assigned to each sample collected and relationships were developed between ANC and flow percentile as described in Table A-1 and associated text to provide flow-adjusted ANC values. These equations were used to depict the responses of fish to future deposition scenarios by adjusting ANC to estimated values at the 27th percentile of daily mean flow based on the mean among days when fish samples were collected (Table A-4).

3.1.7 Model testing

Two statistical criteria were used to assess model performance: normalized mean error (NME) and normalized mean absolute error (NMAE; Janssen & Heuberger, 1995). The NME provides a comparison of model-simulated values to observed values on an average basis. A negative value of NME indicates underestimation and a positive value indicates overestimation by model simulation. The NMAE indicates the absolute discrepancy between model predictions and observations. The NMAE is used to evaluate the performance of the model in capturing measured trends. An NMAE value of zero is considered optimal and indicates full agreement between model simulation and observed data. NME and NMAE are defined as:

$$NME = \frac{\bar{s}-\bar{o}}{\bar{o}} \tag{3-4}$$

$$NMAE = \frac{\sum_{t=1}^{n}(\lceil s_t - o_t \rceil)}{n\bar{o}} \tag{3-5}$$

where $\bar{s}$ and $\bar{o}$ are the average of model-simulated values and observed values, s_t is the model-simulated value at time t, o_t is the observed value at time t, and n is the number of observations.

3.2 Results and discussion

3.2.1 Model evaluation

Model performance varied among sites and stream solutes, partly due to differences in stream water sampling intensity and length of record (Figure 3-3, Table A-5). The best model performance was evident for Archer Creek, Buck Creek and the tributaries of Buck Creek, attributable to the relatively long records of observations at these sites, whereas other stream sites had relatively few observations that were largely collected during spring high flow conditions.

Overall, there was good agreement between model-simulated and measured stream discharge and ambient chemistry of soil and stream waters of the Adirondack watersheds. The model-simulated annual stream discharge (652 ± 133 mm) for Archer Creek was close to the measured value (705 ± 135 mm; NME = -0.07, NMAE = 0.10). Mean NME and NMAE values indicated good agreement between measured and model-simulated SO_4^{2-} across all sites (NME = 0.04 ± 0.05; NMAE = 0.08 ± 0.05; Table A-5). Simulated stream Ca^{2+} and ANC agreed well with observations, except for one high ANC site (S14). Lower ANC sites (< 100 μeq L^{-1}), which were the major focus of this study, showed good agreement between measured and modeled stream Ca^{2+} and ANC (Ca^{2+}: NME = -0.02± 0.03 and NMAE = 0.06 ± 0.05; ANC: NME = -0.08 ± 0.11 and NMAE = 0.13 ± 0.06). The simulated DOC concentrations also agreed well with measured data at lower concentrations (<600 μmol C L^{-1}), but somewhat underestimated DOC at higher values. Modeled stream NO_3^- showed relatively large discrepancies with observed values in comparison to other stream chemical variables (Figure 3-3, Table A-5). These relatively large discrepancies can be attributed to the relatively simple representation of the complex N cycle of

forested watersheds depicted by PnET-BGC (e.g., assumption of low denitrification loss) and/or the challenges in characterizing historical land disturbances and meteorological conditions in model simulations. Furthermore, the limited number of samples collected from some streams likely do not represent annual volume weighted NO_3^- concentrations. Model-simulated soil % base saturation (BS) generally agreed with the measured values (NME = -0.26 ± 0.15), especially for BS < 25% (Figure 3-3).

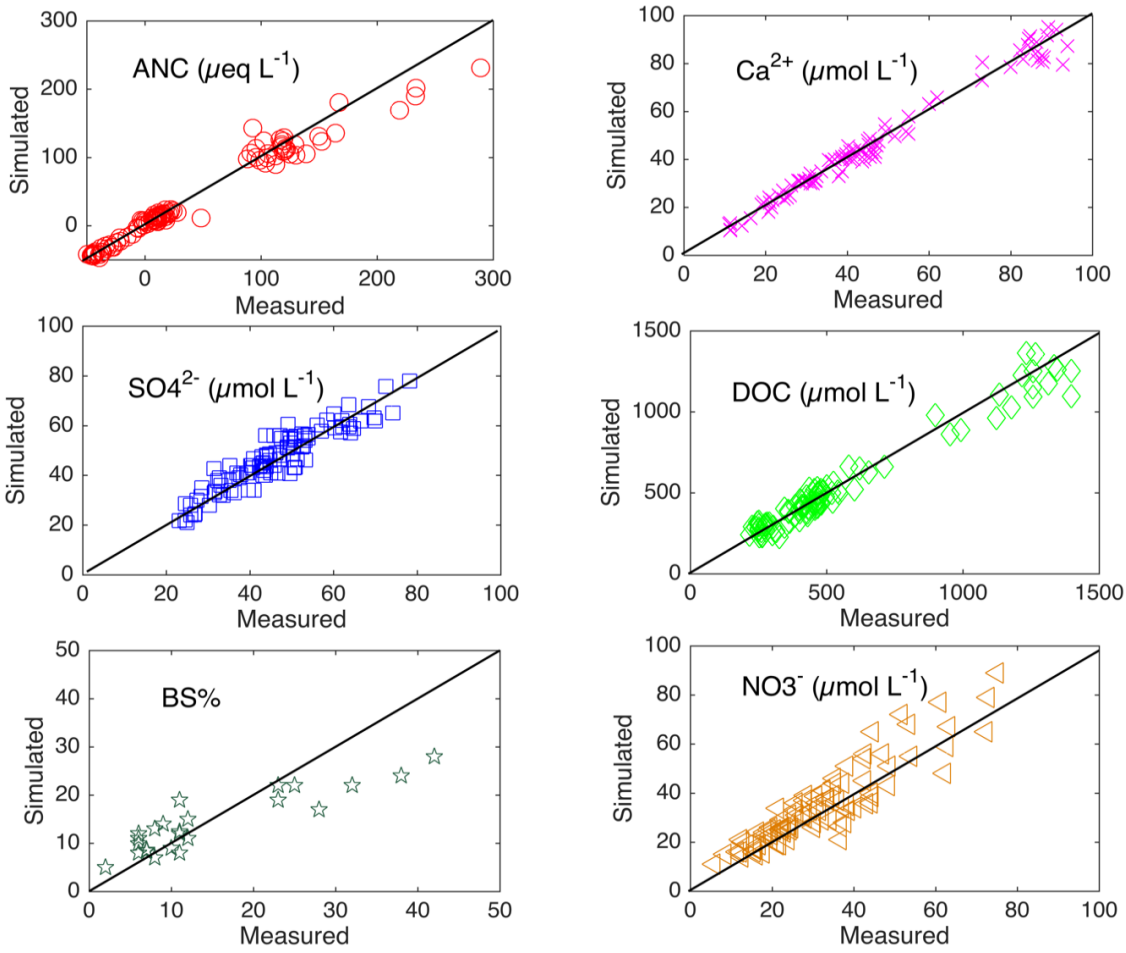

Figure 3-3. Comparison of model-simulated and observed stream chemistry (ANC, Ca^{2+}, SO_4^{2-}, DOC and NO_3^-) and soil base saturation for 24 modeled streams (the high ANC site S14 is not included due to high ANC values). The measured values are represented as mean annual values for years having available data. The solid black lines are the 1:1 line of model simulated values and measured values.

3.2.2 Historical acidification and recovery

Model simulations were conducted to examine time series of annual volume-weighted concentrations of stream chemistry and soil % BS from 1850 to 2200 for the 25 model sites (Figure 3-4). The model hindcast scenarios suggest that stream SO_4^{2-} concentrations were historically low (mean+ std. dev; 12 ± 5 µmol L^{-1}) during the pre-industrial period (1850), increasing to maximum concentrations of 62 ± 21 µmol L^{-1} by approximately 1980 and then

decreasing to ambient concentrations in 2015 (at 35 ± 11 µmol L^{-1}). These patterns coincide with increases in atmospheric S deposition at the start of the Industrial Revolution, followed by decreases in atmospheric deposition associated with controls on SO_2 emissions from the Clean Air Act and associated rules (Figures 3-2, 3-4). Simulated stream SO_4^{2-} concentrations remained relatively high in 2015, about three-fold higher than projected pre-industrial levels. The magnitude of the simulated stream SO_4^{2-} response to decreases in atmospheric S deposition varied among study sites (Figure 3-4). This variability can be explained by differences among sites due to atmospheric deposition, elevation, climate, vegetation, soils, land cover, and model-calibrated soil SO_4^{2-} adsorption capacity.

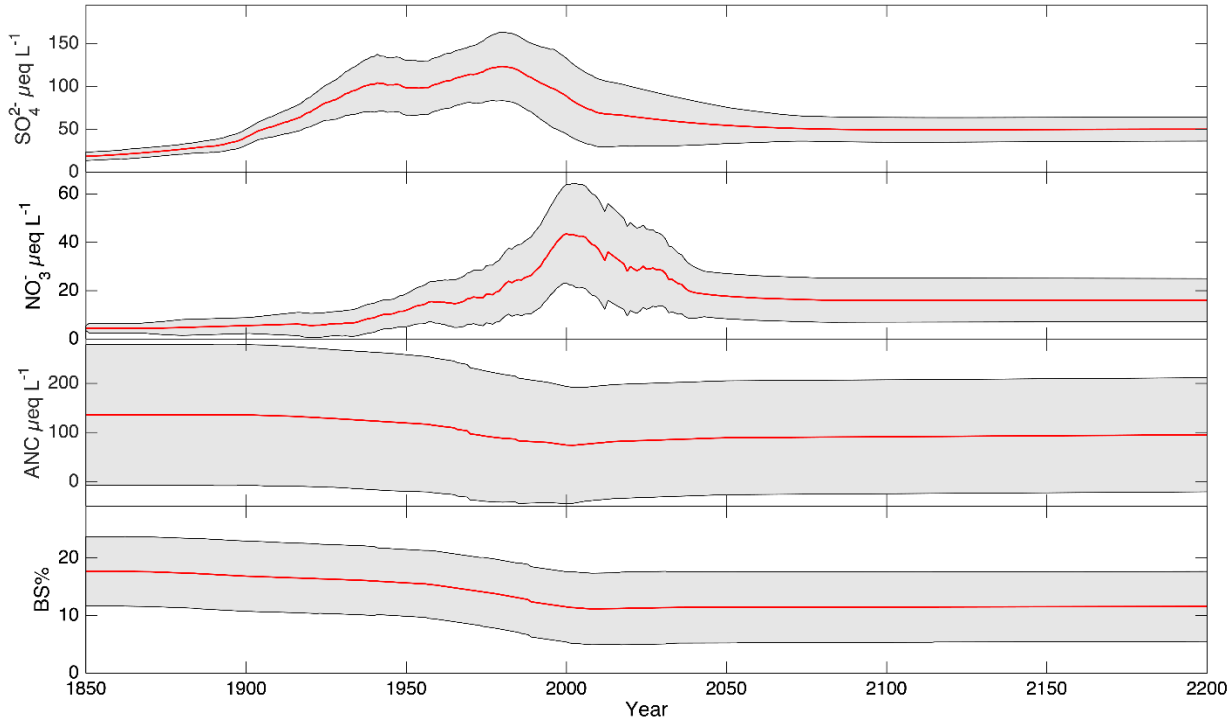

Figure 3-4. Mean (± standard deviation) of model-predicted selected stream chemistry (SO_4^{2-}, NO_3^- and ANC) and soil base saturation (BS) for the 25 simulated Adirondack streams during the period 1850–2200. [Future projections are shown for the "business-as-usual" scenario.]

Simulated long-term patterns of stream NO_3^- contrasted with those of SO_4^{2-}. The model-simulated pre-industrial NO_3^- concentrations were low for all 25 streams (2.1 ± 0.6 μmol L^{-1}) and did not show significant increasing trends until the 1930s. The hindcast concentrations of NO_3^- increased after the 1930s and peaked in the early 2000s at 43 ± 21 μmol L^{-1}. These long-term increases in stream NO_3^- can be attributed to increases in NO_X emissions and deposition coupled with decreases in forest demand for N with increasing stand age and the effects of disturbance associated with the blowdown events and salvage logging in the 1950s and 1960s in the Adirondacks. Consistent with decreases in NO_3^- deposition resulting from implementation of the CAA and subsequent rules (e.g., the NO_x Budget Trading Program, Cross State Air Pollution Rule), decreases in stream NO_3^- concentration started around the 2000s. However, the mean value of stream NO_3^- for the 25 sites remained high in 2015 compared to estimated pre-industrial concentrations (2015: 16.4 ± 8.5 μmol L^{-1}, pre-industrial: 2.1 ± 0.6 μmol L^{-1}). Hindcast trends in stream NO_3^- were not only associated with decreases in atmospheric NO_x deposition, but also changes in meteorological conditions (most notably increases in maximum monthly air temperature). Climatic drivers likely play a more important role in regulating monthly and yearly variation in stream NO_3^- concentrations than stream SO_4^{2-} concentrations because of strong N cycling through the forest vegetation and microbial processes which are influenced by meteorological conditions (McDonnell et al., 2018; also see Chapter 4). The differences in stream NO_3^- response to historical changes in N deposition among study sites could also be attributed to inaccurate estimates of atmospheric N deposition to individual watersheds, watershed characteristics (particularly watershed retention of N), and the accuracy of the characterization of the land disturbance history of the watersheds.

The mean simulated pre-industrial stream ANC was 136 ± 184 μeq L^{-1} for the modeled sites. Only one stream (#35014, ANC = 10.1 μeq L^{-1}) had simulated pre-industrial ANC less than 20 μeq L^{-1}. Eight streams had simulated pre-industrial ANC between 20 and 50 μeq L^{-1}. The remaining 16 streams had model-simulated pre-industrial ANC higher than 50 μeq L^{-1} (Table A-7). Coinciding with increases in concentrations of simulated stream SO_4^{2-} and NO_3^-, the simulated stream ANC decreased to minimum values around the year 2000 (75 ± 158 μeq L^{-1}), followed by a slight increasing trend in more recent years (2000 to 2015: +0.55 μeq L^{-1} yr^{-1}). Model hindcasts suggested that across the 25 modeled streams, acid deposition resulted in decreases in ANC of about 50 μeq L^{-1} on average from pre-industrial conditions (1850).

Historical increases in acid deposition to the modeled watersheds not only acidified the streams, but also acidified the forest soil. Hindcast simulations of soil chemistry suggest decreases in soil % BS from pre-industrial levels of 17.2% ± 6.9% to minimum levels of 11.3% ± 6.1% in about 2010, with no significant recovery thereafter. This marked decrease in soil % BS is the result of soil exchangeable cation depletion resulting from elevated historical anthropogenic N and S deposition and strong acid anion leaching, coupled with relatively low base cation weathering rates. The calibrated weathering rates of total base cations was from 0.28 to 1.82 keq ha^{-1} yr^{-1} with a median of 0.47 keq ha^{-1} yr^{-1}, with the model-calibrated weathering rate for Na^+ from 0.12 to 0.24 keq ha^{-1} yr^{-1}, Mg^{2+} from 0.06 to 0.33 keq ha^{-1} yr^{-1}, K^+ from 0.009 to 0.07 keq ha^{-1} yr^{-1}, and Ca^{2+} from 0.09 to 1.18 keq ha^{-1} yr^{-1}. For many of the modeling sites, the estimated base cation weathering rates were close to the lower limit of long-term estimates of an acid-sensitive Adirondack watershed as described by April et al. (1986) (0.62 ± 0.21 keq ha^{-1} yr^{-1}).

3.2.3 Simulations of stream ANC recovery under different future deposition scenarios

To evaluate potential future recovery of stream ANC, response curves (examples shown in Figure 3-5) were developed for each stream by depicting simulated future ANC values corresponding with deposition reduction levels (-15, 0, 25, 50, 75 and 100%) for each of the three deposition conditions (SO_4^{2-} alone; SO_4^{2-} and NO_3^-; SO_4^{2-}, NO_3^-, and NH_4^+). Note that none of the streams simulated were able to recover to their pre-industrial ANC values by 2200, even under the scenario of 100% reduction of anthropogenic S and N deposition to pre-industrial values. Nevertheless, model projections indicate that stream ANC will increase in proportion to decreases in acid deposition. Our model projections also suggest that to achieve the same level of recovery in stream ANC for the target year of 2150 at 21 of the 25 modeled streams, the scenarios that considered decreases in atmospheric SO_4^{2-}, NO_3^-, and NH_4^+ deposition in combination required a smaller percentage reduction than either decreases in SO_4^{2-} plus NO_3^- deposition or decreases in SO_4^{2-} deposition alone (Figure 3-5). For the remaining four streams, there is no significant difference in deposition reduction percentage among the three deposition conditions. However, for the target year of 2050, the number of modeled streams with limited differences in ANC recovery among the three deposition scenarios increased to 11. Therefore, the effectiveness of controls on NO_3^- and NH_4^+ deposition is manifested over a longer period, than those of SO_4^{2-} alone. The increases in stream ANC per unit equivalent decrease in SO_4^{2-} is greater than values for decreases in N deposition, likely due to relatively high watershed retention of N deposition. Simultaneous reduction of SO_4^{2-}, NO_3^-, and NH_4^+ deposition that provides larger reductions may be the most effective approach to achieve greatest overall recovery of Adirondack stream ANC over the long-term, followed by decreases in SO_4^{2-} plus NO_3^- deposition, and lastly SO_4^{2-} deposition alone. Also, projected ANC recovery by 2150

exceeds values in 2050 due to the longer period for weathering reactions to resupply exchangeable base cations that had been depleted due to historical acid deposition.

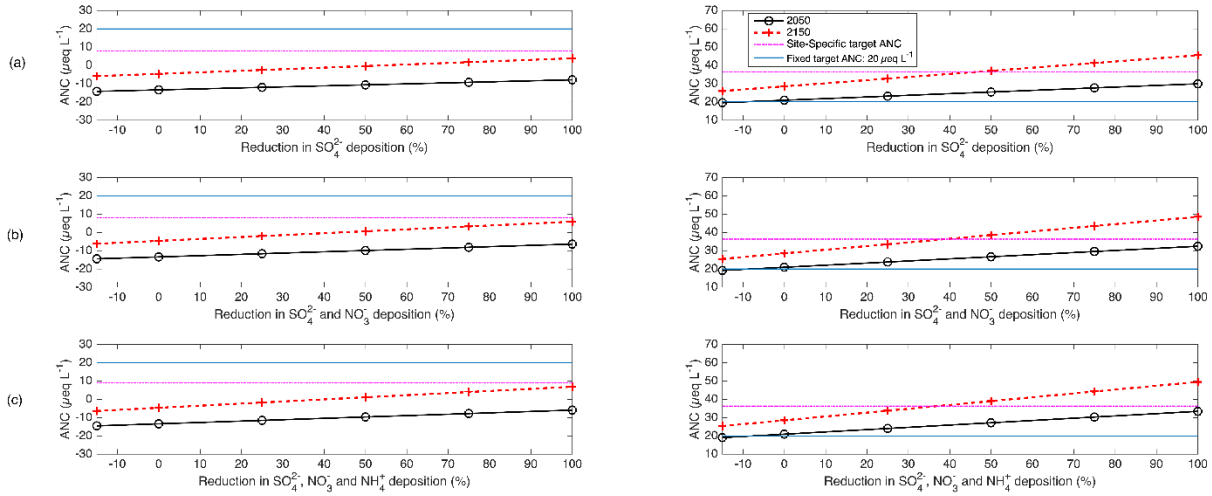

Figure 3-5. Example projections of ANC at T24 (left) and Buck Creek (right) in response to different load reduction scenarios: (a) SO_4^{2-} load reduction, (b) SO_4^{2-} and NO_3^- load reduction and (c) SO_4^{2-}, NO_3^-, and NH_4^+ load reduction for different target years (2050 and 2150) in relation to ANC targets of 20 μeq L^{-1} and preindustrial ANC –20 μeq L^{-1}.

The 25 modeled streams were grouped into three recovery classes for both ANC criteria (fixed and site specific) based on whether they: 1) could achieve the ANC criterion without further load reductions; 2) could achieve the ANC criteria but only with additional load reductions; or 3) were unable to attain the ANC criterion even if atmospheric depositions were decreased to pre-industrial levels and then held there until the year 2200 (Figure 3-6; Table A-8). For example, relatively insensitive streams like Archer Creek (observed ANC in 2013: 138 μeq L^{-1}) do not require any additional decrease in acid deposition to achieve an ANC criterion of 20 μeq L^{-1}. Of the 25 simulated streams 13 and 14 did not require additional decreases in acid deposition by the years 2050 and 2150, respectively, to achieve the ANC criterion of 20 μeq L^{-1}

(Figure 3-6 a). In contrast, model projections suggested that 7 and 6 study streams cannot achieve the ANC criterion of 20 µeq L^{-1} by 2050 and 2150, respectively, even with a 100% reduction in SO_4^{2-}, NO_3^-, and NH_4^+ deposition. For these watersheds, the field ANC values used in model calibration were all negative, suggesting that these sites are sensitive and have been impacted by historical acid deposition (Table A-1). These data were obtained from sampling during elevated spring flows (flow percentile values ranging from 62% to 79%), except for watershed WF (Table A-4, Table A-8). These highly acid-sensitive watersheds are characterized by low rates of base cation supply from weathering. Many of these streams also experience elevated inputs of naturally occurring organic acids. The sensitivity of these watersheds can be put into regional context by comparison with stream survey results conducted in the western and east-central Adirondack regions, which together are representative of the full Adirondack Region (Lawrence et al., 2018). These stream surveys were conducted during elevated (but not peak) spring snowmelt are approximate to the calibration data with regard to flow conditions. Sampling of approximately 400 randomly selected accessible headwater streams in the western Adirondack region indicated that 36 % of the streams had negative ANC values (Lawrence et al., 2008). Sampling of a similar number of randomly selected accessible headwater streams in the east-central Adirondack region indicated that 8 % of the streams had negative ANC values (Lawrence et al., 2018). When compared to the modeling results, these percentages provide a rough approximation of the percentage of headwater Adirondack streams that may not be capable of achieving the ANC criterion of 20 µeq L^{-1} by 2050 and 2150. Finally, five streams of the 25 simulated can achieve the ANC criterion of 20 µeq L^{-1} with additional reductions in acid deposition. For example, the south tributary of Buck Creek is projected to achieve the ANC

criterion of 20 µeq L^{-1} by the year 2150, but only with an 18% reduction in SO_4^{2-}, NO_3^-, and NH_4^+ deposition (Table 3-2).

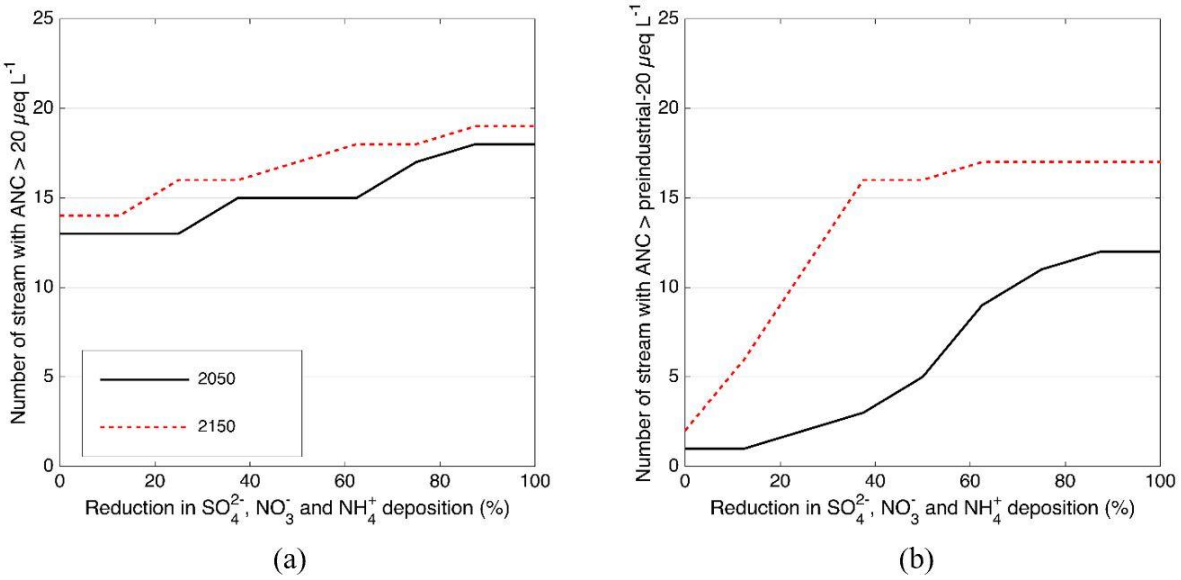

Figure 3-6. Number of modeled streams (out of 25) expected to attain the ANC criteria of 20 µmol L^{-1} (a) and preindustrial ANC-20 µmol L^{-1} (b) by the years 2050 and 2150 as a result of decreasing ambient atmospheric SO_4^{2-}, NO_3^-, and NH_4^+ deposition.

In contrast to the fixed ANC endpoint of 20 µeq L^{-1}, model simulations of the level of deposition needed to achieve the site-specific endpoint of the estimated pre-industrial ANC minus 20 µeq L^{-1} showed that only one stream would attain the TL by 2050 and two streams by 2150 with no additional reduction in SO_4^{2-}, NO_3^-, and NH_4^+ deposition (Figure 3-6). With additional reduction in SO_4^{2-}, NO_3^-, and NH_4^+ deposition, the number of streams achieving their estimated pre-industrial ANC minus 20 µeq L^{-1} increased to 12 (out of 25) by 2050 and increased further to 17 by 2150 with decreases in atmospheric deposition to pre-industrial levels.

3.2.4 TLs of acidity for modeled streams

Target loads calculated for this study provide estimates of the deposition loads of S and N (NO_3^- and NH_4^+) necessary to return stream ANC to the fixed level of 20 µeq L^{-1} and to within 20 µeq L^{-1} of simulated pre-industrial values, including the one stream for which this value is less than 20 µeq L^{-1}. Most streams were unable to recover to pre-industrial ANC values by 2150 due to depletion of soil exchangeable base cations resulting from historical acid deposition. In general, more substantial deposition reductions would be required in the future to achieve site-specific ANC recoveries (to within 20 µeq L^{-1} of pre-industrial values) or to reach ANC benchmarks earlier, by the year 2050 for example, as compared with chemical recovery by 2150. Target load simulations suggested that some of the damage to stream acid-base chemistry may be irreversible, although some streams likely had relatively low ANC prior to the advent of acid deposition. Thus, benchmarks based on model-simulated pre-industrial ANC as criteria for recovery may be more appropriate than fixed ANC benchmarks as a basis for establishing recovery goals and should be considered as a viable approach in the development of future TLs.

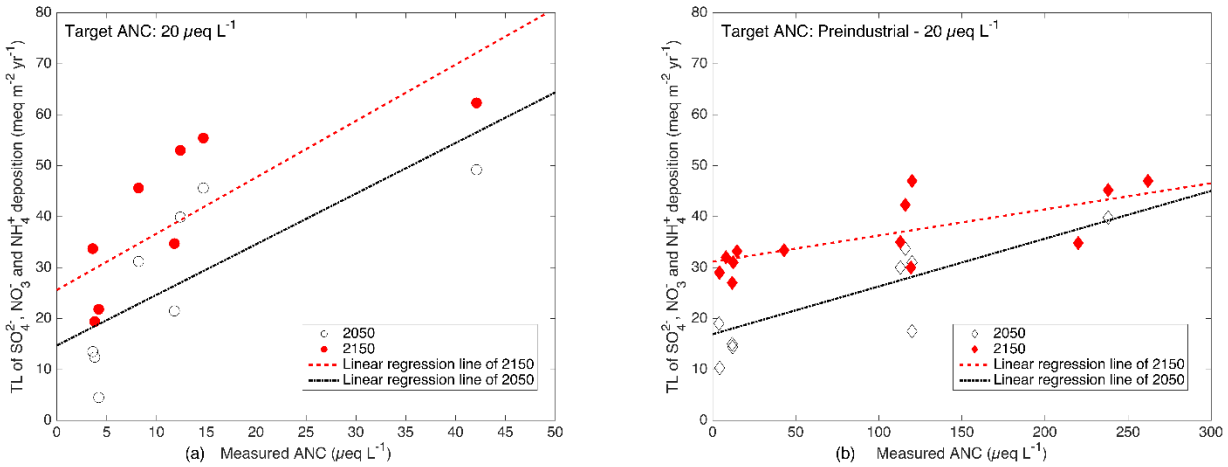

Figure 3-7. The (a) TLs of SO_4^{2-}, NO_3^-, and NH_4^+ deposition needed to achieve the ANC criterion of 20 μeq L^{-1} plotted against the mean of observed ANC for the years 2004-2005 for 9 Adirondack streams that were able to reach ANC = 20 μeq L^{-1} and (b) the TLs of the same deposition constituents needed to increase ANC to pre-industrial ANC less 20 μeq L^{-1} for the years 2050 and 2150.

The TLs needed to protect stream ANC were developed for the watersheds that were modeled to be recoverable with respect to the fixed (20 μeq L^{-1}) and site-specific ANC criteria (pre-industrial ANC less 20 μeq L^{-1}) under the SO_4^{2-}, NO_3^-, and NH_4^+ deposition reductions for the years 2050 and 2150 (Table A-8). I found strong, positive correlations between measured stream ANC and the TLs at the individual modeled sites (Figure 3-7). This pattern illustrates that streams with higher ANC are more likely to be associated with TLs that are higher than ambient or expected future acid deposition and therefore are of low concern with respect to effects from acid deposition. These sites require smaller reduction percentages in acid deposition to achieve their ANC criterion values compared with more acid-sensitive and impacted streams (Figure 3-7). The linear regression models that estimated TLs of acidity using measured stream ANC for the fixed and site-specific ANC criterion values for the years 2050 and 2150 are summarized in Table 3-3. For a given measured stream ANC, the TLs are higher for the year 2150 than for 2050, indicating that less reduction in acid deposition is needed to achieve the same ANC target

if a longer recovery period is considered (Table 3-3). These results could be used to extrapolate the TLs to populations of streams in the region.

Table 3-3. Linear regression statistics for predicting the TLs of acidity as functions of mean observed stream ANC in 2004 and 2005 (TLs = slope × ANC + intercept) for various target years of 2050 and 2150, and ANC criterion of pre-industrial ANC - 20 μeq L^{-1} on control of SO_4^{2-}, NO_3^-, and NH_4^+ deposition. [Coefficients are significant at P < 0.05.]

		Linear Regression Coefficients		
Target Year	**ANC Criterion**	Slope (m yr^{-1})	Intercept (meq m^{-2} yr^{-1})	R^2
2050	20 μeq L^{-1}	0.99	14.71	0.57
	Pre-industrial ANC -20 μeq L^{-1}	0.09	16.92	0.65
2150	20 μeq L^{-1}	1.11	25.59	0.66
	Pre-industrial ANC -20 μeq L^{-1}	0.05	31.17	0.52

3.2.5 Stream biology in response to changes in acid deposition

The hydrological analysis defined the relationship between low-flow stream ANC and the rate at which ANC declines as stream discharge increases, which is consistent across the region (Lawrence et al., 2004). Using this relationship, I was able to estimate ANC values under the summer base flow conditions using simulated annual average ANC values. Based on the nonlinear relationships of fish response metrics and adjusted model-simulated ANC, estimated fish density and fish biomass for model projections of the 25 streams are summarized in Table A-9 and Table A-10, respectively. During the pre-industrial period, projected estimates of fish density ranged from 162 to 690 fish per 0.1 ha (mean: 387), and fish biomass ranged from 946 to 3034 g per 0.1 ha with an average of 1828 g per 0.1 ha across the study watersheds. Projections of fish density for the 25 streams in 2015 decreased to a range of 16 to 689 fish per 0.1 ha with

the average of 306, and fish biomass decreased to a range of 0 to 2810 g per 0.1 ha, with an average of 1359 g per 0.1 ha. These decreases coincided with increases in atmospheric S and N deposition and decreases in stream ANC.

Model projections under the different deposition reduction scenarios generally indicate that Adirondack streams could gain fish density and biomass by the year 2150, compared to ambient conditions (in 2015). Estimates of fish density and fish biomass increased under the most aggressive future reduction scenario of a 100% decrease in S and N deposition, with an average increase of 52 fish per 0.1 ha (range from -55 to 126) and 303 g per 0.1 ha (range from 10 to 714) among the 25 streams. However, for most of the study sites (24 of 25), even under this most aggressive emissions reduction scenario, simulated fish density and fish biomass could not be restored to pre-industrial conditions. The average simulated fish density and fish biomass recoveries relative to pre-industrial level were 87% and 86%, respectively, with a range from 40% to 100% and 22% to 100%, respectively. The modeled scenario of a 15% increase in deposition suggests that there would be no significant deterioration in fish density or fish biomass between ambient conditions (year 2015) and those in the year 2150. However, a comparison between a scenario of 15% increase in deposition and a scenario of business as usual suggests that streams could lose fish density and fish biomass in the year 2150 with average decreases of 15 fish per 0.1 ha and 95 g per 0.1 ha, respectively, if the deposition of S and N increased. An integrated analysis suggests that surface water acidification from acid deposition has led to the loss of fish density and biomass for modeled streams (Baldigo et al. 2019b). Projected responses to potential decreases in acid deposition indicate that future emissions controls could help recover density and biomass of fish communities. A 100% reduction in N and S deposition beyond a U.S. Environmental Protection Agency proposal to control carbon

dioxide emissions from electric utilities was the most effective modeled emissions scenario for biological recovery and would allow fish communities to most closely return to pre-industrial conditions.

Although these integrated analyses of the extent of acidification and recovery can be directly related to the predictable measure of ANC, the biological scenario results rely on ANC as the only factor limiting recovery of fish communities in the study streams. We essentially invoke a spatial relationship of fish biomass and density with ANC and assume it is applicable to through time with changes in stream ANC. Other chemical, physical, and biological stressors may also impair fish assemblages and affect their ability to fully recover from decreases in acidification (Driscoll et al., 2001). Fish assemblages typically react directly to pH and Al_i concentrations, and indirectly to ANC levels. Long- or short-term shifts in other factors, such as climate (temperatures and precipitation), stocking policy, invasive species, and habitat quality may also affect the rate and level of biological recovery in headwater streams across the region.

3.2.6 Management implications

This research has improved our understanding of the historical acidification and possible future recovery of water chemistry and biology in acid-sensitive streams of the Adirondacks. Results suggest that simultaneous decreases in atmospheric SO_4^{2-}, NO_3^-, and NH_4^+ deposition are the best means of fostering the chemical recovery of acid-impacted Adirondack streams. Results of this research indicate that 12 low-order streams, especially in the southwestern portion of the Adirondack Park, have low TLs needed to achieve fixed or site-specific target ANC and are highly sensitive to acidification. This information will help in the management of natural

resources, and to determine whether and to what extent further emissions reductions or other restoration options are needed to further mitigate acidification. The findings that some streams may not be able to regain their pre-industrial water chemistry or fisheries in response to further reductions in the emissions and deposition of S and N, and in some cases may be unable to regain values within 20 μeq L^{-1} of pre-industrial ANC, suggest that intervention in the form of liming of some watersheds or streams might be a viable management option (Lawrence et al., 2016). Also, the quantitative relations among ANC and fishery metrics in Adirondack streams may be used not only to characterize how acidification currently affects local fish assemblages, but also to forecast and assess how changes in acid deposition will likely affect biological recovery in the Adirondacks.

Chapter 4. The response of streams to projected changes of climate and sulfur and nitrogen deposition in the Adirondacks

4.1 Methods

4.1.1 Study sites

The Adirondack Park (44.12° N, 73.87° W) is a large park in northern New York State, comprising about 24,000 km^2 of predominantly forested land, with approximately 2800 lakes (>2000 m^2 surface area) and a dense network of streams (Driscoll et al., 1991). The mean air temperature is 18 ^oC in July and -10 ^oC in January. The annual mean precipitation is 110 cm ranging from 76 to 154 cm during 1980 to 2016 (http://nadp.slh.wisc.edu/). The acidic deposition in the Adirondack region has experienced pronounced temporal and spatial gradients changes, generally decreasing from southwest to northeast, and shows highly variable surface water chemistry (Driscoll et al., 2016; Ito et al., 2002) (Figure 4-1). The legacy of past and current acidic deposition interacts with changing patterns in temperature, precipitation, and snowpack dynamics making the Adirondack Park an important region to explore the hydrologic and biogeochemical interplay between possible future acidic deposition and climate change (Arseneau et al., 2016).

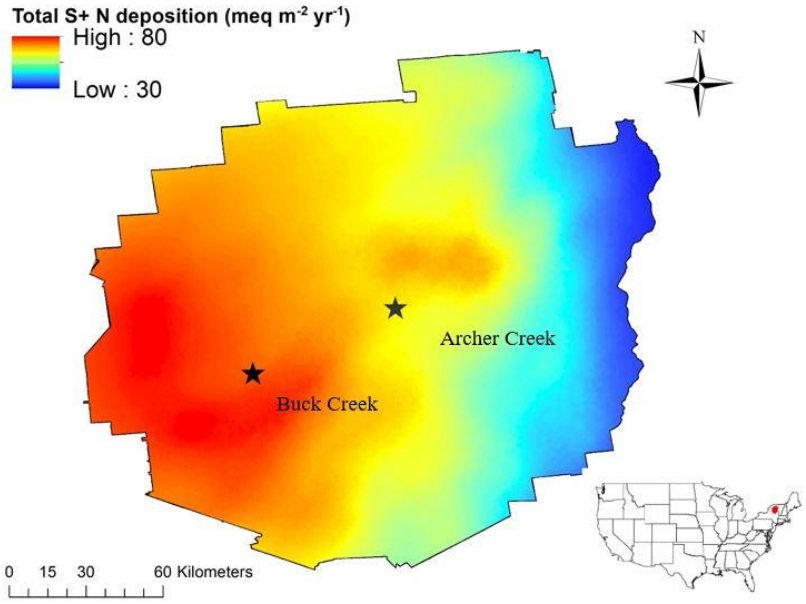

Figure 4-1. Estimated total sulfur plus nitrogen (S+N) deposition in the Adirondack Park and location of Archer Creek and Buck Creek watersheds, sites at which PnET-BGC was applied in this study. The deposition data were developed from TDep Version 2016.01. Values are an average of years 2014 and 2015.

Archer Creek is the main inlet to Arbutus Lake located near the center of the Adirondacks, with a drainage area of about 1.4 km^2 (Figure 4-1). The underlying bedrock is dominated by granitic gneiss with small outcrops of amphibolite and biotite-rich gneiss (April et al., 1986). Overlying the bedrock is glacial till from the most recent period of continental glaciation. High sand (75%) and low clay (<10%) content result in well-drained soils (Mitchell et al., 2006). The presence of minerals with moderately fast weathering rates (e.g., hornblende, pyroxenes, garnet, recrystallized calcite) provide relatively elevated acid neutralizing capacity (ANC) to drainage waters and as a result the watershed is insensitive to acidic deposition (April et al., 1986; Foster et al., 1992). Vegetation consists of northern hardwood forest. Meteorological and wet and dry deposition data are measured at the Huntington Forest, the site of Archer Creek (SUNY-ESF; http://www.esf.edu/hss/em/huntington/ackerman. html; NADP;

http://nadp.slh.wisc.edu/data/sites/siteDetails.aspx? net=NTN&id=NY20, accessed on May 11, 2018). Water chemistry data and stream flow data are available for Archer Creek from 1996-2017 (https://www.esf.edu/hss/em/huntington/archive.html, accessed on Jun 21, 2018).

Buck Creek is a second order stream with a drainage area of 3.1 km^2 and mean topographic gradient of about 50 m km^{-1}. Buck Creek watershed is well drained except for a small wetland area of less than 0.03 km^2 located in a mid-elevation tributary (Lawrence et al., 2008). Soils in the Buck Creek watershed are largely Spodosols derived from glacial till. The underlying bedrock is composed primarily of interlayered metasedimentary rocks and various forms of gneiss (Lawrence, 2002). The shallow deposits of glacial till and weathering resistant bedrock have resulted in relatively low values of stream ANC in Buck Creek. Stream flow and water chemistry data are available for Buck Creek from 2001 to 2017. Soil and water sampling and chemical analysis procedures are described in (Lawrence et al., 2008)

4.1.2 PnET-BGC model

PnET-BGC is a comprehensive biogeochemical model that has been used to evaluate the responses of forested ecosystems to changes in atmospheric deposition, climatic and land disturbance (Fakhraei et al., 2014, 2016; Gbondo-Tugbawa et al., 2001; Pourmokhtarian et al., 2012, 2017; Valipour et al., 2018). The model was formulated by linking two sub-models: PnET-CN (Gbondo-Tugbawa et al., 2001; Pourmokhtarian et al., 2012) and BGC which considers the cycling of major elements (Ca^{2+}, Mg^{2+}, K^+, Na^+, Al^{3+}, Cl^-, F^-, S, P, and Si) through biogeochemical processes (Gbondo-Tugbawa et al., 2001; Pourmokhtarian et al., 2012). The model considers major ecosystem processes, including tree photosynthesis, growth and

productivity, litter production and decay, CO_2 effects on vegetation, mineralization of soil organic matter and associated major elements, immobilization of N, nitrification, interactions of major elements with vegetation and organic matter, abiotic soil exchange/adsorption processes, solution speciation, and surface water processes (Gbondo-Tugbawa et al., 2001; Pourmokhtarian et al., 2012).

The model simulations run on a monthly time step and require monthly inputs of meteorological data (maximum and minimum temperature, precipitation, solar radiation, and atmospheric CO_2 concentration), atmospheric deposition (both wet and dry) and parameters that need to be calibrated (e.g., weathering rate of major elements, soil SO_4^{2-}, DOC adsorption constants, and chemical equilibrium constants). A detailed description of the methods for reconstruction of historical meteorological and atmospheric deposition data for the study sites is available in Shao et al. (2020). Forest vegetation type, and soil physical and chemical characteristics were assumed to be constant over the simulation period. Land disturbance history was incorporated into model simulations, including clear-cut forest harvesting in the 1880s and salvage harvests following the 1950 hurricane (McMartin, 1994). A detailed description of the model structure, input data development, model calibration processes and detailed sensitivity and uncertainty analysis of parameters are available in Gbondo-Tugbawa et al. (2001) and Fakhraei et al. (2017, 2014)

4.1.3 Future scenarios

The focus of this paper is to assess potential effects of climate change on the recovery of stream water from historical acidification. For projected future deposition scenarios, I only

consider changes in S and N deposition, and hold other components of atmospheric deposition constant at ambient levels (average of 2015 to 2017) for the future projections. Following model hindcasts, future simulations were implemented starting in year 2017. Deposition changes were linearly ramped to target values by 2030 and then held constant through the simulation period to 2100 (Figure 4-2). Simulations considered future deposition scenarios (for SO_4^{2-}, NO_3^- and NH_4^+), including a "business-as-usual" scenario that held ambient deposition (average of 2015 to 2017) constant until the end of the simulation period; a "pre-industrial" scenario in which deposition was linearly decreased from the ambient levels to the estimated pre-industrial deposition of 1850; and an "increasing deposition" scenario in which deposition was increased 20% from ambient levels (2017) to 2030 and then held constant (Figure 4-2). These three scenarios were chosen to bracket what I believe to be the full range of likely future emissions patterns.

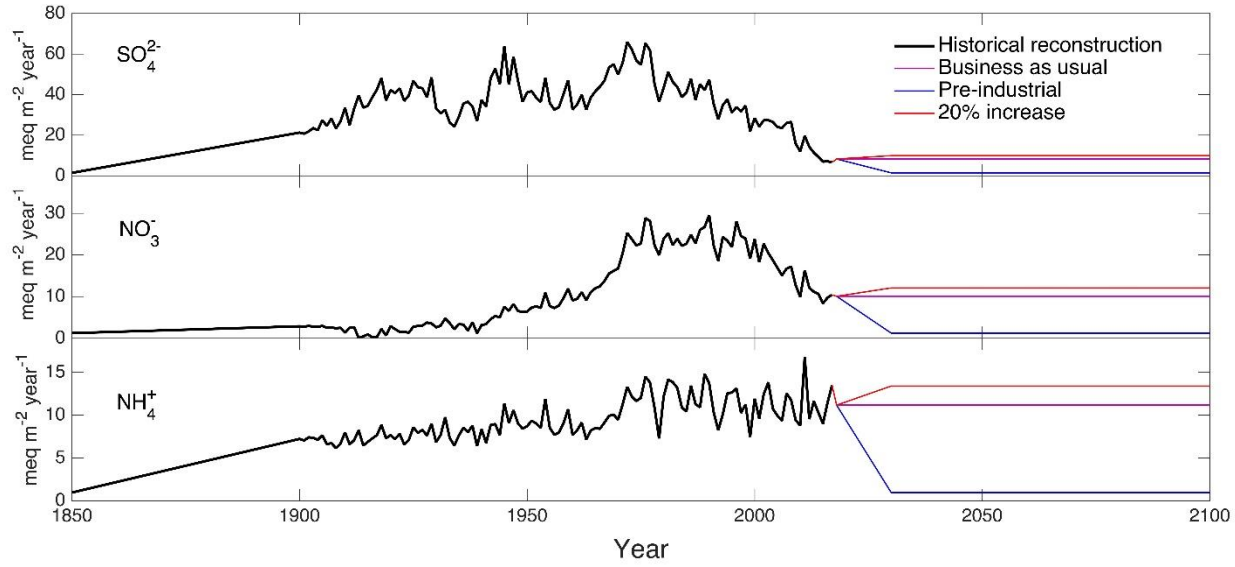

Figure 4-2. Reconstructions of wet atmospheric deposition of SO_4^{2-}, NO_3^- and NH_4^+ in the Adirondacks for the period 1850-2100. [Future projections (2017-2100) are shown under the "business as usual" scenario, a 20% increase scenario, and a 100% reduction in anthropogenic emissions (return to preindustrial levels).]

Statistically downscaled meteorology data for the Adirondacks were derived from the Coupled Model Inter-Comparison Project Phase 5 (CMIP5) models (http://cmip-pcmdi.llnl.gov/) (Figure 4-3). The CMIP5 archive includes more than 50 climate models with results of simulations that consider representative concentration pathways (RCPs). Models in the CMIP5 archive must meet a suite of rigorous requirements, including consistency with both past and present observations and with fundamental physical principles. Seventeen atmosphere-ocean general circulation models (AOGCMs) from the CMIP5 archive were applied in this study: the Beijing Climate Center Climate System Model version 1.1 and 1.1 (m) (Tongwen, 2012), the Canadian Earth System (Flato et al., 2000), the France Centre of Meteorological Research (Salas-Mélia et al., 2005), Commonwealth Scientific and Industrial Research Organization/Queensland Climate Model (Rotstayn et al., 2012), NOAA Geophysical Fluid Dynamics Laboratory Earth System Model, version 2G and 2M (Dunne et al., 2012), Hadley

Global Environment Model 2 version Carbon Cycle and Earth System (Collins et al., 2011), Institute Pierre Simon Laplace Model version CM5A-LR, CM5A-MR and CM5B-LR (Tan et al., 2020), Model for Interdisciplinary Research on Climate version 5, ESM, and ESM-CHEM (Watanabe et al., 2011), and Japan Meteorological Research Institute Coupled General Circulation Model version 3 (Yukimoto et al., 2012). Two representative concentration pathways (RCP 4.5 and RCP 8.5 refer to the radiative forcing projected for the year 2100) were applied to represent lower and higher climate scenarios utilized in this study (Moss et al., 2010). This approach captures the range of greenhouse gas emissions uncertainty reported by (IPCC, 2000). Monthly precipitation and temperature data for each model and RCP from observed (1950–2006) and predicted (2007–2100) periods were obtained at a resolution of 1/8° rectangular grid. A statistical approach was used where probability density functions for modeled climate data were mapped onto those of gridded historical observed data. Overlapping periods of Parameter-elevation Relationships on Independent Slopes Model (PRISM: https://prism.oregonstate.edu/) and AOGCM data (1950–2006) were compared to determine bias resulting from the coarse model resolution and the complex topography of the study sites. The temperature and precipitation data from each AOGCM were regressed versus PRISM data, with the resulting equations used to downscale modeled data to align with site observations.

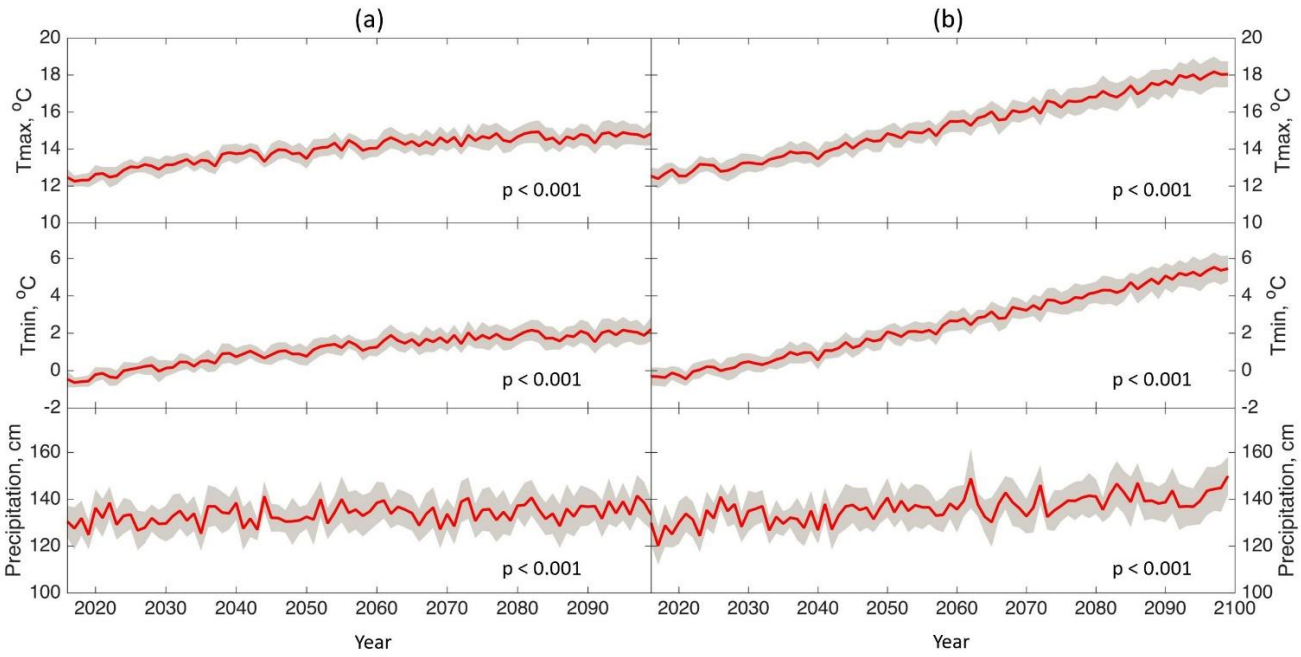

Figure 4-3. Statistically downscaled climate data for the Adirondack region of New York from 17 atmosphere-ocean general circulation models (AOGCMs) for two representative concentration pathways (RCPs) 4.5 (a) and 8.5 (b). The red line represents the average values among 17 models and the gray area represents the 95% confidence interval. The Mann-Kendall Trend test was applied to each climate variable to assess significant trend direction (p values indicate statistical significance of the relationship).

4.1.4 Model calibration and implementation

Soil and stream chemistry and stream flow data were used for chemical and hydrological calibration of the model. Weathering rates for major elements and other soil parameters (e.g., soil SO_4^{2-} and DOC adsorption capacity and adsorption constants) for the two watersheds were determined through model calibration by adjusting input parameters until simulated soil and stream water chemistry outputs matched observed values. The Mann-Kendall Trend test was applied to each climate variable over the period of 2006-2100 to assess significant trend direction. The magnitude of the trends for each variable was evaluated by the non-parametric Theil-Sen Slope.

The model spin-up period started at the year 1000 to achieve steady state for the soil and vegetation pools (e.g., net ecosystem production of the simulated forest watershed remains close to zero). The simulations started from 1000 to 2017 using reconstructed and measured atmospheric deposition and meteorology data (Shao et al., 2020). Model forecasts continued for the remainder of the simulation (2018–2100) using statistically downscaled meteorology data and projected future atmospheric deposition control scenarios described previously.

I examine the impacts of changes in temperature and precipitation on discharge and the acid-base chemistry of the streams using a range of temperature and precipitation ramps in the PnET-BGC model over the period 2018–2100. These ramps are referred to by the change in average annual temperature and precipitation from 2018 to 2100 and are expressed relative to 1990-2010 averages from PRISM data. The upper and lower bounds of the ramps are determined by the changes expected in the downscaled climate scenarios. Temperature ramps ranged from 0 to an increase of 5 ^{o}C at 0.5 °C intervals, and precipitation ramps ranged from 0 to an increase of 25 cm at 5 cm intervals. The temperature and precipitation ramps were distributed equally across 12 months. Applying every combination of these ramps resulted in 50 combinations of varying temperature and precipitation scenarios. The climate scenario with no change in precipitation or temperature is considered the reference climate scenario.

4.2 Results and discussion

4.2.1 Model evaluation

In general, PnET-BGC effectively simulated the hydrology of streams at the Adirondack watersheds (Figure 4-4; Table 4-1). Measured annual discharge (Archer Creek: 785 ± 95 mm;

Buck Creek: 762 ± 87 mm) closely approximated model simulated values for both sites (Archer Creek: NME=0.03; Buck Creek: NME=0.02). PnET-BGC simulations also reproduced the time series of stream chemistry for both streams over the measurement period (Figure 4-4; Table 4-1). Simulations depict decreasing trends in SO_4^{2-} concentrations for both streams, which is consistent with decreases in atmospheric S deposition input to the model (Figure 4-2). The model simulated stream SO_4^{2-} concentrations agreed well with measured values at both sites (Table 4-1). The model simulated annual volume-weighted NO_3^- concentrations also generally agreed with measured data, but with larger departures from the measured data than observed for SO_4^{2-} as indicated by higher NME and NMAE values (Table 4-1). PnET-BGC simulates ANC as an analog of measured ANC by Gran plot analysis (Gran, 1952). Accurate simulations of ANC require effective depiction of concentrations in all major solutes (Fakhraei & Driscoll, 2015; Gbondo-Tugbawa et al., 2001). Simulations showed good agreement between modeled and measured ANC for both sites, despite considerably different ANC values due to differences in estimated mineral basic cation weathering rates (Archer Creek: 0.84 keq ha^{-1} yr^{-1}; Buck Creek: 0.43 keq ha^{-1} yr^{-1}) estimated through model calibration. The mean model simulated ANC values over the monitoring period (Archer Creek: 113 ± 8 μeq L^{-1}; Buck Creek: 16 ± 3 μeq L^{-1}) were similar to the measured values (Figure 4-4). Both sites had a pattern of increasing ANC over the monitoring period, however, increases at Buck Creek were more prominent (Archer Creek: + 1.4 μeq L^{-1} yr^{-1}; Buck Creek: + 2.1 μeq L^{-1} yr^{-1}). A naturally occurring organic acid algorithm is included in PnET-BGC (Fakhraei and Driscoll 2015), which considers protonation and Al binding of dissolved organic matter based on simulation of DOC, pH, and Al as well as partitioning with soil surfaces. This algorithm is important in the simulation of ANC and the

speciation of dissolved Al. Generally, the model simulation results show good agreement between modeled and measured DOC values for both sites (Table 4-1).

Table 4-1. Summary of metrics of model performance (normalized mean error (NME), normalized mean absolute error (NMAE)) in the simulation of annual volume-weighted concentrations of SO_4^{2-}, NO_3^-, ANC, and DOC and annual stream discharge for Archer Creek and Buck Creek.

Sites	**Stream Constituent**	**NME[a]**		**NMAE[b]**	
		Mean	SD	Mean	SD
Archer Creek	**Flow**	0.03	0.08	0.13	0.10
	SO_4^{2-}	0.02	0.05	0.06	0.03
	NO_3^-	0.11	0.12	0.13	0.18
	ANC	-0.06	0.11	0.09	0.10
	DOC	-0.10	0.13	0.12	0.13
Buck Creek	**Flow**	0.02	0.07	0.11	0.08
	SO_4^{2-}	0.01	0.04	0.05	0.03
	NO_3^-	0.12	0.09	0.15	0.16
	ANC	-0.08	0.12	0.11	0.11
	DOC	-0.09	0.12	0.13	0.14

[a] NME - normalized mean error;

[b] NMAE - normalized mean absolute error.

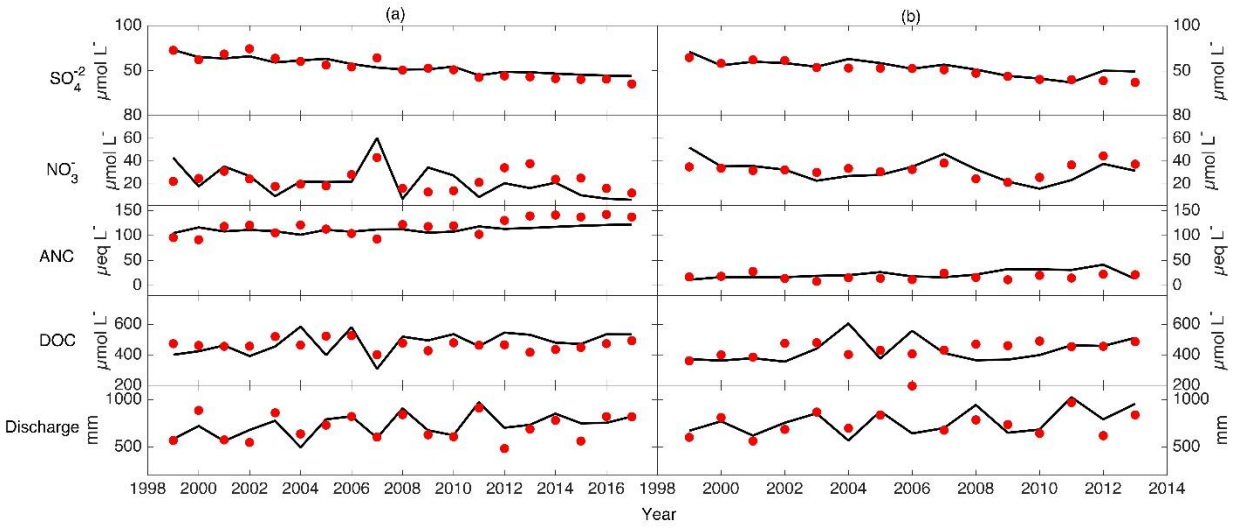

Figure 4-4. Comparisons of measured (red circle) and model simulated (black lines) annual values of SO_4^{2-}, NO_3^-, ANC, DOC and stream flow over the period 1999–2013 at Archer Creek (a) and Buck Creek (b).

4.2.2 Future projections

The results of statistically downscaled time series of the annual average maximum air temperature (T_{MAX}, ^oC), minimum air temperature (T_{MIN}, ^oC), and precipitation (PPT, cm) for RCP 4.5 and 8.5 are shown in Figure 4-3. All climate variables had significant increasing trends over the study period under both emission scenarios (Figure 4-3). Compared to average values from 2006–2015, the average values for 2091-2100 are projected to increase by 2.48 ^oC and 5.58 ^oC for mean maximum air temperature, by 2.63 ^oC and 5.84 ^oC for mean minimum air temperature, and by 13.10 cm and 17.11 cm for mean precipitation under RCP 4.5 and RCP 8.5, respectively, for the Adirondack region based on output from the 17 GCMs. Overall, the downscaled climate data suggest that projections of maximum air temperature increases will range from 0.6 - 8.3 °C, minimum air temperature increases range from 0.4 - 8.0 °C, and annual precipitation increases range from 2 - 31 cm by the end of the century (2091–2100) compared to recent conditions (2006–2015) across all 17 models under the two climate scenarios.

The time series of projections of soil and stream water chemistry and their variation for Archer Creek and Buck Creek for "pre-industrial" and "20% increased deposition scenarios using statistically downscaled meteorological data derived from each AOGCM and RCP are depicted in Figures 4-5 and 4-6. Projected average annual volume-weighted stream concentrations of SO_4^{2-}, NO_3^-, ANC, DOC, and soil BS% (red line) and 95% confidence interval (gray area) are presented in the figures along with a reference scenario (black line) that considered stationary meteorological conditions and the "business as usual" deposition scenario. Model simulations comparing annual average volume-weighted values for the period 2006–2015 to 2091–2100 for SO_4^{2-}, NO_3^-, ANC, soil BS% and stream flow under each AOGCM and RCP are summarized in Table 4-2. Generally, discharge is projected to increase under climate change scenarios by a range of 11.5 to 14.9 cm. Sulfate concentrations are projected to decrease by -45.9 to -24.5 μeq L^{-1} and those of NO_3^- by -23.4 to -9.7 μeq L^{-1} under all scenarios. In contrast, ANC increases under all scenarios, with increases ranging from 3.4 μeq L^{-1} to 31.2 μeq L^{-1}.

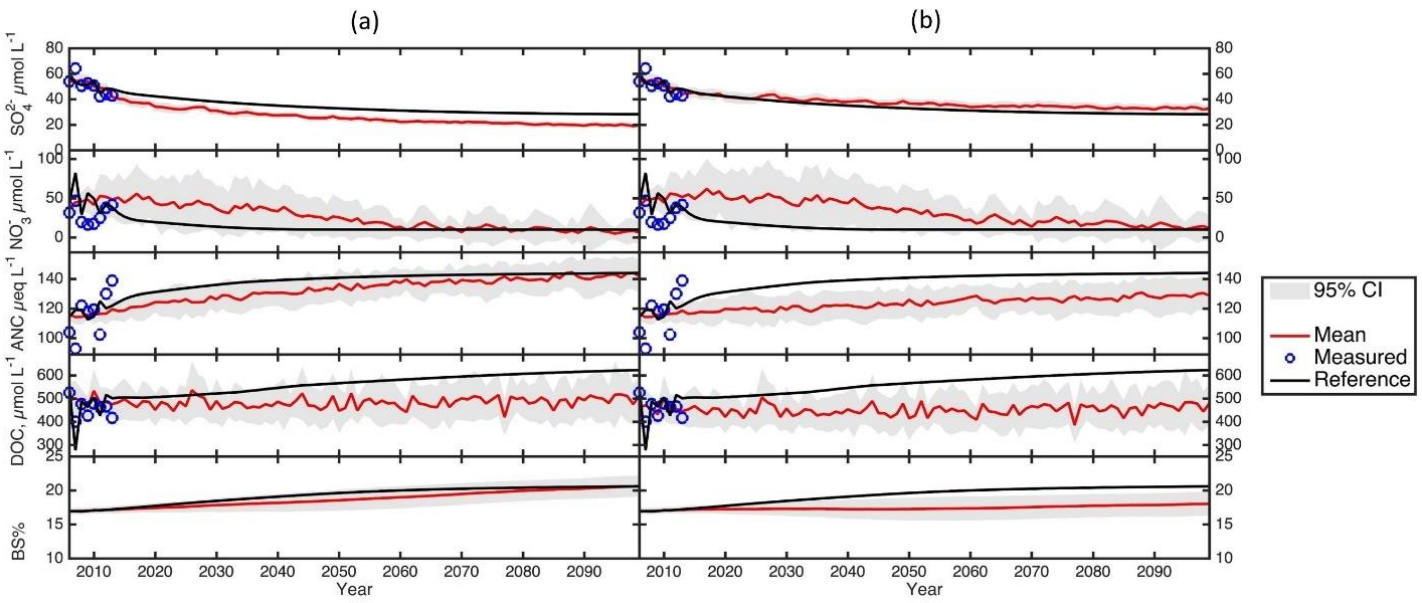

Figure 4-5. Projected annual volume-weighted average of SO_4^{2-}, NO_3^-, ANC, DOC in streamwater and soil BS% at Archer Creek over the period 2000–2100 for scenarios of pre-industrial (a) and 20% increase (b) deposition (red lines) which consider variation of simulations of 17 atmosphere-ocean general circulation models and two RCPs. The gray shaded area represents the 95% confidence interval of this variation. The blue circles represent the measured annual average value. The black line represents the projection for stationary meteorological conditions and business as usual deposition scenario (reference scenario).

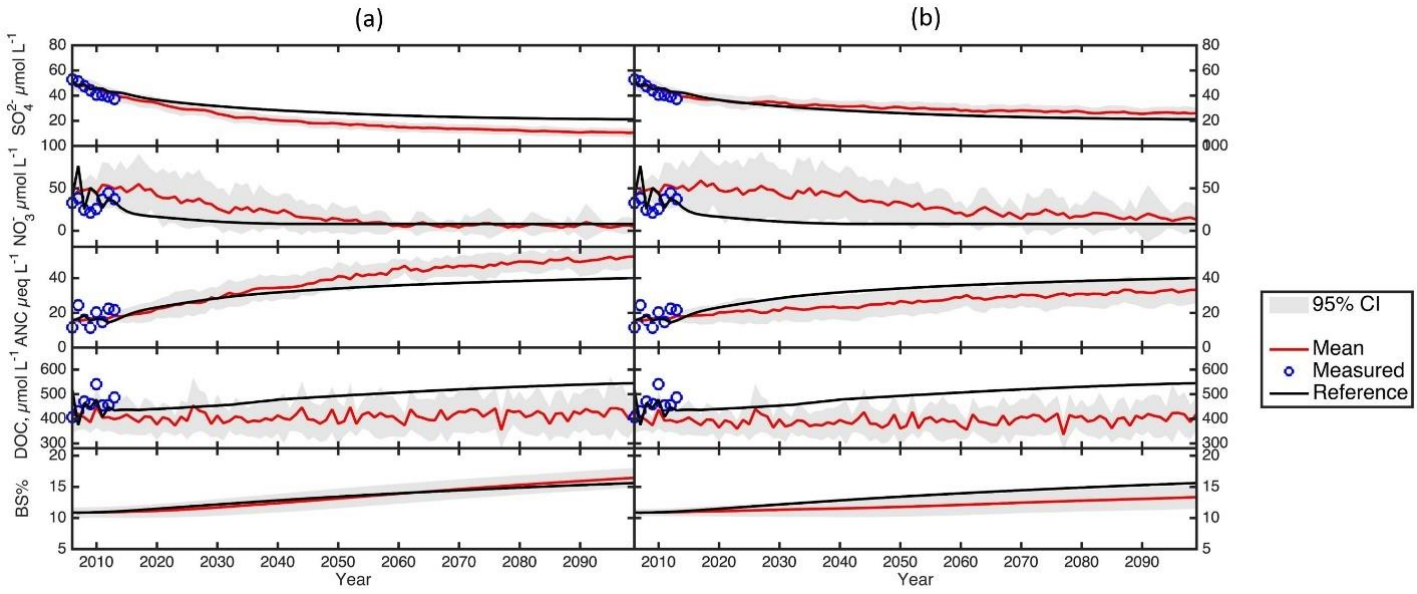

Figure 4-6. Projected annual volume-weighted average of SO_4^{2-}, NO_3^-, ANC, DOC in streamwater and soil BS% at Buck Creek over the period 2000–2100 for scenarios of pre-industrial (a) and 20% increase (b) deposition (red lines) which consider variation of simulations of 17 atmosphere-ocean general circulation models and two RCPs. The gray shaded area represents the 95% confidence interval of this variation. The blue circles represent the measured annual average value. The black line represents the projection for stationary meteorological conditions and business as usual deposition scenario (reference scenario).

In general, SO_4^{2-} and NO_3^- concentrations peaked in the early 2000s followed by long-term decreasing trends. Note that all climate projections showed an extended enrichment in stream NO_3^- starting around 2010 and extending with a long tail to various future dates depending on the deposition scenario, which was not observed in the stationary climate simulations. This increase in NO_3^- is a manifestation of enhanced decomposition rates of soil organic matter and N mineralization under warmer temperatures and an accelerated release of N to streamwater that accumulated in Adirondack soils from elevated historical atmospheric N deposition. This increase in stream NO_3^- under changing climate and the scenario of increases in acid deposition in comparison to stationary climate conditions persists for a longer period than

for the pre-industrial deposition scenario. This pattern simply reflects the effects of ongoing atmospheric N deposition compared to the scenario of aggressive mitigation of emissions. Soil BS and stream ANC are projected to be relatively low during the 2000s and then increase for the two sites under all deposition scenarios ("business as usual", "20% increases" and "pre-industrial") reflecting varying degrees of recovery from historical acid deposition.

Under the scenario of increased acidic deposition, increases in concentrations of SO_4^{2-} and NO_3^- are projected for both streams, impairing recovery from historical acidification by reducing stream ANC and soil BS% when compared to the reference scenario. For the scenario where deposition decreases to pre-industrial conditions, concentrations of stream SO_4^{2-} decrease somewhat offsetting the projected increases in NO_3^-. PnET-BGC has an algorithm of pH-dependent soil partitioning of DOC to simulate increases in stream DOC that have been observed in Adirondack waters (Fakhraei and Driscoll 2015; Driscoll et al. 2016), a phenomenon referred to as "browning". Simulations under the stationary scenarios all depict increases in DOC associated with increases in soil pH and decreases in soil partitioning of dissolved organic matter, consistent with our expectation. In contrast, under the varying climate scenarios simulations of DOC concentrations decrease in comparison to the reference scenario. These decreases would seem to be inconsistent with the hypothesis that climate change would drive increases in stream water DOC that was also reported by Pourmokhtarian et al. (2012). Since the higher temperature and CO_2 fertilization increase the NPP (Net primary production) and litterfall, therefore an increase in the decomposition of SOM will led to a higher DOC concentration in stream water.

Table 4-2. Projected average changes and standard deviation in stream variables at Archer Creek and Buck Creek by Atmosphere-Ocean General Circulation Model RCP scenarios and deposition scenarios, determined by comparing average annual values from 2006–2015 to 2091–2100.

Deposition	Stream	RCP	Stream flow (cm)	SO_4^{2-} (µeq L^{-1})	NO_3^- (µeq L^{-1})	ANC (µeq L^{-1})
Business as usual	Archer Creek	Static	-1.5±0.3	-27.1±3.2	-15.2±3.6	10.4±2.1
		4.5	11.7±1.5	-28.5±3.6	-12.7±5.0	8.7±2.4
		8.5	14.9±2.1	-30.2±4.1	-10.9±6.2	7.8±1.9
	Buck Creek	Static	-1.4±0.3	-28.2±3.5	-14.3±3.8	13.8±2.4
		4.5	11.5±1.4	-31.2±4.1	-13.5±4.9	10.5±2.1
		8.5	14.8±2.3	-32.8±4.9	-12.8±5.7	8.3±2.0
20% increase	Archer Creek	Static	-1.5±0.2	-25.6±2.8	-15.3±3.5	6.7±1.8
		4.5	11.7±1.2	-27.1±3.1	-14.1±4.9	4.8±1.7
		8.5	14.9±2.8	-28.5±4.4	-13.2±5.9	3.4±1.5
	Buck Creek	Static	-1.4±0.2	-24.5±2.8	-12.1±3.7	11.1±2.0
		4.5	11.5±1.4	-25.8±3.2	-10.5±4.7	7.7±1.8
		8.5	14.8±2.6	-27.1±4.8	-9.7±5.6	5.1±1.4
Pre-industrial	Archer Creek	Static	-1.5±0.2	-36.5±2.9	-18.7±3.6	24.9±3.4
		4.5	11.7±1.5	-37.8±3.7	-17.5±5.2	21.2±2.7
		8.5	14.9±2.4	-39.4±4.8	-15.2±5.3	18.9±2.6
	Buck Creek	Static	-1.4±0.2	-41.2±3.1	-23.4±3.8	31.2±3.5
		4.5	11.5±1.9	-43.8±4.9	-20.1±3.6	24.9±3.1
		8.5	14.8±2.7	-45.9±5.5	-18.7±4.1	17.2±2.8

4.2.3 Acidification recovery under changing climate

Despite reductions in acidic deposition that have occurred across the northeast United States in response to the Clean Air Act (CAA) and associated rules, recovery of surface water chemistry has been limited primarily due to three factors. First, long-term depletion of soil exchangeable base cations due to decades of acidic deposition has limited the ability of the soil

to neutralize ongoing inputs of S and N deposition (Johnson et al., 2008b). Second, declines in S and N deposition are increasingly buffered by internal legacy soil sources of SO_4^{2-} and NO_3^- to surface waters (Mitchell et al., 2011). Third, increases in DOC concentrations have been observed in many acid-impacted surface waters during recovery period. Increases in strongly acidic functional groups associated with DOC have likely slowed the rate of recovery in stream pH and ANC (Driscoll et al., 2016; Lawrence et al., 2011). These effects are likely to become exacerbated under future climate change. For example, the increases of NO_3^- leaching due to temperature-driven increases in net mineralization and nitrification would lead to an accelerated loss of cations (e.g., Ca^{2+}) that contribute to the ongoing depletion of soil exchangeable base cations (Campbell et al., 2009; Huntington, 2005; Watmough et al., 2005). Previous studies also indicate that under a warmer and wetter climate, elevated leaching of NO_3^- and DOC would be expected from catchment soils which therefore affects the hydrochemistry of streams (Evans, 2005; Sebestyen et al., 2009). Our study focused on addressing the effects of climate change in assessment of the recovery of surface water chemistry from acidification, which has been ignored in most previous studies (Fakhraei et al., 2014, 2016; Shao et al., 2020; Zhou et al., 2015). Because the time scale of climate change effects is comparable to that of acidification recovery and as climate change fundamentally affects hydrologic and biogeochemical processes affecting solute transformations and transport, I would advocate that climate change effects be incorporated in assessments of air pollution impacts, such as the determination of critical loads/target loads of ecosystems (Von Schneidemesser et al., 2020).

The model simulations were conducted to project changes in ANC for Archer Creek and Buck Creek under future deposition and climate scenarios (Figure 4-7). Model simulations with stationary climate projections corresponding to three different deposition projections are

represented by color coded solid lines. The difference between each solid line could be considered as the change in stream ANC in response to a deposition control strategy (red arrow in Figure 4-7). For example, the simulations suggest that ANC would increase by 7.9 μeq L^{-1} for Archer Creek by year 2100 if acidic depositions were reduced from business-as-usual scenario to pre-industrial scenario (red arrow up from the solid black line to the solid blue line). For Buck Creek, the projected ANC gain from emission control is even greater, 12.8 μeq L^{-1}. The gap between solid line and dash line of the same color represents a simulated offset of stream ANC recovery due to climate change (blue arrow in Figure 4-7). For example, model projections indicate that if climate change is considered in model simulations, stream ANC would be reduced by 8.5 μeq L^{-1} relative to stationary climate under a pre-industrial deposition level for Archer Creek by year 2100 (blue arrow down from solid blue line to dash blue line). For Buck Creek, the projected ANC loss from climate change has diminished by 0.4 μeq L^{-1}. The comparison of simulation results for the two sites suggests that the acid-sensitive watersheds like Buck Creek would gain more ANC from an emission control strategy, while the acid-insensitive site Archer Creek would experience a larger offset of ANC increases due to climate change, however both sites are simulated to experience a decrease in ANC under changing climate compared to stationary climate.

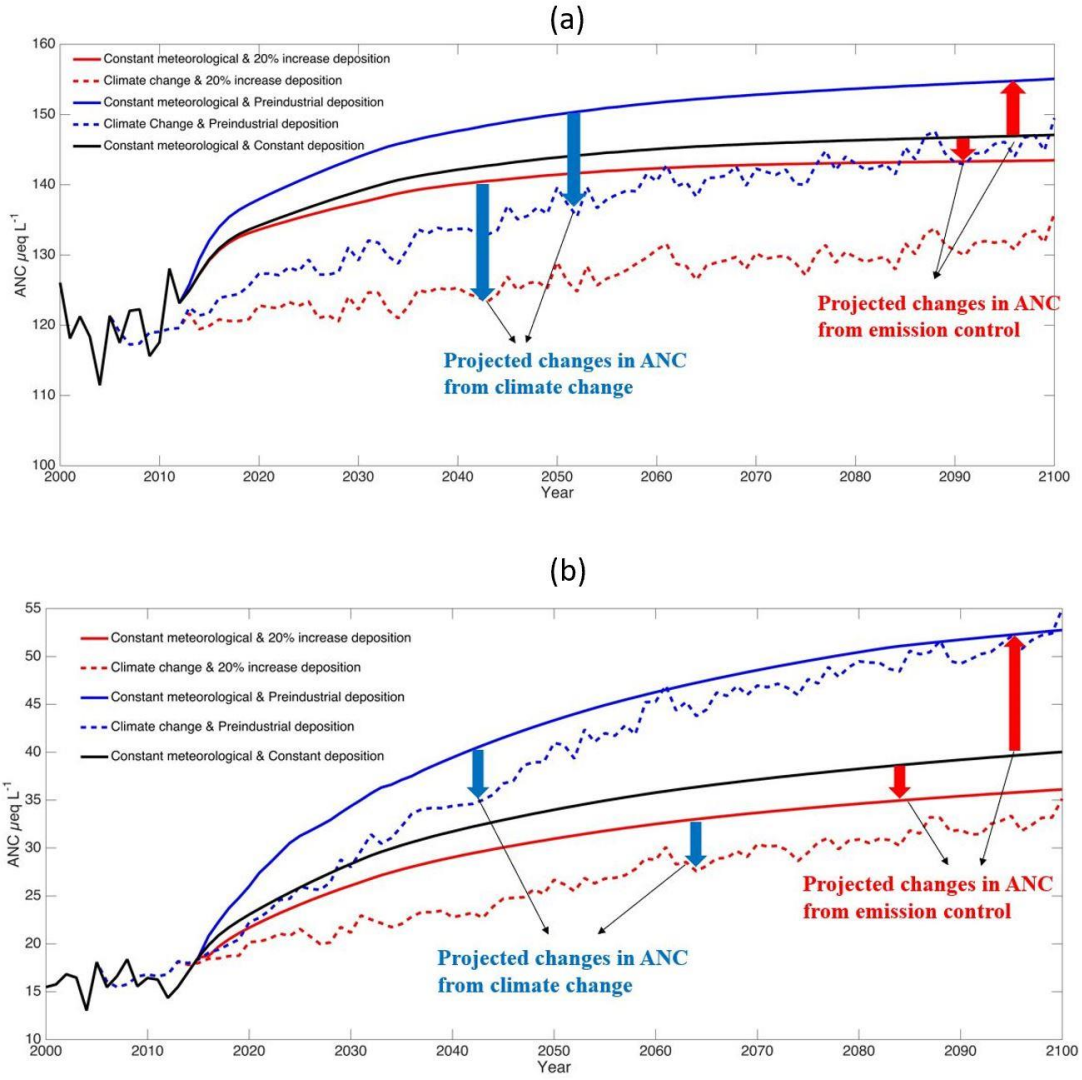

Figure 4-7. Time-series of model simulations of ANC for Archer Creek (a) and Buck Creek (b), comparing deposition only scenarios with combined climate and deposition scenarios. The solid lines represent the scenarios in which climate remains at current conditions with deposition change (business as usual, 20% increase and 100% reduction from current levels). The dashed lines represent scenarios in which predicted changes in climate (average of 34 model simulations) are simulated together with changes in deposition.

Target loads (TLs) provide an estimate of the levels of atmospheric deposition above which ecosystem services become compromised and the ecosystem transitions from a sustaining

to a non-sustaining condition (Sullivan et al., 2011). Note that values of TLs decrease with increases in ecosystem sensitivity to atmospheric deposition. Previously, I developed TLs to achieve site-specific benchmarks of ANC at Archer Creek and Buck Creek for an end year 2150 without considering climate change (Archer Creek: 35.2 meq m^{-2} yr^{-1}, Buck Creek: 33.2 meq m^{-2} yr^{-1}) (Shao et al., 2020). The site-specific target ANC was 20 µeq L^{-1} less than the simulated pre-industrial ANC, reflecting recovery to within 20 µeq L^{-1} of the pre-industrial ANC value at a given site. To illustrate the impact of changing climate on TLs, I incorporated climate projections developed for this analysis into the TL approach described in Shao et al. (2020). The resulting TLs for Archer Creek and Buck Creek to achieve site-specific target ANC at year 2150 decreased from 35.2 and 33.2 meq m^{-2} yr^{-1} to 17.8 and 26.9 meq m^{-2} yr^{-1} under RCP 4.5 and to 13.7 and 23.4 meq m^{-2} yr^{-1} under RCP 8.5. These decreases in TLs indicate that further reductions in acidic deposition may be necessary for these watersheds to support healthy fisheries or other ecosystem services under changing climate compared to projections assuming a stationary climate.

4.2.4 The influence of temperature and precipitation on stream water chemistry

To evaluate the extent to which climate variables may affect recovery in stream chemistry from acidic deposition, I conducted model simulations to compare changes in stream flow and chemistry resulting from temperature and precipitation (Figures 4-8 & 4-9). These hypothetical model simulations indicate that stream flow is positively correlated with precipitation amount and negatively correlated with temperature (Figures 4-8a & 4-9a). Stream flow as depicted in the PnET-BGC model is the sum of drainage and fast flow. The fast flow

fraction allows for rapid response of streamflow when the water holding capacity of the soil is exceeded (Aber & Federer, 1992). A fraction of the total input water goes to drainage and is calculated by numerical integration of water inputs to satisfy soil and transpiration demand by vegetation over each month. In the model, increases in air temperature cause a higher vapor pressure deficit (VPD) and lowers the water use efficiency, resulting in greater transpiration and a decrease in stream discharge (Aber & Federer, 1992).

The contour plot for SO_4^{2-} is similar to that of stream flow (Figures 4-8b & 4-9b) indicating that changes in simulated SO_4^{2-} concentration in stream are primarily controlled by temperature and precipitation similar to that of stream discharge. Higher precipitation increases stream flow, thereby directly diluting SO_4^{2-} concentrations in stream water. The SO_4^{2-} dynamics in soil are mainly controlled by adsorption and desorption processes rather than by weathering sources and the mineralization process (Gbondo-Tugbawa et al., 2002). Adsorption and desorption are simulated as being insensitive to soil temperature, but are dependent on soil moisture (Bohn et al., 1979). Mitchell and Likens (2011) and Hinckley et al. (2020) observed that with decreases in atmospheric S deposition, stream SO_4^{2-} concentrations shift from deposition control to climate control. Our simulations are consistent with this change in SO_4^{2-} behavior.

Stream NO_3^- exhibits a completely different pattern than SO_4^{2-}. The changes in NO_3^- concentration are more sensitive to temperature than precipitation (Figures 4-8c & 4-9c). Although increases in precipitation also enhance dilution of NO_3^-, the response of NO_3^- to changes in precipitation is much less than that of SO_4^{2-}. More importantly in PnET-BGC, biotic processes play a greater role in N dynamics than in S dynamics. Changes in temperature and precipitation have a considerable effect on N processes because they are strongly biologically

mediated. Previous studies have demonstrated that changes in temperature and soil moisture affect rates of soil microbiological processes in the northeastern United States (Davidson & Janssens, 2006; Fierer & Schimel, 2003). In general, soil biological activity doubles for every 10 ^{o}C increase in temperature (Bohn et al., 1979). Melillo et al. (2002) showed experimentally that increasing soil temperature by 5 ^{o}C resulted in a near doubling of N mineralization rates in the soil Oa horizon at Harvard Forest. The amount of N taken up by vegetation also plays a role in controlling the amount of NO_3^- available for stream export. Water stress lessens plant N demand and increases N availability for nitrification and therefore increases NO_3^- leaching in drainage waters (Aber et al., 1997; Aber & Federer, 1992). In addition to temperature and precipitation, many other factors, including nutrient availability, tree species composition, and land disturbance affect N mineralization, nitrification and denitrification in a complex manner, and therefore predictions of NO_3^- concentrations in stream water have high uncertainty.

PnET-BGC simulates ANC as an analog to measured ANC by Gran plot analysis (Gran 1952). Theoretically, the variability in ANC should be equivalent to sum of variability in SO_4^{2-}, NO_3^-, cations (Ca^{2+}, Mg^{2+}, K^+, Na^+, Al^{3+}) and naturally occurring organic acids (Fakhraei & Driscoll 2015). The dilution effect is the main factor affecting stream concentrations of SO_4^{2-} and base cations in response to changes in temperature and precipitation in ours and other analyses (Robison & Scanlon, 2018). As directional changes in concentrations of SO_4^{2-} and base cations have counteracting effects in controlling ANC, dilution caused by climate change alone is expected to have little effect on ANC. This interaction likely explains why the contour plots of ANC and NO_3^- (Figures 4-8 & 4-9) show similar structure under low precipitation change but high temperature change conditions, however, note that the magnitude of changes of ANC are much larger than those of NO_3^-.

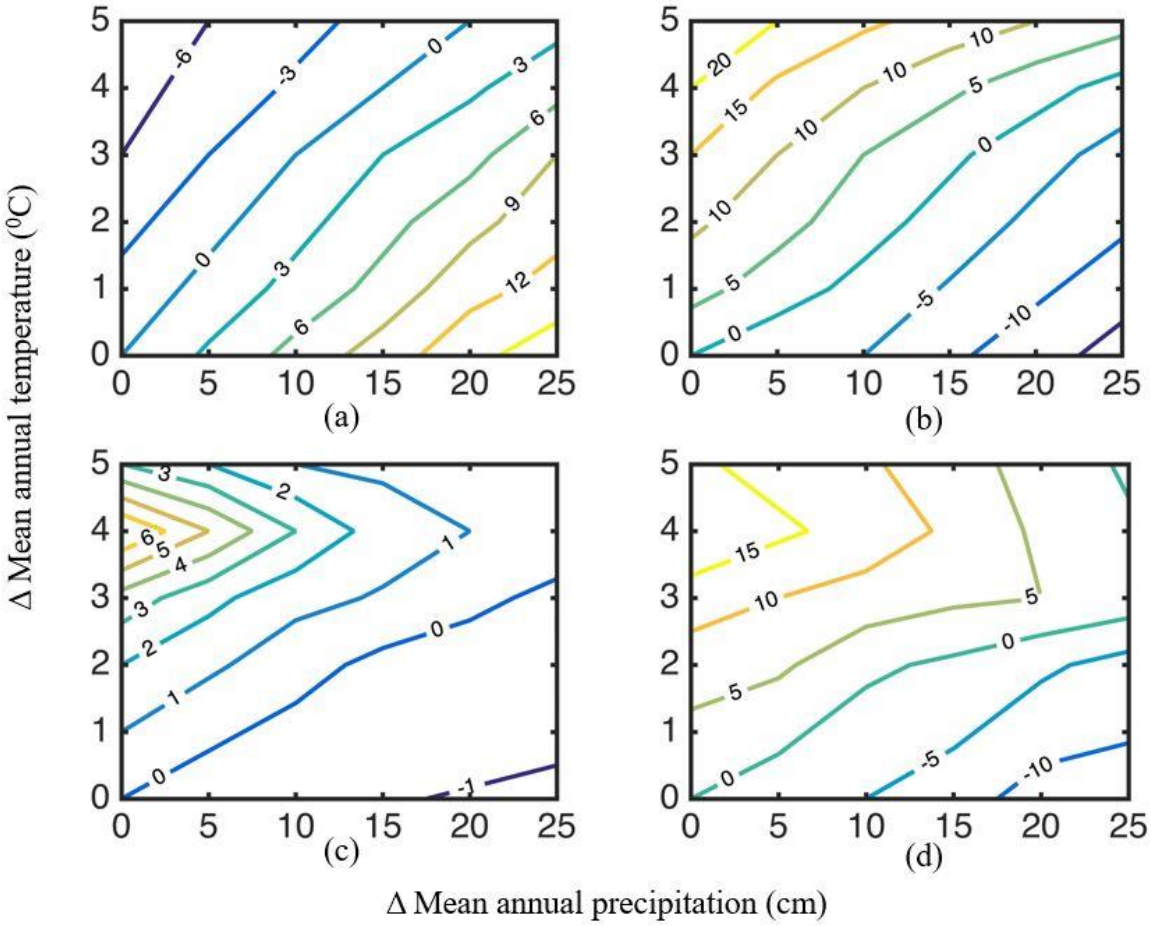

Figure 4-8. Contour plots illustrating the sensitivity of (a) annual discharge (in cm), (b) SO_4^{2-} (as µeq L^{-1}), (c) NO_3^- (as µeq L^{-1}) and (d) ANC (as µeq L^{-1}) in Archer Creek to changes in mean annual precipitation and temperature relative to stationary climate.

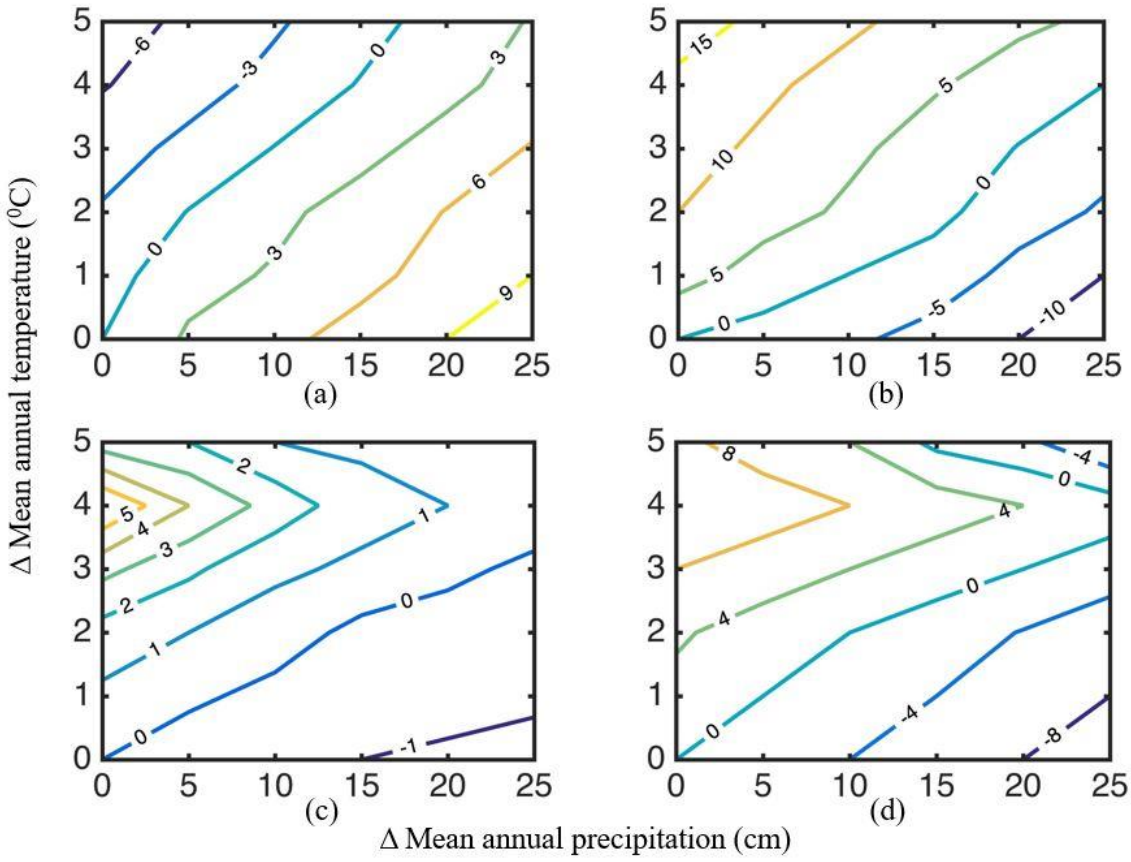

Figure 4-9. Contour plots illustrating the sensitivity of (a) annual discharge (in cm), (b) SO_4^{2-} (as µeq L^{-1}), (c) NO_3^- (as µeq L^{-1}) and (d) ANC (as µeq L^{-1}) in Buck Creek to changes in mean annual precipitation and temperature relative to stationary climate.

4.2.5 Limitation of modeling approach

Although the algorithms in PnET-BGC such as the depiction of the temperature and moisture dependence on the decomposition of organic matter and changes in stomatal conductance with variation in atmospheric CO_2 concentration that address changes in fixation of atmospheric CO_2, provide a useful framework to better understand how forest ecosystems may respond to future changes in climate and acidic deposition, simulation are limited by uncertainty in process representation and responses to changing climatic conditions.

A major limitation of PnET-BGC is the lack to a process basis for element weathering that allows for a response of mineral weathering rates with increasing temperature and changes in precipitation. PnET-BGC assumed a fixed element weathering rate throughout the simulation period based on model calibration with measured water quality and discharge. Previous studies have suggested that climate change may increase weathering rates and replenish exchangeable base cations in soil, thus accelerating recovery (Aherne et al., 2012; Akselsson et al., 2016).

PnET-BGC can be parameterized to simulate ambient concentrations of DOC and to depict its effects on the acid-base chemistry of surface waters (Gbondo-Tugbawa et al. 2001; Fakhraei & Driscoll 2015), however it is not able to effectively simulate the production of DOM from decomposition of plant detrital materials or microbial reprocessing of these carbon sources or factors affecting DOM partitioning with soil and changes in these processes under changing climatic conditions. Previous studies have demonstrated the importance of organic acids in controlling the acid-base behavior of surface waters, especially for waters with high DOC concentration (Fakhraei & Driscoll, 2015) and recent patterns of increases in DOM in surface waters or browning (Driscoll et al., 2016). A related short coming is the failure of models including PnET-BGC to simulate the dynamics of nutrients associated with soil organic matter (SOM) and DOM, particularly N, S and P, and the response of these processes to changing climatic conditions. For example, Mitchell and Likens (2011) indicated that with decreases in atmospheric S deposition, soil S mineralization is becoming the major source of SO_4^{2-} to streams and lakes, and increases in soil S mineralization would act to decrease ANC and slow recovery from acidic deposition. There are improved tools, such as isotopes for determining the age of C (e.g., Balesdent et al. 2018) and approaches for characterizing fractions and sources of organic C (e.g., LoRusso et al. 2020) that should facilitate improvements in model formulation and

parameterization. Given the ongoing changes in climatic conditions, decreases in acidic deposition and effects of browning, improved representation of SOM and DOM would seem to be an important focus of future modeling efforts.

PnET-BGC does not consider the changes in vegetation that may occur as climate changes and assumes a homogeneous distribution of vegetation and constant forest composition during simulations. It would be useful to evaluate the influence of shifts in vegetation composition under the changing climate condition or to link PnET-BGC with a forest community model that projects changes in species assemblages. Moreover, a single soil layer version of PnET-BGC model was used in this study. An algorithm of multiple soil layers that better depicts seasonal variation in stream chemical constituents and discharges could potentially improve the model performance by better simulating the dynamics of soil processes (Chen & Driscoll, 2005a; Valipour et al., 2018). Related to these limitations, PnET-BGC is incapable of depicting tipping points or fundamental structural changes that could occur to forest ecosystems particularly in response to extreme climate events (e.g., wildfire, hurricanes). Projecting the conditions leading to such an occurrence would be a valuable modeling endeavor.

Chapter 5. Sensitivity and uncertainty analysis of PnET-BGC modeling stream acidity in the Adirondacks

5.1 Methods

5.1.1 Sensitivity analysis

Sensitivity analysis was conducted to analyze the influence of changes in parameters on the results of an output of interest. In this study, I conducted sensitivity analysis of model parameters to identify those parameters with a greater impact on model output. The purpose of this analysis is to reduce the workload of analyzing the impact of each parameter on the model. Sensitivity analysis can be divided into local and global sensitivity approaches (Andrea Saltelli, K. Chan, 2009). Local sensitivity analysis is used to evaluate the effect of a single variable on the output of the model, and global sensitivity analysis considers the influence of multiple parameters on system output when they change simultaneously.

Local sensitivity analysis was used as a screening tool to evaluate which parameters and inputs have a significant impact on model outputs. The most widely used and simplest local sensitivity analysis, also known as the “One-at-A-Time” (OAT) method, considers only one input factor at a time on the local response of the parameters on the output of the model, where the other parameters remain constant in model simulation. Local sensitivity analysis mainly calculates the gradient of a variable near a fixed value to measure the sensitivity of the parameter. That is, the greater the gradient, the greater is the sensitivity of parameters. In this study, an OAT sensitivity analysis was conducted by examining the relative change in model output divided by the relative change in parameter values. This method is a simple approach to

evaluate general sensitivity of model parameters and inputs. The sensitivity index of a parameter Y_i is defined as (Jorgensen, 1994):

$$S_{Parameter,Y_i} = \frac{\partial X/X}{\partial Y_i/Y_i} \quad (5\text{-}1)$$

where the ∂X is the relative change in the model output X, and ∂Y_i is the relative change in the model input factor Y_i. The higher the value of $S_{Parameter,Y_i}$, the more sensitive the model is to the parameter of interest. Stream ANC was selected as the model output of interest since it is an integrating indicator of watershed sensitivity to acidic deposition. Sensitivity analyses were conducted on 16 model parameters and inputs. The analysis was conducted by examining the change in model output under pre-industrial (~1850) and future (2050) conditions in response to a change in a model parameter or input of interest. The model was run for each site to estimate the degree of sensitivity by applying a 15% change in model inputs and parameters, except for air temperature which was changed by 2 ^{o}C (i.e., increase and decrease). The most sensitive parameters were identified by comparing the average of calculated $S_{Parameter,Y_i}$ values for 25 modeled streams that were described in section 3.2.2.

5.1.2 Latin hypercube sampling method

Latin hypercube sampling (LHS) is a stratified sampling method proposed by McKay et al. (1979). The main idea of this method is to divide the entire design space into several non-overlapping subintervals. Each variable is sampled in its own interval to produce a random number (Helton & Davis, 2003). The advantage of this method is that it provides better coverage of the sampling area. The LHS method avoids the accumulation of sampling points formed by multiple sampling using a simple random sampling method and improves sampling efficiency.

The main steps of the LHS method are as follows: first, set the number of samples as n =500; then divide each of the variables into n subintervals of equal probability that do not overlap and cover the region of feasible parameter values, and for each parameter, generate a random number in each interval to obtain a set of sample combinations with n sample values. Compared with traditional random sampling, the LHS method can achieve better sample coverage using fewer iterations of sampling. When the number of samplings is large, insufficient sample concentration can be avoided.

5.1.3 Uncertainty analysis

The discrepancy between measured and model simulated stream and soil chemistry can originate from measurement uncertainty, model calibration processes, and model inadequacy. Monte Carlo uncertainty analysis was employed to describe the uncertainty in model outputs. Using the Monte Carlo technique, ± 15% uncertainty in the input factors was applied to the model output. Monte Carlo simulations were conducted to estimate uncertainty in model-predicted ANC by imposing this uncertainty on input factors. A uniform distribution ranging ± 15% around the calibrated and/or observed inputs were assigned to the input factors that were screened via OAT sensitivity analysis. A set of 500 samples was drawn from the uniform distribution of input factors using the Latin Hypercube Sample scheme. Monte Carlo simulation of Latin Hypercube samples resulted in 500 predictions for concentrations of major elements and ANC in stream and soil chemistry for the period of simulation. The distribution of model predictions provided an estimate of model uncertainty in response to the uncertainty in model inputs.

5.2 Results and discussion

5.2.1 First-order sensitivity analysis

The overall results of the local one-factor-at-a-time sensitivity analysis of model-simulated ANC to 16 model parameters and inputs for all 25 streams are shown in Table A-6. Although the most sensitive parameters are generally the same for different streams, there are differences in the magnitude of sensitivity of a given parameter from one watershed to another. The range of the first-order sensitivity index of model simulated ANC of 25 steams are summarized in Figure 5-1. The different physical characteristics of the study sites and the complex interactions among various components of the model contribute to the magnitude of variation in ANC change in model simulations. Overall, the sensitivity analysis indicated that the model is most sensitive to variation in precipitation quantity, Ca^{2+} and Na^{+} weathering rates, maximum monthly air temperature, SO_4^{2-} wet deposition, and DOC site density. This analysis (Table A-6) suggests that to improve the accuracy in simulating ANC, it is important to specify the values of these model inputs and parameters in model calibration processes and application. The model predicted ANC was relatively insensitive to changes in the other parameters, such as the aluminum solubility constant ($K_{Al(OH)3}$), organic acid dissociation constant (pK_{a1}, pK_{a2} and

pK_{a3}) and organic acid and Al binding constant (pK_{Al1}, pK_{Al2} and pK_{al3}).

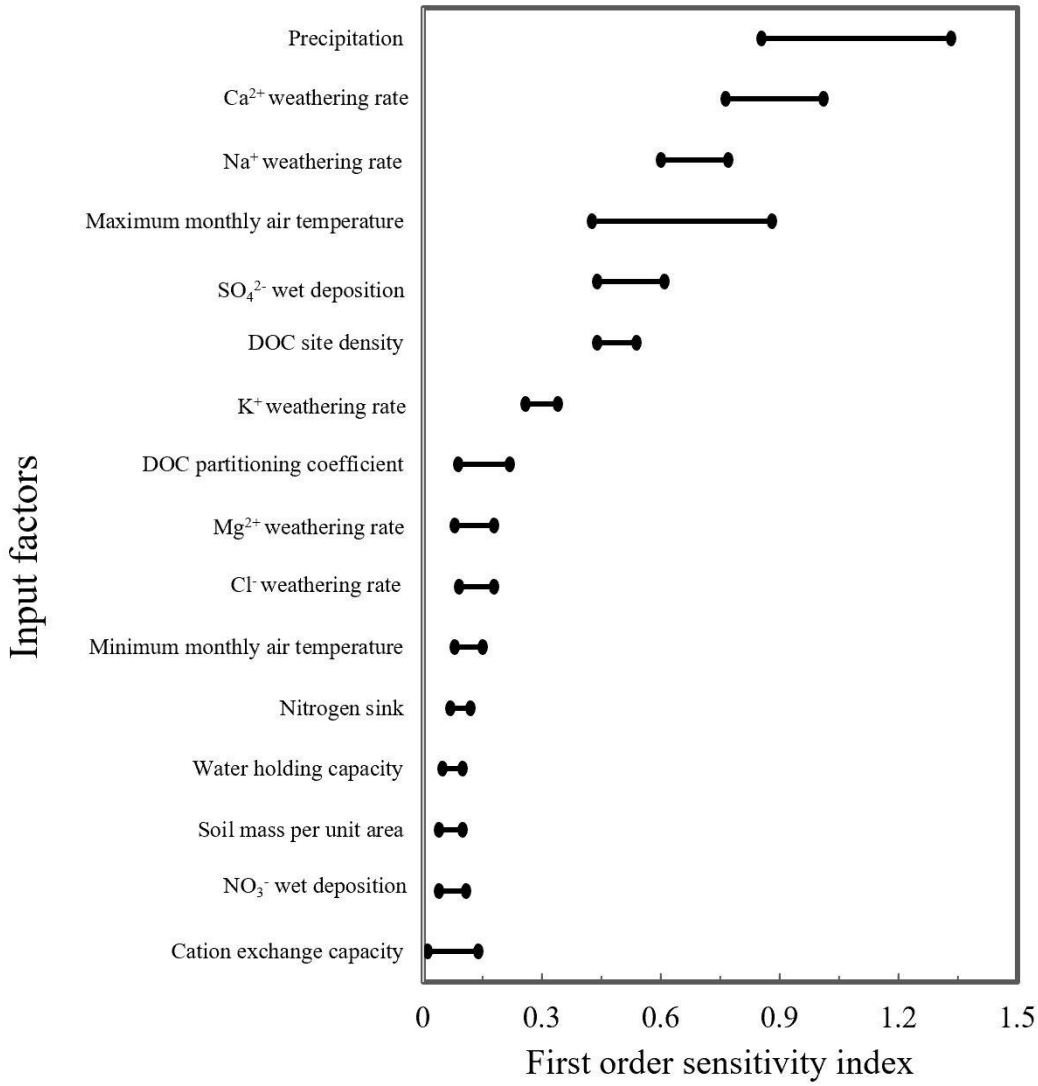

Figure 5-1. The range of the first-order sensitivity index of ANC simulated for 25 streams in the Adirondack region in 2050 based on a 15% variation in parameter or input values, except for air temperature which was changed by 2 ^{o}C change (i.e., increase and decrease).

5.2.2 Monte Carlo

Monte Carlo analysis was conducted to evaluate the uncertainty in the calibrated parameters which were screened using 'OAT' first-order sensitivity index of the model simulated ANC for year 2050. The Monte Carlo analysis under the assumption of a 30% interval uncertainty (± 15%) for the 16 input factors resulted in 500 simulations that were normally distributed around the original simulated stream ANC (the simulated ANC using the calibrated parameters) for year 2050 with a standard deviation of 15.3 μeq L^{-1} and 7.2 μeq L^{-1} for Archer Creek and Buck Creek, respectively (Figure 5-2).

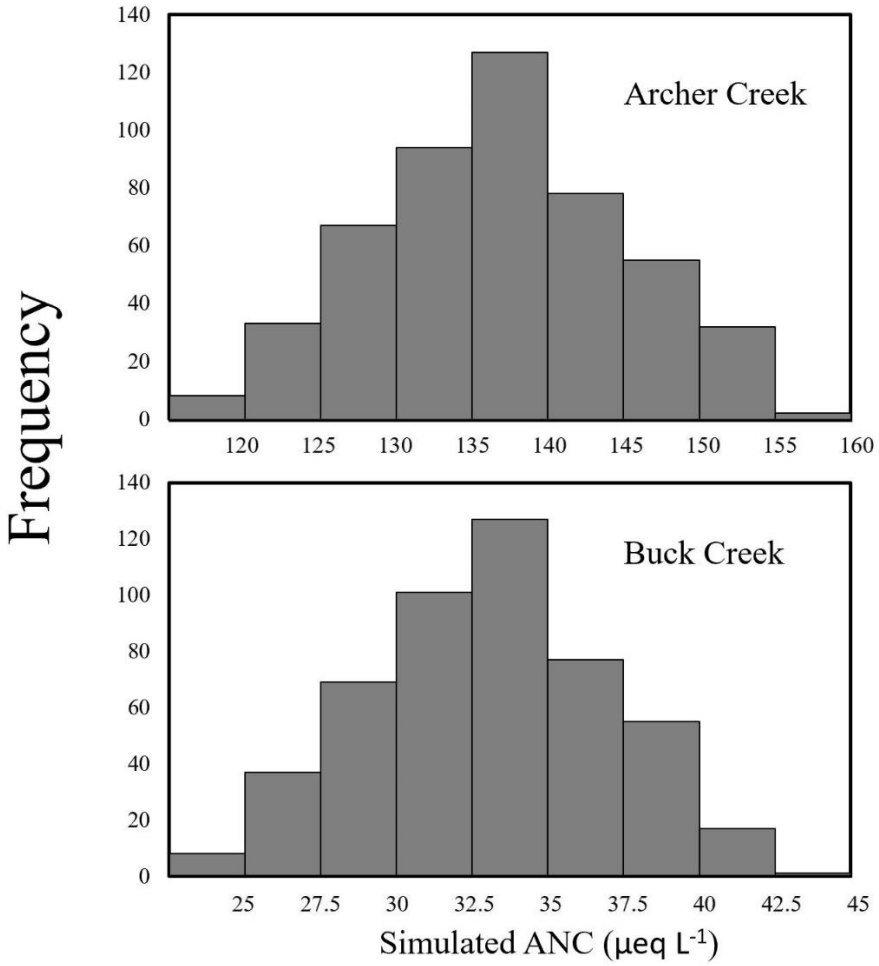

Figure 5-2. Frequency distribution of 500 Monte Carlo simulated ANCs for Archer Creek (top) and Buck Creek (bottom) in year 2050 in response to 30 % of uncertainty in 16 input factors.

The Spearman correlation coefficients (ρ) between Monte Carlo simulations and each perturbed input factor were calculated to evaluate the sensitivity of these input factors on the model simulated ANC (Table 5-1). The absolute value of the Spearman correlation coefficients (ρ) can be used to evaluate the influences of the perturbed input factors to the simulation of ANC (the positive values indicate the positive correlation, and the negative values indicate the inverse correlation between input factors and model simulated ANC). For Archer Creek, precipitation quantity (ρ = -0.62), Ca^{2+} weathering rate (ρ = 0.34), maximum monthly air temperature (ρ =

0.31), SO_4^{2-} wet deposition (ρ = -0.21), and Na^+ weathering rate (ρ = 0.18) were identified as the most important input factors for simulation of stream ANC. (Table 5-1). The overall results of the Spearman correlation coefficients (ρ) between input factors and model simulated ANC were consistent between Archer Creek and Buck Creek except soil cation exchange capacity (CEC), where it was positive for Archer Creek but negative for Buck Creek (Archer Creek: ρ = 0.03, Buck Creek: ρ= -0.01). Also, the ranking of the most important input factors was slightly different between two sites. The precipitation quantity (ρ = -0.39), Ca^{2+} weathering rate (ρ = 0.36), Na^+ weathering rate (ρ = 0.27), SO_4^{2-} wet deposition (ρ = -0.24), and maximum monthly air temperature (ρ = 0.17) were identified as the most important input factors for Buck Creek. The order of significance of these 16 input factors were found to be slightly different to the results of 'OAT' first-order sensitivity index analysis. The difference in the results of these two methods was due to the interaction effect between input factors that is considered in the Monte Carlo method, but is not addressed in the first-order sensitivity analysis (Table 5-1, Table A-6).

Table 5-1. Spearman correlation coefficients ($\rho < 0.05$) between input factors and model predicted ANC in 2050 for Archer Creek and Buck Creek.

Parameters	**Notation**	**Unit**	**ρ (Archer Creek)**	**ρ (Buck Creek)**
Precipitation	PPT	cm $month^{-1}$	-0.62	-0.39
Ca^{2+} weathering rate	Weathering Ca	g m^{-2} $month^{-1}$	0.34	0.36
Na^{+} weathering rate	Weathering Na	g m^{-2} $month^{-1}$	0.18	0.27
Maximum monthly air temperature	Tmax	˚C	0.31	0.17
SO_4^{2-} wet deposition	WetSO4	g S m^{-2} $month^{-1}$	-0.21	-0.24
DOC site density		(mol site) (mol C)$^{-1}$	-0.11	-0.07
K^{+} weathering rate	Weathering K	g m^{-2} $month^{-1}$	0.08	0.12
DOC partitioning coefficient	DOCPart		-0.06	-0.08
Mg^{2+} weathering rate	Weathering Mg	g m^{-2} $month^{-1}$	0.05	0.09
Cl^{-} weathering rate	Weathering Cl	g m^{-2} $month^{-1}$	-0.02	-0.03
Minimum monthly air temperature	Tmin	˚C	0.11	0.02
Nitrogen sink	Nsink	%	-0.08	-0.09
Water holding capacity	WHC	cm	0.06	0.08
Soil mass per unit area	SoilMass	kg m^{-2}	0.04	0.02
NO_3^{-} wet deposition	WetNO3	g S m^{-2} $month^{-1}$	-0.07	-0.12
Cation exchange capacity	CEC	mol kg^{-1}	0.03	-0.01

5.2.3 Comparison with other studies

The results of my sensitivity analysis and previous studies that have applied PnET-BGC to simulate surface water chemistry of forested watersheds were generally similar, but with some differences among studies conducted at different regions or at different sites or were conducted with different foci in terms of model inputs or parameters of interest (Fakhraei et al., 2017, 2014; Gbondo-Tugbawa et al., 2001; Zhou et al., 2015). Zhou et al. (2015) applied first-order

sensitivity analysis to Constable Pond in the Adirondack Park. Their results indicated that the model simulated surface water ANC was most sensitive to SO_4^{2-} wet deposition, NO_3^- wet deposition, cation exchange capacity (CEC), and soil mass. Gbondo-Tugbawa et al. (2001) applied first-order sensitivity analysis to the 21 parameters in the PnET-BGC model for simulations of stream water chemistry of a forested watershed at the Hubbard Brook Experimental Forest. They found that model prediction of ANC is most responsive to CEC, the adsorption coefficient of DOC, soil mass, and partial pressure of CO_2 in soil. In the study conducted by Fakhraei (2016), the results of sensitivity analysis indicated that the PnET-BGC model prediction of surface water ANC in the Adirondack park were most sensitive to Ca^{2+} and Na^+ weathering rates, partial pressure of CO_2 in soil and the adsorption coefficient of DOC. Another study by Fakhraei et al. (2017) evaluated the sensitivity of model inputs (e.g., meteorological data, atmospheric deposition) using first-order sensitivity analysis and Monte Carlo analysis, and found that meteorological input variables such as precipitation quantity are more influential than watershed characteristics parameters and deposition inputs variables in simulation of stream ANC in the Great Smokey Mountain, which is consistent with my study. My analysis suggests that PnET-BGC simulations of surface water ANC are most sensitive to the climatic drivers that are used as model inputs (e.g., precipitation, maximum monthly temperature). Therefore, accurate reconstruction of historical climate data and application of well constrained future climate predictions are important for accurate prediction of surface water ANC. In addition, if field or laboratory experiments are conducted to characterize soil properties and model parameter values (e.g., base cation weathering rate, CEC, soil selectivity coefficients and soil mass), improved accuracy of these values will also improve the accuracy in prediction of future surface water ANC using the PnET-BGC model.

Chapter 6. Conclusions

In phase 1 of the dissertation (Chapter 3), I applied the biogeochemical model PnET-BGC to 25 stream watersheds in the Adirondack region of New York to evaluate the recovery of ANC in response to different atmospheric emissions control scenarios. The model performance was directly proportional to the amount of time series data available to support model calibration and testing. Model simulations suggest that simultaneous controls of SO_4^{2-}, NO_3^- and NH_4^+ deposition would achieve the greatest recovery of Adirondack streams from acidification. Model hindcasts indicate that Adirondack streams had a broad range of pre-industrial (~1850) ANC values, ranging from about 10 to over 894 μeq L^{-1}. I applied two approaches to calculate TLs for stream acidity: a fixed ANC target of 20 μeq L^{-1} was used to protect the fish communities and a site-specific target was based on model-simulated pre-industrial ANC. The TLs analysis suggests that less reduction in acid deposition is needed to achieve the same ANC target if a longer recovery period is considered (e.g., 2150 vs. 2050). Based on this analysis, streams were categorized into three classes: streams that could achieve the ANC targets without further load reductions; streams that could achieve the ANC targets, but only with additional load reductions; streams that were unable to attain the ANC targets even under a scenario of complete elimination of anthropogenic acid deposition. Positive correlations between measured stream ANC and the TLs suggest that acid-sensitive stream sites that have lower ANC require more reduction in acid deposition to achieve the TL as compared with less acid-sensitive streams. The application of empirical equations indicate that historical acidification has impacted fish communities, including loss of fish density and biomass, but they could recover to some degree under the acid deposition reduction control scenarios. Integrated analysis of stream chemistry modeling,

variation in stream chemistry under varying hydrologic conditions and fish health surveys were used to project changes in stream chemistry and fish communities in response to changes in acid deposition to inform resource management and provide a framework for decision-making.

In phase 2 of this study (Chapter 4), I applied the biogeochemical model PnET-BGC to two forest watersheds in the Adirondack region of New York State to evaluate the response of soils and streams to projected future changes in the combined effects of climate and acidic deposition. Statistically downscaled results from 17 AOGCMs indicated that the mean maximum and minimum air temperature and precipitation would increase in the Adirondack region by the end of 2100 under the RCP 4.5 and RCP 8.5 scenarios. Model simulations indicate that stream concentrations of SO_4^{2-} and NO_3^- are projected to decrease and stream ANC and soil BS% increase at both sites in response to acidic deposition reduction scenarios. However, when simulating simultaneous changes in acidic deposition and climate, the extent of this recovery is diminished. Model simulations indicated that changes in temperature and precipitation influence stream discharge, concentrations of SO_4^{2-} and NO_3^-, and ANC through physical, chemical and biological processes depicted in the model. Emission control strategies designed to reduce acidic deposition have and can further accelerate recovery from historical acidification at both watershed sites, but with contrasting patterns due to differences in their inherent sensitivity to acid deposition. The simulation results suggest acid-sensitive watersheds like Buck Creek would gain more ANC from deposition control strategies, while the acid-insensitive site Archer Creek would experience a larger offset of ANC increases due to effects of climate change. In the study, TLs that consider both deposition and climate changes were calculated and compared to stationary climate values to help inform policy makers and natural resource managers on the

extent to which further emissions reductions will be necessary to achieve a given level of recovery under the changing climate.

In phase 3 of this study (Chapter 5), the first-order sensitivity and Latin Hypercube sampling-Monte Carlo analysis was applied to evaluate PnET-BGC model simulation of stream ANC in the Adirondack region. Among 16 input factors which were examined in this analysis, I identified that precipitation quantity, Ca^{2+} weathering rate, Na^{+} weathering rate, maximum monthly air temperature, SO_4^{2-} wet deposition, DOC site density, K^{+} weathering rate and DOC partitioning coefficient as the most influential input factors for model simulation of stream ANC of Adirondack streams. The results of this analysis suggest that if the uncertainty of these most sensitive input factors can be reduced, the accuracy of future prediction of stream ANC will be improved. In Chapter 3, I assumed stationarity in meteorological inputs (mean of recent observations) for future projections. However, the sensitivity analysis indicates that prediction of stream water ANC is highly sensitive to changes in precipitation quantity and air temperature. Therefore, the future studies that evaluate the recovery of surface water from historical acidification using PnET-BGC model simulation should incorporate projections of temperature, precipitation, and atmospheric concentrations of carbon dioxide. This research helps identify important data collection and laboratory and/or field experiments needed to improve the predictions of future ANC. For example, by increasing the number of meteorological and deposition monitoring stations inside or close to the Adirondack Park and conducting lab and field experiments to estimate of Ca^{2+} and Na^{+} weathering rates will reduce the uncertainty of these input factors and improve the accuracy of simulation stream water ANC. Accurate prediction of stream ANC can be used to calculate the target loads to protect forest and fishery resources for the region.

Chapter 7. Future research recommendations

In this study, I performed the sensitivity and uncertainty analysis for PnET-BGC model simulation of stream ANC. The results indicated that ANC is most sensitivity to the input factors, involving meteorological inputs and base cation weathering. Therefore, accurate reconstruction of the historical meteorological data and future projections of meteorological condition will significantly reduce the uncertainty in model simulation of ANC. Future work could focus on evaluation of different statistical methods used to downscale the climate projection from larger scale simulations to local scale conditions. Also, future research should conduct more field/lab work to provide direct measurement of base cation weathering rate and other improved parameterization, like SO_4^{2-} adsorption rate.

Future work might include the development of a comprehensive atmospheric-watershed modeling framework. For example, the CMAQ (Community Multiscale Air Quality Modeling System) and PnET-BGC model could be linked as a decision-making tool. PnET-BGC is a comprehensive biogeochemical model and CMAQ is a comprehenisve air quality model. This framework could enable decision makers to directly link the emission scenarios to watershed chemical indicators to address environmental management questions.

Future work could be conducted to improve the representation of hydrologic flow paths in PnET-BGC. In this study, a single soil layer version of PnET-BGC was used. An algorithm of multiple soil layers may better depict the temporal patterns in stream chemistry. Parameterizing the model with multi-layer soil profile would potentially improve the model performance by better simulating the dynamics of soil processes and effects of hydrological flowpaths.

In this study, the projections of DOC under climate change scenarios decreased in comparison to the reference scenario. These decreases are inconsistent with the hypothesis that climate change would drive increases in stream water DOC. DOC will likely continue to have an increasing trend at the Adirondacks based on the long-term monitoring data (Driscoll et al. 2016). One possible explanation for this pattern is due to recent increases on pH associated with decreases in acidic deposition. With increasing pH, the partitioning of DOC with soil would decrease. PnET-BGC includes simple pH dependent algorithm for DOC adsorption, which represented by analog organic anions (Fakhraei et al. 2015; e.g. $XOrg^{3-}$, $XHOrg^{2-}$ and XH_2Org^{-}). The equilibrium constants were obtained based on calibration of Carry Lake in Adirondack. Future work could focus on improving the pH dependent for DOC adsorption algorithm and parameterization of this algorithm.

PnET-BGC assumed a fixed element weathering rate throughout the simulation period based on model calibration with measured water quality and discharge. Previous studies have suggested that climate change may increase weathering rates and help replenish base cations depleted under historical acid deposition, thus accelerating recovery (Aherne et al., 2012; Akselsson et al., 2016). Future study should consider adding an algorithm to allow changing mineral weathering rates with increasing temperature and changes in precipitation.

Future research should consider linking PnET-BGC with a forest community model that projects changes in vegetation species assemblages. Such a simulator would be useful to evaluate the influence of shifts in vegetation composition under the changing climate condition.

Appendices

Table A-1. Site IDs, sample dates or date ranges, and data sources for chemistry data from 25 Adirondack streams that were applied to calibrate the PnET-BGC model. Observed acid neutralizing capacity (ANC) of 25 study streams (that were simulated using the PnET-BGC model), and the average ratio of estimated SO_4^{2-} and NO_3^- deposition at each site to SO_4^{2-} and NO_3^- deposition at Huntington Forest (HF).

Project Site ID	USGS Site ID	Samples Dates Applied in Model Calibration	ANC	Deposition ratio	Source of Data	USGS Gage ID for Flow Percentile Estimate
North Buck Creek	04253295	1998-2014 (n=697)	-42.5	1.02	1	04253295
35014	432910075001001	10/27/03, 3/31/04, 8/16/04, 3/31/05	-32.1	1.21	1	04253296
27026	434154074445701	10/28/03, 3/29/04, 8/17/04	-26.9	1.06	1	04253296
T24	0134277112	2011-2015 (n=104)	-26.2	1.03	1	04256000
22019	435115075093901	8/26/03, 10/28/03, 3/31/04, 8/17/04, 3/30/05	-8.9	1.22	1	04253296
12003	440151075084801	10/29/03, 3/31/04, 8/18/04, 3/31/05	-13.2	1.18	1	04253296
WF	434816074494201	5/5/2011	-3.7	1.06	1	04253296
South Buck Creek	04253294	1998-2014 (n=689)	14.0	1.05	1	04253294
13008	440201075053401	10/29/03, 3/31/04, 8/18/04, 3/31/05	20.6	1.13	1	04253296
24002	434544074411101	8/25/03, 10/28/03, 3/31/04, 8/18/04, 3/30/05	21.0	1.05	1	04253296
28011	433918074403501	8/25/03, 10/29/03, 3/29/04, 8/17/04, 3/29/05	32.4	1.08	1	04253296
28014	433820074410001	8/26/03, 10/29/03, 3/30/04, 8/17/04, 3/30/05	11.5	1.02	1	04253296
NW	434836074030201	5/5/2011	12.4	1.02	1	01312000
Buck Creek	04253296	ANC & pH 1991-2014 (n=1536), other constituents 1997-2014 (n=867)	17.7	1.09	1	04253296
AMP	441424074155501	5/18/2011	42.1	0.96	1	01312000
27019	434256074453801	8/26/03, 10/28/03, 3/29/04, 8/17/04, 3/29/05	70.0	1.07	1	04253296
Archer Creek	Not USGS data	1996-2015	137.5	1.00	2	01312000
30009	433553075062101	8/26/03, 10/28/03, 3/29/04, 8/17/04, 3/29/05	97.0	1.23	1	04253296
26008	434001075045401	8/27/03, 10/29/03, 3/29/04, 8/17/04, 3/31/05	102.6	1.19	1	04253296
30019	433548075110101	10/28/03, 3/31/04, 8/17/04, 3/30/05	127.7	1.28	1	04253296
29012	433324075165001	8/25/03, 10/29/03, 3/29/04, 8/16/04, 3/29/05	147.7	1.35	1	04253296
28030	434500074441601	10/29/03, 3/31/04, 8/18/04, 3/31/05	217.9	1.09	1	04253296
N1	440034074184801	5/18/2011	238.0	0.96	1	01312000
24001	434606074424901	8/25/03, 10/29/03, 3/31/04, 8/18/04, 3/30/05	369.9	1.09	1	04253296

S14	Not USGS data	2009-2015 (n=365)	758.3	0.93	2	01312000

1 – https://waterdata.usgs.gov/nwis
2 - https://www.esf.edu/hss/em/huntington/archive.html

Table A-2. Regression models used to reconstruct the historical wet deposition at Huntington Forest between 1900 and 1978.

The regression models were developed using annual national emissions (Tg yr^{-1}) and concentration in precipitation (mg L^{-1}) measured at an NADP site in the Adirondacks (NY20) during the period 1979-2015.

Concentration in Precipitation	=	Intercept	+	Slope	x	National Emission	R^2	P-Value
Ca^{2+}		1.701		0.681		PM_{10}	0.63	<0.001
Mg^{2+}		-0.151		0.358		PM_{10}	0.59	<0.001
K^{+}		0.126		0.047		PM_{10}	0.34	<0.001
Na^{+}		-0.321		0.598		PM_{10}	0.49	<0.001
NH_4^{+}		6.07		0.201		NO_x	0.09	0.065
NO_3^{-}		-6.603		1.202		NO_x	0.75	<0.001
Cl^{-}		0.986		0.388		PM_{10}	0.43	<0.001
SO_4^{2-}		-3.012		1.893		SO_2	0.70	<0.001

Table A-3. Summary of the model inputs and parameters used in the PnET-BGC model.

Model Inputs	Notation	Unit
Precipitation	PPT	cm $month^{-1}$
Maximum monthly air temperature	Tmax	˚C
Minimum monthly air temperature	Tmin	˚C
Daily solar radiation	PAR	μmol m^{-2} s^{-1}
Mean monthly atmospheric CO_2 concentration	CO2c	ppm
SO_4^{2-} wet atmospheric deposition	Wet $_{SO4}$	g S m^{-2} $month^{-1}$
NO_3^- wet atmospheric deposition	Wet $_{NO3}$	g N m^{-2} $month^{-1}$
NH_4^+ wet atmospheric deposition	Wet $_{NH4}$	g N m^{-2} $month^{-1}$
Na^+ wet atmospheric deposition	Wet $_{Na}$	g m^{-2} $month^{-1}$
Mg^{2+} wet atmospheric deposition	Wet $_{Mg}$	g m^{-2} $month^{-1}$
K^+ wet atmospheric deposition	Wet $_{K}$	g m^{-2} $month^{-1}$
AL^{3+} wet atmospheric deposition	Wet $_{Al}$	g m^{-2} $month^{-1}$
F^- wet atmospheric deposition	Wet $_{F}$	g m^{-2} $month^{-1}$
Cl^- wet atmospheric deposition	Wet $_{Cl}$	g m^{-2} $month^{-1}$
SO_4^{2-} dry to wet atmospheric deposition ratio	DWR $_{SO4}$	
NO_3^- dry to wet atmospheric deposition ratio	DWR $_{NO3}$	
NH_4^+ dry to wet atmospheric deposition ratio	DWR $_{NH4}$	
Na^+ dry to wet atmospheric deposition ratio	DWR $_{Na}$	
Mg^{2+} dry to wet atmospheric deposition ratio	DWR $_{Mg}$	
K^+ dry to wet atmospheric deposition ratio	DWR $_{K}$	
Al^{3+} dry to wet atmospheric deposition ratio	DWR $_{Al}$	
F^- dry to wet atmospheric deposition ratio	DWR $_{F}$	
Cl^- dry to wet atmospheric deposition ratio	DWR $_{Cl}$	
Site characteristics and biogeochemistry parameters		
Water holding capacity	WHC	cm
Nitrogen sink	Nsink	%
Soil mass per unit area	SoilMass	kg m^{-2}
SO_4^{2-} adsorption coefficient	K $_{XSO4}$	
DOC adsorption coefficient	K $_{XDOC}$	
Cation exchange capacit	CEC	mol kg^{-1}
DOC site density	m	(mol site) (mol C)$^{-1}$
DOC partitioning coefficient	DOCPart	
Fast flow fraction	Fast flow frac	%
Ca weathering rate	Weathering Ca	g m^{-2} $month^{-1}$
Na weathering rate	Weathering Na	g m^{-2} $month^{-1}$
Mg weathering rate	Weathering Mg	g m^{-2} $month^{-1}$
Al weathering rate	Weathering Al	g m^{-2} $month^{-1}$
K weathering rate	Weathering K	g m^{-2} $month^{-1}$
Cl weathering rate	Weathering Cl	g m^{-2} $month^{-1}$

Table A-3. (Continued).

Model Inputs	Notation	Unit
S weathering rate	Weathering S	g m^{-2} $month^{-1}$
P weathering rate	Weathering P	g m^{-2} $month^{-1}$
F weathering rate	Weathering F	g m^{-2} $month^{-1}$
Selectivity coefficient of Mg^{2+} against H^{+}	K_{X2Mg}	
Selectivity coefficient of Ca^{2+} against H^{+}	K_{X2Ca}	
Selectivity coefficient of K^{+} against H^{+}	K_{XK}	
Selectivity coefficient of Al^{3+} against H^{+}	K_{X3Al}	
Selectivity coefficient of Na^{+} against H^{+}	K_{XNa}	
First organic acid dissociation constant	pKa1	
Second organic acid dissociation constant	pKa2	
Third organic acid dissociation constant	pKa3	
Aluminum solubility constant	$K_{Al(OH)3}$	
First organic acid and Al binding constant	$pKAl_1$	
Second organic acid and Al binding constant	$pKAl_2$	
Third organic acid and Al binding constant	$pKAl_3$	
First apparent soil acidity constant	K_{XOH2}	
Second apparent soil acidity constant	K_{XO}	

Table A-4. Mean flow percentile and observed ANC based on samples at each site that were applied in model calibration of PnET-BGC. ANC values were adjusted to the Q_{27} flow percentile according to the approach described in the section 3.1.6.

Site	Flow Percentile	ANC (□eq L^{-1})	ANC at Q_{27} Flow Percentile (□eq L^{-1})
North Buck	63.4	-42.0	-33.9
35014	79.2	-35.2	-26.2
27026	74.5	-27.1	-27.6
T24	55.1	-24.3	-7.7
22019	75.4	-16.2	1.4
12003	62.4	-3.8	5.4
WF	10.4	-3.7	-7.1
South Buck	63.4	9.5	29.2
13008	73.0	3.8	24.9
24002	71.7	4.2	39.8
28011	74.5	8.2	-1.4
28014	83.6	14.8	39.1
NW	3.6	12.4	4.2
Buck Creek	63.4	16.6	36.3
AMP	11.5	42.1	32.6
27019	83.0	112.4	367.2
Archer	57.0	111.1	125.5
30009	82.0	118.2	270.4
26008	83.6	115.9	225.1
30019	63.8	119.7	231.5
29012	83.0	158.3	345.9
28030	63.4	226.2	309.6
N1	11.5	238.0	201.5
24001	71.7	262.2	438.6
S14	54.1	784.9	848.7

Table A-5. Summary of metrics of model performance in the simulation of Ca^{2+}, SO_4^{2-}, NO_3^- ANC and DOC concentrations for all 25 modeled Adirondack streams and soil base saturation of their watersheds.

Stream Constituent	NME[a]		NMAE[b]	
	Mean	SD	Mean	SD
Ca^{2+}	-0.13	0.12	0.16	0.11
SO_4^{2-}	0.04	0.05	0.08	0.05
NO_3^-	0.18	0.14	0.35	0.24
ANC	-0.11	0.17	0.18	0.15
DOC	-0.15	0.11	0.17	0.10
% BS	-0.26	0.15	0.26	0.15

[a] NME - normalized mean error;

[b] NMAE - normalized mean absolute error.

Table A-6. Summary of sensitivity analysis of the PnET-BGC simulated ANC (2050) in response to variation in 16 input factors used in the model. Average values of the first-order sensitivity index for 25 modeled streams are sorted by absolute value.

Parameters	Notation	Unit	S_{ANC}
Precipitation	PPT	cm $month^{-1}$	1.09
Ca^{2+} weathering rate	Weathering Ca	g m^{-2} $month^{-1}$	0.93
Na^{+} weathering rate	Weathering Na	g m^{-2} $month^{-1}$	0.67
Maximum monthly air temperature	Tmax	˚C	0.61
SO_4^{2-} wet deposition	WetSO4	g S m^{-2} $month^{-1}$	0.52
DOC site density		(mol site) (mol C)$^{-1}$	0.52
K^{+} weathering rate	Weathering K	g m^{-2} $month^{-1}$	0.31
DOC partitioning coefficient	DOCPart		0.16
Mg^{2+} weathering rate	Weathering Mg	g m^{-2} $month^{-1}$	0.11
Cl^{-} weathering rate	Weathering Cl	g m^{-2} $month^{-1}$	0.10
Minimum monthly air temperature	Tmin	˚C	0.10
Nitrogen sink	Nsink	%	0.08
Water holding capacity	WHC	cm	0.06
Soil mass per unit area	SoilMass	kg m^{-2}	0.06
NO_3^{-} wet deposition	WetNO3	g S m^{-2} $month^{-1}$	0.04
Cation exchange capacity	CEC	mol kg^{-1}	0.02

Table A-7. Comparisons between PnET-BGC model estimates of preindustrial (Year 1850) chemistry and estimates for Year 2000 and ambient (Year 2015) chemistry (units in µeq L^{-1}) for 25 modeled sites.

	Simulated Preindustrial (Year 1850) Chemistry			Simulated Year 2000 Chemistry			Simulated Ambient (Year 2015) Chemistry		
Site	SO_4^{2-}	NO_3^-	ANC	SO_4^{2-}	NO_3^-	ANC	SO_4^{2-}	NO_3^-	ANC
North_Buck	31.6	6.8	22.8	114.4	24.4	-44.3	67.5	18.6	-42.1
35014	17.5	6.2	10.0	62.1	67.1	-45.8	42.6	70.2	-34.1
27026	15.1	7.5	25.5	81.5	64.7	-31.2	46.4	65.2	-27.8
T24	14.8	3.9	28.7	75.1	18.4	-31.2	53.4	16.8	-22.8
22019	25.5	3.8	23.4	94.1	36.1	-23.5	62.2	13.8	-16.4
12003	20.5	3.9	28.2	75.5	17.8	-14.5	47.6	21.4	-2.3
WF	8.8	7.8	25.9	71.8	45.2	-15.8	53.7	36.8	-3.7
South_Buck	24.4	4.8	53.2	93.4	35.2	7.8	72.4	48.5	9.6
13008	30.4	4.2	38.4	112.8	56.3	2.1	81.6	33.8	4.0
24002	16.1	8.9	37.3	85.4	76.3	-6.8	52.3	58.7	2.8
28011	19.2	4.6	52.6	70.7	43.7	4.8	42.6	46.4	7.6
28014	9.0	7.2	51.8	71.6	58.2	8.7	65.3	33.9	14.8
NW	11.3	3.3	56.5	73.7	19.5	-2.1	67.3	11.8	11.5
Buck Creek	22.9	5.7	56.3	111.7	42.7	12.2	94.4	23.6	19.7
AMP	31.7	4.5	93.1	119.6	29.4	30.8	94.2	30.7	37.5
27019	31.2	6.5	160.6	113.3	57.9	96.4	92.2	31.5	115.7
Archer	42.7	4.8	148.8	112.5	38.8	102.1	85.1	27.9	110.7
30009	36.5	6.1	155.8	127.7	42.9	113.5	74.9	21.1	114.8
26008	33.6	4.1	163.2	102.6	30.8	108.5	62.4	11.5	112.2
30019	10.4	7.3	163.8	63.8	18.5	108.8	45.2	20.5	113.4
29012	27.2	4.0	218.3	116.4	18.1	147.3	77.8	11.2	154.1
28030	7.8	4.2	271.6	74.2	60.7	216.2	49.1	31.2	230.1
N1	20.4	5.5	285.1	102.9	40.7	212.2	70.9	32.2	230.1
24001	30.9	7.9	336.8	137.7	64.8	201.2	105.3	54.8	221.4
S14	41.3	5.2	894.1	145.2	40.5	720.4	128.2	58.5	738.7

Table A-8. Modeled stream recovery classes.

Site	Site could achieve ANC criterion without further deposition reduction		Site could achieve ANC criterion only with further deposition reduction		Site unable to achieve ANC criterion even if deposition is decreased to preindustrial level and held there	
	Year 2050	Year 2150	Year 2050	Year 2150	Year 2050	Year 2150
Target ANC = 20 µeq L^{-1}						
North Buck					X	X
35014					X	X
27026					X	X
T24					X	X
22019					X	X
12003				X	X	
WF					X	X
South Buck			X	X		
13008			X	X		
24002			X	X		
28011		X	X			
28014			X	X		
NW	X	X				
Buck Creek	X	X				
AMP	X	X				
27019	X	X				
Archer	X	X				
30009	X	X				
26008	X	X				
30019	X	X				
29012	X	X				
28030	X	X				
N1	X	X				
24001	X	X				
S14	X	X				
Target ANC = Site-Specific						
North Buck					X	X
35014					X	X
27026					X	X
T24					X	X
22019				X	X	
12003			X	X		
WF			X	X		
South Buck					X	X
13008			X	X		
24002			X	X		

Table A.8 (continued)

Site	Site could achieve ANC criterion without further deposition reduction		Site could achieve ANC criterion only with further deposition reduction		Site unable to achieve ANC criterion even if deposition is decreased to preindustrial level and held there	
	Year 2050	Year 2150	Year 2050	Year 2150	Year 2050	Year 2150
28011				X	X	
28014			X	X		
NW			X	X		
Buck Creek				X	X	
AMP				X	X	
27019					X	X
Archer			X	X		
30009			X	X		
26008			X	X		
30019			X	X		
29012					X	X
28030				X	X	
N1	X	X				
24001		X	X			
S14					X	X

Table A-9. Predicted fish density (# of fish/0.1 ha) for the 25 model sites under preindustrial (1850), ambient (2015), and future (2150) scenario summer baseflow ANC Q_{27} conditions.

Site	Preindustrial (1850)	Ambient (2015)	Future Scenario (2150)							Target Load
			1	2	3	4	5	6	7	Site-Specific
North Buck	196	16	63	64	70	77	83	90	44	143
35014	162	39	57	59	60	62	64	65	27	108
27026	182	35	52	55	57	62	68	72	21	129
T24	228	92	142	145	150	157	165	173	137	177
22019	221	117	132	145	148	154	164	171	106	170
12003	208	128	151	153	157	165	176	190	148	157
WF	174	94	115	117	120	125	128	133	98	120
South Buck	296	191	213	216	220	226	234	239	201	250
13008	265	180	198	204	211	219	226	234	192	216
24002	300	218	231	237	246	256	265	275	229	253
28011	227	110	149	162	177	198	213	224	127	177
28014	304	216	225	231	244	270	292	300	210	257
NW	241	125	161	170	183	193	212	231	140	191
Buck Creek	297	209	230	235	244	256	264	281	223	250
AMP	330	200	242	256	267	285	303	326	210	286
27019	690	681	684	684	685	686	687	687	681	688
Archer	476	407	424	426	428	433	438	442	397	441
30009	652	617	630	631	635	640	644	649	613	636
26008	623	566	583	592	594	602	610	619	570	603
30019	628	574	598	601	605	613	619	627	579	609
29012	690	672	679	680	681	683	685	687	673	687
28030	675	651	658	660	662	666	669	671	647	665
N1	603	534	573	577	581	588	594	599	546	580
24001	631	689	647	646	645	642	638	634	652	647
S14*	NA	NA	NA	NA	NA	NA	NA	NA	NA	NA
Mean	519	432	462	466	471	479	486	494	446	488
Median	300	209	230	235	244	256	265	281	210	253

* Stream S14 was not analyzed for predicting fish metrics because its ANC was very high, well beyond the level used to develop the fish metric equations. The acid-base chemistry of this lake would support relatively high richness over time, irrespective of acidic deposition; NA = not applicable.

Table A-10. Predicted fish biomass (g/0.1 ha) for the 25 model sites under preindustrial (1850), ambient (2015), and future (2150) scenario summer baseflow ANC Q_{27} conditions.

Site	Preindustrial (1850)	Ambient (2015)	Future Scenario (2150) 1	2	3	4	5	6	7	Target Load Site-Specific
North	1140	-287	191	202	257	321	365	427	3	829
35014	946	-44	129	148	159	175	194	210	-177	572
27026	1066	-85	83	111	133	177	232	271	-233	731
T24	1297	447	819	836	870	919	966	1011	788	1038
22019	1268	646	750	840	860	899	963	1001	560	999
12003	1204	725	882	894	914	968	1032	1107	858	914
WF	1018	459	630	642	666	698	726	758	493	666
South	1567	1115	1226	1240	1259	1291	1327	1347	1166	1392
13008	1454	1054	1153	1184	1218	1255	1290	1324	1122	1245
24002	1578	1251	1314	1338	1379	1419	1455	1490	1303	1407
28011	1295	586	867	948	1035	1154	1228	1279	717	1035
28014	1591	1242	1284	1310	1371	1471	1551	1579	1215	1424
NW	1356	701	945	994	1072	1128	1224	1312	807	1115
Buck	1568	1209	1307	1330	1368	1420	1450	1513	1277	1393
AMP	1675	1161	1361	1419	1460	1526	1591	1663	1212	1530
27019	2810	2810	2816	2817	2818	2819	2820	2820	2810	2820
Archer	2060	1882	1927	1932	1937	1950	1961	1972	1856	1969
30009	2696	2544	2600	2605	2620	2641	2662	2682	2527	2627
26008	2568	2342	2403	2438	2449	2481	2514	2550	2355	2483
30019	2591	2372	2462	2475	2493	2525	2552	2586	2390	2508
29012	2812	2781	2804	2806	2810	2815	2818	2819	2785	2820
28030	2790	2690	2721	2733	2738	2755	2769	2777	2674	2751
N1	2485	2233	2365	2381	2397	2422	2446	2470	2272	2395
24001	3034	2782	2867	2873	2888	2913	2957	3000	2830	2867
S14*	NA	NA	NA	NA	NA	NA	NA	NA	NA	NA
Mean	2185	1947	2025	2035	2048	2069	2090	2110	1983	2094
Median	1578	1209	1307	1330	1371	1420	1455	1513	1215	1407

* Stream S14 was not analyzed for predicting fish metrics because its ANC was very high, well beyond the level used to develop the fish metric equations. The acid-base chemistry of this lake would support relatively high richness over time, irrespective of acidic deposition; NA = not applicable.

References

Aber, J. D., & Freuder, R. (2000). Variation among solar radiation data sets for the Eastern US and its effects on predictions of forest production and water yield. *Climate Research*, *15*(1), 33–43. https://doi.org/10.3354/cr015033

Aber, John D., & Federer, C. A. (1992). A generalized, lumped-parameter model of photosynthesis, evapotranspiration and net primary production in temperate and boreal forest ecosystems. *Oecologia*. https://doi.org/10.1007/BF00317837

Aber, John D., Ollinger, S. V., & Driscoll, C. T. (1997). Modeling nitrogen saturation in forest ecosystems in response to land use and atmospheric deposition. *Ecological Modelling*. https://doi.org/10.1016/S0304-3800(97)01953-4

Aherne, J., Posch, M., Forsius, M., Lehtonen, A., & Härkönen, K. (2012). Impacts of forest biomass removal on soil nutrient status under climate change: A catchment-based modelling study for Finland. *Biogeochemistry*, *107*(1–3), 471–488. https://doi.org/10.1007/s10533-010-9569-4

Akselsson, C., Olsson, J., Belyazid, S., & Capell, R. (2016). Can increased weathering rates due to future warming compensate for base cation losses following whole-tree harvesting in spruce forests? *Biogeochemistry*, *128*(1–2), 89–105. https://doi.org/10.1007/s10533-016-0196-6

Andrea Saltelli, K. Chan, E. M. S. (2009). *Sensitivity Analysis*. WILEY.

April, R., Newton, R., & Coles, L. T. (1986). Chemical weathering in two Adirondack watersheds: past and present-day rates. *Geological Society of America Bulletin*, *97*(10),

1232–1238. https://doi.org/10.1130/0016-7606(1986)97<1232:CWITAW>2.0.CO;2

Arseneau, K. M. A., Driscoll, C. T., Cummings, C. M., Pope, G., & Cumming, B. F. (2016). Adirondack (NY, USA) reference lakes show a pronounced shift in chrysophyte species composition since ca. 1900. *Journal of Paleolimnology*, *56*(4), 349–364. https://doi.org/10.1007/s10933-016-9922-2

Baldigo, B. P., George, S. D., Lawrence, G. B., & Paul, E. A. (2019). Acidification Impacts and Goals for Gauging Recovery of Brook Trout Populations and Fish Communities in Streams of the Western Adirondack Mountains, New York, USA. *Transactions of the American Fisheries Society*, *148*(2), 373–392. https://doi.org/10.1002/tafs.10137

Baldigo, B. P., George, S. D., Sullivan, T. J., Driscoll, C. T., Burns, D. A., Shao, S., & Lawrence, G. B. (2019). Probabilistic relations between acid–base chemistry and fish assemblages in streams of the Western Adirondack mountains, New York, USA. *Canadian Journal of Fisheries and Aquatic Sciences*, *76*(11), 2013–2026. https://doi.org/10.1139/cjfas-2018-0260

Baldigo, B. P., Lawrence, G., & Simonin, H. (2007). Persistent Mortality of Brook Trout in Episodically Acidified Streams of the Southwestern Adirondack Mountains, New York. *Transactions of the American Fisheries Society*, *136*(1), 121–134. https://doi.org/10.1577/t06-043.1

Balesdent, J., Basile-Doelsch, I., Chadoeuf, J., Cornu, S., Derrien, D., Fekiacova, Z., & Hatté, C. (2018). Atmosphere–soil carbon transfer as a function of soil depth. *Nature*, *559*(7715), 599–602. https://doi.org/10.1038/s41586-018-0328-3

Beier, C. M., Caputo, J., Lawrence, G. B., & Sullivan, T. J. (2017). Loss of ecosystem services

due to chronic pollution of forests and surface waters in the Adirondack region (USA). *Journal of Environmental Management*, *191*, 19–27. https://doi.org/10.1016/j.jenvman.2016.12.069

Beniston, M., Diaz, H. F., & Bradley, R. S. (1997). Climatic change at high elevation sites: An overview. *Climatic Change*, *36*(3–4), 233–251. https://doi.org/10.1023/a:1005380714349

Bobbink, R., Hicks, K., Galloway, J., Spranger, T., Alkemade, R., Ashmore, M., Bustamante, M., Cinderby, S., Davidson, E., Dentener, F., Emmett, B., Erisman, J. W., Fenn, M., Gilliam, F., Nordin, A., Pardo, L., & De Vries, W. (2010). Global assessment of nitrogen deposition effects on terrestrial plant diversity: A synthesis. *Ecological Applications*, *20*(1), 30–59. https://doi.org/10.1890/08-1140.1

Bohn, H. L., McNeal, B. L., & O'connor, G. A. (1979). Soil chemistry. In *Soil chemistry*. https://doi.org/10.1201/9781315137322-6

Burns, D. A. and T. J. S. (2015). *Critical loads of Atmospheric Deposition to Adirondack Lake Watersheds: A Guide for Policymakers*. 14.

Campbell, J. L., Rustad, L. E., Boyer, E. W., Christopher, S. F., Driscoll, C. T., Fernandez, I. J., Groffman, P. M., Houle, D., Kiekbusch, J., Magill, A. H., Mitchell, M. J., & Ollinger, S. V. (2009). Consequences of climate change for biogeochemical cycling in forests of northeastern North America. *Canadian Journal of Forest Research*, *39*(2), 264–284. https://doi.org/10.1139/X08-104

Chen, L., & Driscoll, C. T. (2004). An evaluation of processes regulating spatial and temporal patterns in lake sulfate in the Adirondack region of New York. *Global Biogeochemical Cycles*, *18*(3). https://doi.org/10.1029/2003GB002169

Chen, L., & Driscoll, C. T. (2005a). Regional application of an integrated biogeochemical model to northern new england and maine. *Ecological Applications*, *15*(5), 1783–1797. https://doi.org/10.1890/04-1052

Chen, L., & Driscoll, C. T. (2005b). Regional assessment of the response of the acid-base status of lake watersheds in the Adirondack region of New York to changes in atmospheric deposition using PnET-BGC. *Environmental Science and Technology*, *39*(3), 787–794. https://doi.org/10.1021/es049583t

Collins, W. J., Bellouin, N., Doutriaux-Boucher, M., Gedney, N., Halloran, P., Hinton, T., Hughes, J., Jones, C. D., Joshi, M., Liddicoat, S., Martin, G., O'Connor, F., Rae, J., Senior, C., Sitch, S., Totterdell, I., Wiltshire, A., & Woodward, S. (2011). Development and evaluation of an Earth-System model - HadGEM2. *Geoscientific Model Development*, *4*(4), 1051–1075. https://doi.org/10.5194/gmd-4-1051-2011

Cosby, B. J., Hornberger, G. M., Galloway, J. N., & Wright, R. F. (1985). Modeling the Effects of Acid Deposition: Assessment of a Lumped Parameter Model of Soil Water and Streamwater Chemistry. *Water Resources Research*, *21*(1), 51–63. https://doi.org/10.1029/WR021i001p00051

Cronan, C. S., Reiners, W. A., Reynolds, R. C., & Lang, G. E. (1978). Forest floor leaching: Contributions from mineral, organic, and carbonic acids in New Hampshire subalpine forests. *Science*, *200*(4339), 309–311. https://doi.org/10.1126/science.200.4339.309-a

Cukier, R. I., Levine, H. B., & Shuler, K. E. (1978). Nonlinear sensitivity analysis of multiparameter model systems. *Journal of Computational Physics*, *26*(1), 1–42. https://doi.org/10.1016/0021-9991(78)90097-9

Davidson, E. A., & Janssens, I. A. (2006). Temperature sensitivity of soil carbon decomposition and feedbacks to climate change. *Nature*, *440*(7081), 165–173. https://doi.org/10.1038/nature04514

Dong, Z., Driscoll, C. T., Campbell, J. L., Pourmokhtarian, A., Stoner, A. M. K., & Hayhoe, K. (2019a). Projections of water, carbon, and nitrogen dynamics under future climate change in an alpine tundra ecosystem in the southern Rocky Mountains using a biogeochemical model. *Science of the Total Environment*, *650*, 1451–1464. https://doi.org/10.1016/j.scitotenv.2018.09.151

Dong, Z., Driscoll, C. T., Johnson, S. L., Campbell, J. L., Pourmokhtarian, A., Stoner, A. M. K., & Hayhoe, K. (2019b). Projections of water, carbon, and nitrogen dynamics under future climate change in an old-growth Douglas-fir forest in the western Cascade Range using a biogeochemical model. *Science of the Total Environment*, *656*, 608–624. https://doi.org/10.1016/j.scitotenv.2018.11.377

Driscoll, C. T., Driscoll, K. M., Fakhraei, H., & Civerolo, K. (2016). Long-term temporal trends and spatial patterns in the acid-base chemistry of lakes in the Adirondack region of New York in response to decreases in acidic deposition. *Atmospheric Environment*, *146*, 5–14. https://doi.org/10.1016/j.atmosenv.2016.08.034

Driscoll, C. T., Driscoll, K. M., Roy, K. M., & Dukett, J. (2007). Changes in the chemistry of lakes in the Adirondack region of New York following declines in acidic deposition. *Applied Geochemistry*, *22*(6), 1181–1188. https://doi.org/10.1016/j.apgeochem.2007.03.009

Driscoll, C. T., Lehtinen, M. D., & Sullivan, T. J. (1994). Modeling the acid-base chemistry of organic solutes in Adirondack, New York, lakes. *Water Resources Research*, *30*(2), 297–

306. https://doi.org/10.1029/93WR02888

Driscoll, C. T., Newton, R. M., Gubala, C. P., Baker, J. P., & Christensen, S. W. (1991). Adirondack Mountains. In *Acidic Deposition and Aquatic Ecosystems*. https://doi.org/10.1007/978-1-4613-9038-1_8

Driscoll, C., Whitall, D., Aber, J., Boyer, E., Castro, M., Cronan, C., Goodale, C., Groffman, P., Hopkinson, C., Lambert, K., Lawrence, G., & Ollinger, S. (2001). Acidic deposition in the northeastern United States: sources and inputs, ecosystem effects, and management strategies. *BioScience*, *53*(4), 357–374. http://www.jstor.org/stable/10.1641/0006-3568(2001)051[0180:ADITNU]2.0.CO;2

Dunne, J. P., John, J. G., Adcroft, A. J., Griffies, S. M., Hallberg, R. W., Shevliakova, E., Stouffer, R. J., Cooke, W., Dunne, K. A., Harrison, M. J., Krasting, J. P., Malyshev, S. L., Milly, P. C. D., Phillipps, P. J., Sentman, L. T., Samuels, B. L., Spelman, M. J., Winton, M., Wittenberg, A. T., & Zadeh, N. (2012). GFDL's ESM2 global coupled climate-carbon earth system models. Part I: Physical formulation and baseline simulation characteristics. *Journal of Climate*, *25*(19), 6646–6665. https://doi.org/10.1175/JCLI-D-11-00560.1

Evans, C. D. (2005). Modelling the effects of climate change on an acidic upland stream. *Biogeochemistry*, *74*(1), 21–46. https://doi.org/10.1007/s10533-004-0154-6

Fakhraei, H. (2016). *Modeling the effects of acid deposition and natural organic acids on surface waters*. http://surface.syr.edu/etd/432/%5Cnhttp://surface.syr.edu/cgi/viewcontent.cgi?article=1432&context=etd

Fakhraei, H., & Driscoll, C. T. (2015). Proton and aluminum binding properties of organic acids

in surface waters of the northeastern U.S. *Environmental Science and Technology*, *49*(5), 2939–2947. https://doi.org/10.1021/es504024u

Fakhraei, H., Driscoll, C. T., Kulp, M. A., Renfro, J. R., Blett, T. F., Brewer, P. F., & Schwartz, J. S. (2017). Sensitivity and uncertainty analysis of PnET-BGC to inform the development of Total Maximum Daily Loads (TMDLs) of acidity in the Great Smoky Mountains National Park. *Environmental Modelling and Software*, *95*, 156–167. https://doi.org/10.1016/j.envsoft.2017.06.013

Fakhraei, H., Driscoll, C. T., Renfro, J. R., Kulp, M. A., Blett, T. F., Brewer, P. F., & Schwartz, J. S. (2016). Critical loads and exceedances for nitrogen and sulfur atmospheric deposition in Great Smoky Mountains National Park, United States. *Ecosphere*, *7*(10). https://doi.org/10.1002/ecs2.1466

Fakhraei, H., Driscoll, C. T., Selvendiran, P., DePinto, J. V., Bloomfield, J., Quinn, S., & Rowell, H. C. (2014). Development of a total maximum daily load (TMDL) for acid-impaired lakes in the Adirondack region of New York. *Atmospheric Environment*, *95*, 277–287. https://doi.org/10.1016/j.atmosenv.2014.06.039

Fierer, N., & Schimel, J. P. (2003). A Proposed Mechanism for the Pulse in Carbon Dioxide Production Commonly Observed Following the Rapid Rewetting of a Dry Soil. *Soil Science Society of America Journal*, *67*(3), 798. https://doi.org/10.2136/sssaj2003.0798

Flato, G. M., Boer, G. J., Lee, W. G., McFarlane, N. A., Ramsden, D., Reader, M. C., & Weaver, A. J. (2000). The Canadian centre for climate modelling and analysis global coupled model and its climate. *Climate Dynamics*, *16*(6), 451–467. https://doi.org/10.1007/s003820050339

Foster, N. W., Mitchell, M. J., Morrison, I. K., & Shepard, J. P. (1992). Cycling of acid and base

cations in deciduous stands of Huntington Forest, New York, and Turkey Lakes, Ontario. *Canadian Journal of Forest Research*, *22*(2), 167–174. https://doi.org/10.1139/x92-022

Frumhoff, P., McCarthy, J., Melillo, J. M., Moser, S. C., & Wuebbles, D. J. (2007). Confronting climate change in the US Northeast. In *Union of Concerned Scientists. Cambridge, MA*. http://www.cns.umass.edu/neclimate/sites/www.cns.umass.edu.neclimate/files/confronting-climate-change-in-the-u-s-northeast.pdf

Galloway, J. N., & Cowling, E. B. (2002). Reactive nitrogen and the world: 200 Years of change. *Ambio*, *31*(2), 64–71. https://doi.org/10.1579/0044-7447-31.2.64

Galloway, J. N., Likens, G. E., & Hawley, M. E. (1984). Acid precipitation: Natural versus anthropogenic components. *Science*, *226*(4676), 829–831. https://doi.org/10.1126/science.226.4676.829

Gbondo-Tugbawa, S. S., & Driscoll, C. T. (2003). Factors controlling long-term changes in soil pools of exchangeable basic cations and stream acid neutralizing capacity in a northern hardwood forest ecosystem. *Biogeochemistry*, *63*(2), 161–185. https://doi.org/10.1023/A:1023308525316

Gbondo-Tugbawa, S. S., Driscoll, C. T., Aber, J. D., & Likens, G. E. (2001). Evaluation of an integrated biogeochemical model (PnET-BGC) at a northern hardwood forest ecosystem. *Water Resources Research*, *37*(4), 1057–1070. https://doi.org/10.1029/2000WR900375

Gbondo-Tugbawa, S. S., Driscoll, C. T., Mitchell, M. J., Aber, J. D., & Likens, G. E. (2002). A model to simulate the response of a northern hardwood forest ecosystem to changes in S deposition. *Ecological Applications*, *12*(1), 8–23. https://doi.org/10.1890/1051-0761(2002)012[0008:AMTSTR]2.0.CO;2

Gilliam, F. S., Burns, D. A., Driscoll, C. T., Frey, S. D., Lovett, G. M., & Watmough, S. A. (2019). Decreased atmospheric nitrogen deposition in eastern North America: Predicted responses of forest ecosystems. *Environmental Pollution*, *244*, 560–574. https://doi.org/10.1016/j.envpol.2018.09.135

Gran, G. (1952). Determination of the equivalence point in potentiometric titrations. Part II. *The Analyst*, *77*(920), 661–670. https://doi.org/10.1039/AN9527700661

Greaver, T. L., Sullivan, T. J., Herrick, J. D., Barber, M. C., Baron, J. S., Cosby, B. J., Deerhake, M. E., Dennis, R. L., Dubois, J. J. B., Goodale, C. L., Herlihy, A. T., Lawrence, G. B., Liu, L., Lynch, J. A., & Novak, K. J. (2012). Ecological effects of nitrogen and sulfur air pollution in the US: What do we know? *Frontiers in Ecology and the Environment*, *10*(7), 365–372. https://doi.org/10.1890/110049

Grove-Rasmussen, K. V. (1961). Determination of the equivalence point in potentiometric acid-base titrations. *Dansk Tidsskrift for Farmaci*, *35*, 236–242.

Guilbert, J., Beckage, B., Winter, J. M., Horton, R. M., Perkins, T., & Bomblies, A. (2014). Impacts of projected climate change over the Lake Champlain basin in Vermont. *Journal of Applied Meteorology and Climatology*, *53*(8), 1861–1875. https://doi.org/10.1175/JAMC-D-13-0338.1

Hayhoe, K., Huntington, T. G., Luo, L., Schwartz, M. D., Sheffield, J., Wood, E., Anderson, B., Bradbury, J., DeGaetano, A., Troy, T. J., & Wolfe, D. (2007). Past and future changes in climate and hydrological indicators in the US Northeast. *Climate Dynamics*, *28*(4), 381–407. http://dx.doi.org/10.1007/s00382-006-0187-8

Hayhoe, K., Wake, C., Anderson, B., Liang, X. Z., Maurer, E., Zhu, J., Bradbury, J., Degaetano,

A., Stoner, A. M., & Wuebbles, D. (2008). Regional climate change projections for the Northeast USA. *Mitigation and Adaptation Strategies for Global Change*, *13*(5–6), 425–436. https://doi.org/10.1007/s11027-007-9133-2

Helliwell, R. C., Wright, R. F., Jackson-Blake, L. A., Ferrier, R. C., Aherne, J., Cosby, B. J., Evans, C. D., Forsius, M., Hruska, J., Jenkins, A., Kram, P., Kopáček, J., Majer, V., Moldan, F., Posch, M., Potts, J. M., Rogora, M., & Schöpp, W. (2014). Assessing recovery from acidification of European surface waters in the year 2010: Evaluation of projections made with the MAGIC model in 1995. *Environmental Science and Technology*, *48*(22), 13280–13288. https://doi.org/10.1021/es502533c

Helton, J. C., & Davis, F. J. (2003). Latin hypercube sampling and the propagation of uncertainty in analyses of complex systems. *Reliability Engineering and System Safety*, *81*(1), 23–69. https://doi.org/10.1016/S0951-8320(03)00058-9

Hinckley, E. L. S., Crawford, J. T., Fakhraei, H., & Driscoll, C. T. (2020). A shift in sulfur-cycle manipulation from atmospheric emissions to agricultural additions. *Nature Geoscience*, *13*(9), 597–604. https://doi.org/10.1038/s41561-020-0620-3

Huntington, T. G. (2005). Assessment of calcium status in Maine forests: Review and future projection. *Canadian Journal of Forest Research*, *35*(5), 1109–1121. https://doi.org/10.1139/x05-034

Husar, R. B., Sullivan, T. J., & Charles, D. F. (1991). Historical Trends in Atmospheric Sulfur Deposition and Methods for Assessing Long-Term Trends in Surface Water Chemistry. *Acidic Deposition and Aquatic Ecosystems*, 65–82. https://doi.org/10.1007/978-1-4613-9038-1_4

Iman, R. L., Helton, J. C., & Campbell, J. E. (1981). An Approach to Sensitivity Analysis of Computer Models: Part I—Introduction, Input Variable Selection and Preliminary Variable Assessment. *Journal of Quality Technology*, *13*(3), 174–183.

IPCC. (2000). *Special Report on Emissions Scenarios. A Special Report of Working Group III of the Intergovernmental Panel on Climate Change*.

IPCC. (2014). *Executive summary of the Intergovernmental Panel on Climate Change*.

Janssen, P. H. M., & Heuberger, P. S. C. (1995). Calibration of process-oriented models. *Ecological Modelling*, *83*(1–2), 55–66. https://doi.org/10.1016/0304-3800(95)00084-9

Johnson, A. H., Moyer, A., Bedison, J. E., Richter, S. L., & Willig, S. A. (2008a). Seven Decades of Calcium Depletion in Organic Horizons of Adirondack Forest Soils. *Soil Science Society of America Journal*, *72*(6), 1824–1830. https://doi.org/10.2136/sssaj2006.0407

Johnson, A. H., Moyer, A., Bedison, J. E., Richter, S. L., & Willig, S. A. (2008b). Seven Decades of Calcium Depletion in Organic Horizons of Adirondack Forest Soils. *Soil Science Society of America Journal*, *72*(6), 1824–1830. https://doi.org/10.2136/sssaj2006.0407

Jorgensen, S. E. (1994). Fundamentals of ecological modelling. 2nd edition. *Fundamentals of Ecological Modelling. 2nd Edition*.

Keyes, A. T., Lambert, K. F., Burtraw, D., Buonocore, J. J., Levy, J. I., & Driscoll, C. T. (2019). The Affordable Clean Energy rule and the impact of emissions rebound on carbon dioxide and criteria air pollutant emissions. *Environmental Research Letters*, *14*(4).

https://doi.org/10.1088/1748-9326/aafe25

Lawrence, G. B. (2002). Persistent episodic acidification of streams linked to acid rain effects on soil. *Atmospheric Environment*, *36*(10), 1589–1598. https://doi.org/10.1016/S1352-2310(02)00081-X

Lawrence, G. B., Simonin, H. A., Baldigo, B. P., Roy, K. M., & Capone, S. B. (2011). Changes in the chemistry of acidified Adirondack streams from the early 1980s to 2008. *Environmental Pollution*, *159*(10), 2750–2758. https://doi.org/10.1016/j.envpol.2011.05.016

Lawrence, G. B., Sullivan, T. J., Bailey, S. W., McDonnell, J. J., & Antidormi., M. R. (2017). *Adirondack New York soil chemistry data, 1997-2014: U.S. Geological Survey data release*.

Lawrence, Gregory B., Burns, D. A., & Riva-Murray, K. (2016). A new look at liming as an approach to accelerate recovery from acidic deposition effects. *Science of the Total Environment*, *562*, 35–46. https://doi.org/10.1016/j.scitotenv.2016.03.176

Lawrence, Gregory B., McDonnell, T. C., Sullivan, T. J., Dovciak, M., Bailey, S. W., Antidormi, M. R., & Zarfos, M. R. (2018). Soil Base Saturation Combines with Beech Bark Disease to Influence Composition and Structure of Sugar Maple-Beech Forests in an Acid Rain-Impacted Region. *Ecosystems*, *21*(4), 795–810. https://doi.org/10.1007/s10021-017-0186-0

Lawrence, Gregory B., Momen, B., & Roy, K. M. (2004). Use of Stream Chemistry for Monitoring Acidic Deposition Effects in the Adirondack Region of New York. *Journal of Environment Quality*, *33*(3), 1002. https://doi.org/10.2134/jeq2004.1002

Lawrence, Gregory B., Roy, K. M., Baldigo, B. P., Simonin, H. A., Capone, S. B., Sutherland, J.

W., Nierzwicki-Bauer, S. A., & Boylen, C. W. (2008). Chronic and Episodic Acidification of Adirondack Streams from Acid Rain in 2003-2005. *Journal of Environmental Quality*, *37*(6), 2264–2274. https://doi.org/10.2134/jeq2008.0061

Lawrence, Gregory B., Shortle, W. C., David, M. B., Smith, K. T., Warby, R. A. F., & Lapenis, A. G. (2012). Early Indications of Soil Recovery from Acidic Deposition in U.S. Red Spruce Forests. *Soil Science Society of America Journal*, *76*(4), 1407–1417. https://doi.org/10.2136/sssaj2011.0415

Lilburne, L., Gatelli, D., & Tarantola, S. (2006). Sensitivity analysis on spatial models: A new approach. *Proceedings of ACCURACY 2006 - 7th International Symposium on Spatial Accuracy Assessment in Natural Resources and Environmental Sciences*, 329–338.

Lorusso, N. A., McHale, M., McHale, P., Montesdeoca, M., Zeng, T., & Driscoll, C. T. (2020). Landscape influence on the browning of a lake watershed in the adirondack region of new york, usa. *Soil Systems*, *4*(3), 1–16. https://doi.org/10.3390/soilsystems4030050

Lovett, G. M., Tear, T. H., Evers, D. C., Findlay, S. E. G., Cosby, B. J., Dunscomb, J. K., Driscoll, C. T., & Weathers, K. C. (2009). Effects of air pollution on ecosystems and biological diversity in the eastern United States. *Annals of the New York Academy of Sciences*, *1162*, 99–135. https://doi.org/10.1111/j.1749-6632.2009.04153.x

McDonnell, T. C., Sullivan, T. J., Cosby, B. J., Jackson, W. A., & Elliott, K. J. (2013). Effects of climate, land management, and sulfur deposition on soil base cation supply in national forests of the southern Appalachian Mountains. *Water, Air, and Soil Pollution*, *224*(10). https://doi.org/10.1007/s11270-013-1733-8

McDonnell, T., Sullivan, T., & Beier, C. (2018). Influence of Climate on Long-Term Recovery of Adirondack Mountain Lakewater Chemistry from Atmospheric Deposition of Sulfur and Nitrogen. *Adirondack Journal of Environmental Studies*, *22*(1), 4.

McKay, M. D., Beckman, R. J., & Conover, W. J. (1979). Comparison of three methods for selecting values of input variables in the analysis of output from a computer code. *Technometrics*, *21*(2), 239–245. https://doi.org/10.1080/00401706.1979.10489755

McMartin, B. (1994). *The Great Forest of the Adirondacks*.

Melillo, J. M., Steudler, P. A., Aber, J. D., Newkirk, K., Lux, H., Bowles, F. P., Catricala, C., Magill, A., Ahrens, T., & Morrisseau, S. (2002). Soil warming and carbon-cycle feedbacks to the climate system. *Science*, *298*(5601), 2173–2176. https://doi.org/10.1126/science.1074153

Mitchell, M. J., Piatek, K. B., Christopher, S., Mayer, B., Kendall, C., & McHale, P. (2006). Solute sources in stream water during consecutive fall storms in a northern hardwood forest watershed: A combined hydrological, chemical and isotopic approach. *Biogeochemistry*, *78*(2), 217–246. https://doi.org/10.1007/s10533-005-4277-1

Mitchell, Myron J., & Likens, G. E. (2011). Watershed sulfur biogeochemistry: Shift from atmospheric deposition dominance to climatic regulation. *Environmental Science and Technology*, *45*(12), 5267–5271. https://doi.org/10.1021/es200844n

Mitchell, Myron J., Lovett, G., Bailey, S., Beall, F., Burns, D., Buso, D., Clair, T. A., Courchesne, F., Duchesne, L., Eimers, C., Fernandez, I., Houle, D., Jeffries, D. S., Likens, G. E., Moran, M. D., Rogers, C., Schwede, D., Shanley, J., Weathers, K. C., & Vet, R. (2011). Comparisons of watershed sulfur budgets in southeast Canada and northeast US:

New approaches and implications. *Biogeochemistry*, *103*(1), 181–207. https://doi.org/10.1007/s10533-010-9455-0

Morris, M. D. (1991). Factorial Sampling Plans for Preliminary Computational Experiments. *Technometrics*, *33*(2), 161. https://doi.org/10.2307/1269043

Moss, R. H., Edmonds, J. A., Hibbard, K. A., Manning, M. R., Rose, S. K., Van Vuuren, D. P., Carter, T. R., Emori, S., Kainuma, M., Kram, T., Meehl, G. A., Mitchell, J. F. B., Nakicenovic, N., Riahi, K., Smith, S. J., Stouffer, R. J., Thomson, A. M., Weyant, J. P., & Wilbanks, T. J. (2010). The next generation of scenarios for climate change research and assessment. *Nature*, *463*(7282), 747–756. https://doi.org/10.1038/nature08823

NECIA. (2006). Climate Change in the U.S. Northeast: A report of the Northeast Climate Impacts Assessment. In *October* (Issue October).

Neff, J. C., Townsend, A. R., Gleixner, G., Lehman, S. J., Turnbull, J., & Bowman, W. D. (2002). Variable effects of nitrogen additions on the stability and turnover of soil carbon. *Nature*, *419*(6910), 915–917. https://doi.org/10.1038/nature01136

Nizich, S.V., D. Misenheimer, T.E. Pierce, A. Pope, P. C. (2000). National air pollutant emission trends, 1900-1998. In *EPA Publications* (Issues 454 R-00–002).

NOAA. (2013). *Regional Climate Trends and Scenarios for the U.S. National Climate Assessment: Part 4. Climate of the U.S. Great Plains*. http://www.nesdis.noaa.gov/technical_reports/NOAA_NESDIS_Tech_Report_142-4-Climate_of_the_U.S. Great_Plains.pdf

Ollinger, S. V., Aber, J. D., Lovett, G. M., Millham, S. E., Lathrop, R. G., & Ellis, J. M. (1993).

A spatial model of atmospheric deposition for the northeastern US. *Ecological Applications*, *3*(3), 459–472. https://doi.org/10.2307/1941915

Pourmokhtarian, A., Driscoll, C. T., Campbell, J. L., & Hayhoe, K. (2012). Modeling potential hydrochemical responses to climate change and increasing CO2 at the Hubbard Brook Experimental Forest using a dynamic biogeochemical model (PnET-BGC). *Water Resources Research*, *48*(7). https://doi.org/10.1029/2011WR011228

Pourmokhtarian, A., Driscoll, C. T., Campbell, J. L., Hayhoe, K., Stoner, A. M. K., Adams, M. B., Burns, D., Fernandez, I., Mitchell, M. J., & Shanley, J. B. (2017). Modeled ecohydrological responses to climate change at seven small watersheds in the northeastern United States. *Global Change Biology*, *23*(2), 840–856. https://doi.org/10.1111/gcb.13444

Rangwala, I., & Miller, J. R. (2012). Climate change in mountains: A review of elevation-dependent warming and its possible causes. *Climatic Change*, *114*(3–4), 527–547. https://doi.org/10.1007/s10584-012-0419-3

Robison, A. L., & Scanlon, T. M. (2018). Climate Change to Offset Improvements in Watershed Acid-Base Status Provided by Clean Air Act and Amendments: A Model Application in Shenandoah National Park, Virginia. *Journal of Geophysical Research: Biogeosciences*, *123*(9), 2863–2877. https://doi.org/10.1029/2018JG004519

Rotstayn, L. D., Jeffrey, S. J., Collier, M. A., Dravitzki, S. M., Hirst, A. C., Syktus, J. I., & Wong, K. K. (2012). Aerosol- and greenhouse gas-induced changes in summer rainfall and circulation in the Australasian region: A study using single-forcing climate simulations. *Atmospheric Chemistry and Physics*, *12*(14), 6377–6404. https://doi.org/10.5194/acp-12-6377-2012

Salas-Mélia, D., Chauvin, F., Déqué, M., Douville, H., Gueremy, J., Marquet, P., Planton, S., Royer, J., & Tyteca, S. (2005). Description and validation of the CNRM-CM3 global coupled model. *CNRM Working Note 103*, 36. http://www.cnrm.meteo.fr/scenario2004/paper_cm3.pdf

Saltelli, A., Tarantola, S., & Chan, K. P. S. (1999). A quantitative model-independent method for global sensitivity analysis of model output. *Technometrics*, *41*(1), 39–56. https://doi.org/10.1080/00401706.1999.10485594

Schaberg, P. G., DeHayes, D. H., Hawley, G. J., Strimbeck, G. R., Cumming, J. R., Murakami, P. F., & Borer, C. H. (2000). Acid mist and soil Ca and Al alter the mineral nutrition and physiology of red spruce. *Tree Physiology*, *20*(2), 73–85. https://doi.org/10.1093/treephys/20.2.73

Schwieger, V. (2004). Variance-based sensitivity analysis for model evaluation in engineering surveys. *INGEO 2004 and FIG Regional Central and Eastern European Conference on Engineering Surveying*, 1–10.

Sebestyen, S. D., Boyer, E. W., & Shanley, J. B. (2009). Responses of stream nitrate and DOC loadings to hydrological forcing and climate change in an upland forest of the northeastern United States. *Journal of Geophysical Research: Biogeosciences*, *114*(2). https://doi.org/10.1029/2008JG000778

Shao, S., Driscoll, C. T., Sullivan, T. J., Burns, D. A., Baldigo, B., Lawrence, G. B., & McDonnell, T. C. (2020). The response of stream ecosystems in the Adirondack region of New York to historical and future changes in atmospheric deposition of sulfur and nitrogen. *Science of the Total Environment*, *716*. https://doi.org/10.1016/j.scitotenv.2020.137113

406 Sobol, I. M. (2001). Global sensitivity indices for nonlinear mathematical models and their
407 Monte Carlo estimates. *Mathematics and Computers in Simulation*, *55*(1–3), 271–280.
408 https://doi.org/10.1016/S0378-4754(00)00270-6

409 Sullivan, T. J., Cosby, B. J., Driscoll, C. T., McDonnell, T. C., & Herlihy, A. T. (2011). Target
410 loads of atmospheric sulfur deposition protect terrestrial resources in the Adirondack
411 Mountains, New York against biological impacts caused by soil acidification. *Journal of*
412 *Environmental Studies and Sciences*, *1*(4), 301–314. https://doi.org/10.1007/s13412-011-
413 0062-8

414 Sullivan, T. J., Lawrence, G. B., Bailey, S. W., McDonnell, T. C., Beier, C. M., Weathers, K. C.,
415 McPherson, G. T., & Bishop, D. A. (2013). Effects of acidic deposition and soil
416 acidification on sugar maple trees in the Adirondack Mountains, New York. *Environmental*
417 *Science and Technology*, *47*(22), 12687–12694. https://doi.org/10.1021/es401864w

418 Sullivan, T. J. (2015). Air Pollutant Deposition and Its Effects on Natural Resources in New
419 York State. In *Air Pollutant Deposition and Its Effects on Natural Resources in New York*
420 *State*. https://doi.org/10.7591/9781501700811

421 Sullivan, T. J. (2017). Air Pollutant Deposition and Its Effects on Natural Resources in New
422 York State. In *Air Pollutant Deposition and Its Effects on Natural Resources in New York*
423 *State*. https://doi.org/10.7591/9781501700811

424 Sullivan, T. J., Driscoll, C. T., Beier, C. M., Burtraw, D., Fernandez, I. J., Galloway, J. N., Gay,
425 D. A., Goodale, C. L., Likens, G. E., Lovett, G. M., & Watmough, S. A. (2018). Air
426 pollution success stories in the United States: The value of long-term observations.
427 *Environmental Science and Policy*, *84*, 69–73. https://doi.org/10.1016/j.envsci.2018.02.016

Sutherland, J. W., Acker, F. W., Bloomfield, J. A., Boylen, C. W., Charles, D. F., Daniels, R. A., Eichler, L. W., Farrell, J. L., Feranec, R. S., Hare, M. P., Kanfoush, S. L., Preall, R. J., Quinn, S. O., Rowell, H. C., Schoch, W. F., Shaw, W. H., Siegfried, C. A., Sullivan, T. J., Winkler, D. A., & Nierzwicki-Bauer, S. A. (2015). Brooktrout Lake case study: Biotic recovery from acid deposition 20 years after the 1990 clean air act amendments. *Environmental Science and Technology*, *49*(5), 2665–2674. https://doi.org/10.1021/es5036865

Tan, N., Contoux, C., Ramstein, G., Sun, Y., Dumas, C., Sepulchre, P., & Guo, Z. (2020). Modeling a modern-like *p*CO2 warm period (Marine Isotope Stage KM5c) with two versions of an Institut Pierre Simon Laplace atmosphere-ocean coupled general circulation model. *Climate of the Past*, *16*(1), 1–16. https://doi.org/10.5194/cp-16-1-2020

Tongwen, W. (2012). A mass-flux cumulus parameterization scheme for large-scale models: description and test with observations. *Climate Dynamics*, *38*, 725–744. https://doi.org/10.1029/2001JD001005

U.S. Environmental Protection Agency. (2008). Integrated science assessment for oxides of nitrogen and sulfur-environmental criteria. In *Federal Register* (Vol. 73, Issue 240).

U.S. Environmental Protection Agency. (2010). Review of the secondary national ambient air quality standards for oxides of nitrogen and oxides of sulfur. In *Federal Register* (Vol. 75, Issue 182).

U.S. Geological Survey. (2019). *USGS Water Data for the Nation: U.S. Geological Survey National Water Information System Database*. http://dx.doi.org/10.5066/F7P55KJN

Valipour, M., Driscoll, C. T., Johnson, C. E., Battles, J. J., Campbell, J. L., & Fahey, T. J.

(2018). The application of an integrated biogeochemical model to simulate dynamics of vegetation, hydrology and nutrients in soil and streamwater following a whole-tree harvest of a northern hardwood forest. *Science of the Total Environment*, *645*, 244–256. https://doi.org/10.1016/j.scitotenv.2018.07.066

van Breemen, N., Mulder, J., & Driscoll, C. T. (1983). Acidification and alkalinization of soils. *Plant and Soil*, *75*(3), 283–308. https://doi.org/10.1007/BF02369968

Von Schneidemesser, E., Driscoll, C., Rieder, H. E., & Schiferl, L. D. (2020). How will air quality effects on human health, crops and ecosystems change in the future?: Future Air Quality Effects. *Philosophical Transactions of the Royal Society A: Mathematical, Physical and Engineering Sciences*, *378*(2183). https://doi.org/10.1098/rsta.2019.0330

Watanabe, S., Hajima, T., Sudo, K., Nagashima, T., Takemura, T., Okajima, H., Nozawa, T., Kawase, H., Abe, M., Yokohata, T., Ise, T., Sato, H., Kato, E., Takata, K., Emori, S., & Kawamiya, M. (2011). MIROC-ESM 2010: Model description and basic results of CMIP5-20c3m experiments. *Geoscientific Model Development*, *4*(4), 845–872. https://doi.org/10.5194/gmd-4-845-2011

Watmough, S. A., Aherne, J., Alewell, C., Arp, P., Bailey, S., Clair, T., Dillon, P., Duchesne, L., Eimers, C., Fernandez, I., Foster, N., Larssen, T., Miller, E., Mitchell, M., & Page, S. (2005). Sulphate, nitrogen and base cation budgets at 21 forested catchments in Canada, the United States and Europe. *Environmental Monitoring and Assessment*, *109*(1–3), 1–36. https://doi.org/10.1007/s10661-005-4336-z

Wu, W., & Driscoll, C. T. (2009). Application of the PnET-BGC - An integrated biogeochemical model - To assess the surface water ANC recovery in the Adirondack region of New York

under three multi-pollutant proposals. *Journal of Hydrology*, *378*(3–4), 299–312. https://doi.org/10.1016/j.jhydrol.2009.09.035

Yukimoto, S., Adachi, Y., Hosaka, M., Sakami, T., Yoshimura, H., Hirabara, M., Tanaka, T. Y., Shindo, E., Tsujino, H., Deushi, M., Mizuta, R., Yabu, S., Obata, A., Nakano, H., Koshiro, T., Ose, T., & Kitoh, A. (2012). A new global climate model of the Meteorological Research Institute: MRI-CGCM3: -Model description and basic performance-. *Journal of the Meteorological Society of Japan*, *90*(A), 23–64. https://doi.org/10.2151/jmsj.2012-A02

Zhai, J., Driscoll, C. T., Sullivan, T. J., & Cosby, B. J. (2008). Regional application of the PnET-BGC model to assess historical acidification of Adirondack lakes. *Water Resources Research*, *44*(1). https://doi.org/10.1029/2006WR005532

Zhang, Y., & Rundell, A. (2006). Comparative study of parameter sensitivity analyses of the TCR-activated Erk-MAPK signalling pathway. *IEE Proceedings: Systems Biology*, *153*(4), 201–211. https://doi.org/10.1049/ip-syb:20050088

Zhou, Q., Driscoll, C. T., & Sullivan, T. J. (2015). Responses of 20 lake-watersheds in the Adirondack region of New York to historical and potential future acidic deposition. *Science of the Total Environment*, *511*, 186–194. https://doi.org/10.1016/j.scitotenv.2014.12.044

Zhou, Q., Driscoll, C. T., Sullivan, T. J., & Pourmokhtarian, A. (2015). Factors influencing critical and target loads for the acidification of lake–watersheds in the Adirondack region of New York. *Biogeochemistry*, *124*(1–3), 353–369. https://doi.org/10.1007/s10533-015-0102-7

Vita

SHUAI SHAO

(650)305-1185 ● sshao@syr.edu ●

Education:

M.S., Environmental Engineering, Syracuse University, Syracuse, NY, December 2014

Thesis Topic: Watershed-Level Responses to Calcium Silicate Treatment.

Advisor: Dr. Charles T. Driscoll

B.S., Environmental Engineering, Beijing Jiaotong University (BJTU), Beijing, China, July 2011

Publications:

- **Shao S.,** C.T. Driscoll, C.E. Johnson, T.J. Fahey, J.J. Battles, and J.D. Blum, (2016). Long-term responses in soil solution and stream-water chemistry at the Hubbard Brook after experimental addition of wollastonite. Environmental Chemistry, 13(3), 528-540. doi:10.1071/EN15113

- **Shao S.**, C.T. Driscoll, T.J. Sullivan, D.A. Burns, B.P. Baldigo, G.B. Lawrence and T.C. McDonnell, (2020) The response of stream ecosystems in the Adirondack region of New York to historical and future changes in atmospheric deposition of sulfur and nitrogen, Science of the Total Environment. 716 (10) doi:10.1016/j.scitotenv.2020.137113

- **Shao S.**, D.A. Burns, Y.Chen, A.G. Russell, H.Z. Shen, C.T. Driscoll, (submitted), The responses of streams to projected changes of climate and sulfur and nitrogen depositions in the Adirondacks. Science of the Total Environment.

- Gu. W, C. T. Driscoll, **S. Shao**, and C.E. Johnson, (2017). Aluminum is more tightly bound in soil after wollastonite treatment to a forest watershed. Forest Ecology and Management, 397, 57-66. doi: 10.1016/j.foreco.2017.04.035

- Baldigo, B.P., S.D. George, C.T. Driscoll, **S. Shao**, T.J. Sullivan, D.A. Burns, and G.B. Lawrence. (2019). Probabilistic relationships between indicators of acid-base chemistry

and fish assemblages in streams of the western Adirondack Mountains, New York, USA. Canadian Journal of Fisheries and Aquatic Sciences. DOI: 10.1002/tafs.10137

- Shen H.Z., Y.Chen, Y. Li, A.G. Russell, Y. Hu ,**S. Shao**, C.T. Driscoll et al., Relaxing Energy Policies Coupled with Climate Change Will Significantly Undermine Efforts to Attain US Ozone Standards, (2019), One Earth, DOI: https://doi.org/10.1016/j.oneear.2019.09.006

- Chen Y., H.Z. Shen., Y. Li, A.G. Russell, Y. Hu, **S. Shao**, C.T. Driscoll et al., Greater contribution from agricultural sources to future reactive nitrogen deposition in the United States, Earth's Future, https://doi.org/10.1029/2019EF001453

- McDonnell T.C., C.T. Driscoll, T.J. Sullivan, D.A. Burns, B.P. Baldigo, **S. Shao,** G.B. Lawrence, (2021), Regional target loads of atmospheric nitrogen and sulfur deposition for the protection of stream and watershed soil resources of the Adirondack Mountains, USA, Environmental Pollution, https://doi.org/10.1016/j.envpol.2021.117110.

- Sullivan T.J., C.T. Driscoll, D.A. Burns, B.P. Baldigo, G.B. Lawrence, **S. Shao,** and T.C. McDonnell, (2020) The Response of Streams to Changes in Atmospheric Deposition of Sulfur and Nitrogen in the Adirondack Mountains, Technical Report. DOI: 10.13140/RG.2.2.34239.53926

Technical presentations:

- "Responses of acid-sensitive and insensitive streams to projected changes in climate and S and N deposition in the Adirondacks" Presentation. **2020 Adirondack Research Forum**. Old Forge, NY. February 2020.

- "Responses of acid-sensitive and insensitive streams to projected changes in climate and S and N deposition in the Adirondacks" Presentation. **Environmental Group Seminar**. Syracuse, NY. February 2020.

- "The responses of stream ecosystems to future scenarios of atmospheric deposition derived from changing land use-related emission and projected future meteorological conditions" Presentation. **Environmental Group Seminar**. Syracuse, NY. October 2019.

- "The responses of stream ecosystems to future scenarios of atmospheric deposition derived from changing land use-related emission and projected future meteorological conditions" Presentation. **NADP 2018 Fall meeting.** Albany, NY. November 2018.

- "The responses of stream ecosystems to future scenarios of atmospheric deposition derived from changing land use-related emission and projected future meteorological conditions" Presentation. **AGU Fall Meeting**. Washington, D.C., December 2018.

- "Developing Critical Loads of Acidity for Stream Ecosystems in the Adirondack of New York State" Presentation**. 2018 Adirondack Research Forum**. Old Forge, NY. March 2018.

- "Developing Critical Loads of Acidity for Stream Ecosystems in the Adirondack of New York State" Presentation. **NADP 2017 Fall Meeting**. San Diego, CA, November 2017.

- "The Application of an Integrated Biogeochemical Model (PnET-BGC) to Stream Water in the Adirondacks" Poster. **2017 Conference of the Northeastern Ecosystem Research Cooperative.** Albany, NY. March 2017

- "The application of an integrated biogeochemical model (PnET-BGC) to stream water in the Adirondack" Presentation. **2017 Adirondack Research Forum.** Old Forge, NY. March 2017.

- "Long-term analysis of response of soil solution and stream water of Watershed 1 at Hubbard Brook to the experimental addition of wollastonite" Presentation. **Mater's thesis defense.** Syracuse, NY. August 2014.

- "Long-term analysis of response of soil solution and stream water of Watershed 1 at Hubbard Brook to the experimental addition of wollastonite" Presentation. **HBEF meeting.** Hubbard Brook, NH. April 2014.